

RESEARCH ARTICLE

Open Access



Modelling medieval masonry construction: taxa-specific and habitat-contingent Bayesian techniques for the interpretation of radiocarbon data from Mortar-Entrapped Relict Limekiln Fuels

Mark Thacker* 

Abstract

Using data from simulated and actual case studies, this paper assesses the accuracy and precision of Bayesian estimates for the constructional date of medieval masonry buildings, generated from the radiocarbon evidence returned by different assemblages of wood-charcoal mortar-entrapped relict limekiln fuel (MERLF). The results from two theoretical studies demonstrate how Bayesian model specifications can be varied to generate a chronologically continuous spectrum of distributions from radiocarbon datasets subject Inbuilt Age (IA). Further analysis suggests that the potential for these distributions to contain the date of the constructional event depends largely upon the accuracy of the latest radiocarbon determination within each dataset, while precision is predicated on dataset age range, dataset size and model specification. These theoretical studies inform revised approaches to the radiocarbon evidence emerging from six culturally important Scottish medieval masonry buildings, each of which is associated with a wood-charcoal MERLF assemblage of different botanical character. The Bayesian estimates generated from these radiocarbon datasets are remarkably consistent with the historical and archaeological evidence currently associated with these sites, while age range distributions suggest the IA of each MERLF assemblage has been constrained by the taxa-specific and environmentally contingent lifespans and post-mortem durabilities of the limekiln fuel source. These studies provide further evidence that Bayesian techniques can generate consistently accurate chronological estimates for the construction of medieval masonry buildings from MERLF radiocarbon data, whatever the ecological provenance of the limekiln fuel source. Estimate precision is contingent upon source ecology and craft technique but can be increased by a more informed approach to materials analysis and interpretation.

Keywords: Bayesian, Buildings, Charcoal, Ecology, Masonry, Medieval, Outlier, Radiocarbon

Introduction

Scholars across the world often face significant challenges in ascribing constructional dates to masonry buildings with enough precision to enable meaningful interdisciplinary environmental or historical discourse.

The independent evidence returned by radiocarbon analysis of mortar-entrapped relict limekiln fuel (MERLF) fragments can usefully inform these chronological ascriptions, and the sedimentary context within which these materials survive presents some valuable characteristics to facilitate interpretation of that data. Firstly, the durability of lime mortars can allow them to survive *in-situ* for hundreds and sometimes thousands of years in upstanding masonry contexts, even if the walls within

*Correspondence: mark.thacker@stir.ac.uk
University of Stirling, Stirling, UK

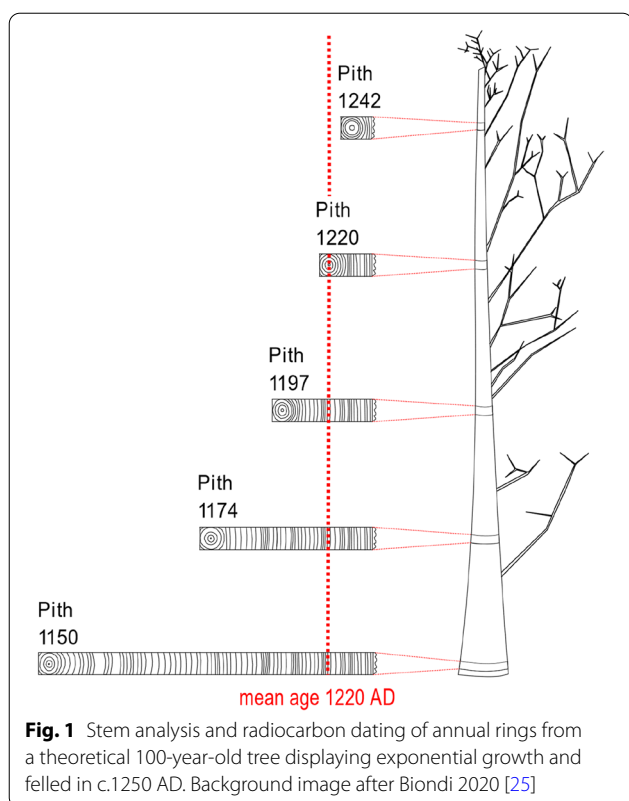
which they were deposited have been incorporated in later buildings or the structure has become ruinous [1–3]. Secondly, mortar compositions are historically and environmentally contingent, and material contrasts noted through field survey and lab-based analyses can inform relative phasing interpretations, even where direct stratigraphic relationships are absent (e. g. [4, 5]). And thirdly, the widespread use of wood fuel in pre-industrial lime-burning practices has often resulted high concentrations of wood-charcoal MERLF fragment inclusions, and this material has well-recognised radiocarbon dating potential [6, 7]. These characteristics of durability, distinctiveness, relative ubiquity, and radiocarbon dating potential are all underpinned by a rapid post-depositional mortar set, which not only allows an unequivocal archaeological association between the mortar's constituent components and the surrounding masonry fabric [8], but also precludes infiltration by other materials in later periods. It is crucial for wider interpretation that mortar phasing is correctly understood, and all radiocarbon measurements are accurate [9], but thereafter the determinations returned by all wood-charcoal relict limekiln fuel fragments are expected to calibrate to dates which are no later than the initial deposition of the masonry mortar within which they were entrapped [10–13].

The extent to which these radiocarbon determinations might calibrate to periods which pre-date the construction of the identified masonry phase will be defined by various interrelated factors. The size of the laboratory measurement error margin and the section of the atmospheric calibration curve to which the determination relates are important factors in defining chronological precision, but an allowance must also be made for any 'inbuilt age' (IA) which might separate the average age of the annual tree rings in the MERLF sample (the cells of which rapidly cease exchanging carbon with the surrounding environment after formation) from the constructional event of interest [14–18]. The 'bridging periods' [14] which might contribute to the IA of a sample must be considered on a context-by-context basis and might include post-limekiln factors such as lime transport, mortar maturation and building construction times. But in the absence of historic evidence for the use of pre-prepared charcoal to fuel limekilns [19], the most significant bridging periods are likely to be associated with the loss of outer tree rings from the sample during post-mortem rot, wood conversion, combustion, and/or mortar mixing: periods limited by the pre-kiln growth and storage ages of the selected wood fuels and essentially defined by ecological parameters [7].

The potential IA of every surviving MERLF sample is influenced by its taxa-specific and habitat-contingent lifespan (constraining growth age), habit (influencing

trunk and branch wood availability), and post-mortem resilience (constraining storage age). These factors are closely interrelated, since higher resource environments and faster growing taxa are almost universally associated with relatively short lifespan plants characterised by low density wood with poor post-mortem resistance to wood-destroying fungi, and low resource environments and slower growing taxa are widely associated with longer lifespan plants characterised by higher density wood with better post-mortem resistance to wood-destroying fungi [20–25]. In general, therefore, an inverse correlation between the growth-rate of the wood fuel source and the potential IA of the MERLF assemblage generally pertains, and this is determined by taxon and habitat.

These relationships have implications for the archaeological resource at different ecological scales. At the broadest scale, IA potential may be determined by the class of the parent tree and the character of the surrounding biome, since gymnosperms are often characterised by extremely long lifespans [26] and boreal forests can be associated with (post-mortem) coarse woody debris many hundreds of years old [27, 28]. Cold, sheltered and phytogeographically marginal environments are also associated with increased tree longevity in temperate woodlands although, with maximum tree lifespans of 3–400 years pertaining across many old-growth northern hemisphere deciduous forests [29], dendroecological meta-data suggests this is generally more limited than records of particularly (probably very slow-growing) ancient individuals might suggest. Even within this reduced range, however, inter-species contrasts in lifespan and post-mortem resilience can be considerable. In the Atlantic-influenced environments of the UK, dense and comparatively slow-growing angiosperms such as *Quercus* sp. mature at around 150 years old, can live to over 500 years, and demonstrate high post-mortem durability; while faster-growing shorter-lived genera such as *Betula* sp. generally mature at around 60 years old, rarely reach 100 years old, and are very rapidly destroyed by fungal attack after death [30–32]. At a finer scale, field reports suggest *Betula pendula* has a much longer lifespan in the colder climates of central Scotland than elsewhere in these islands [31], and yet the lifespan of 'self-coppicing' *Corylus avellana* stems (which generally extend to 30–50 years in England) [30], can be limited to 12–15 years on some thin western Scottish soils [33]. Consideration of woodland ecologies in the immediate locality is often useful for evaluation of IA potential, therefore, and particularly in a country such Scotland which is crossed by numerous Northern European phytogeographical boundaries [34, 35].



Scale of analysis is also important for our interpretations of how the carbon might be distributed within a potential IA range. The distribution of carbon within a woodland exploited for lime-burning fuel will be determined by a complex mix of historically-contingent ecological processes, but although the IA potential of an even-aged stand will tend to increase over time as the population matures and productivity will naturally decline in later years as mortality increases, meta-data gathered from long-term monitoring projects across the globe suggests that aboveground mass growth rates (and so carbon gain) in individual trees generally increases continuously throughout their lifespans [24, 36–38]. Indeed, it has been reported that only 6% of old-growth forest in the western USA is comprised of trees with trunks of over 100 cm diameter, and yet this small population contributes a remarkably high ‘33% of the annual forest mass growth’ [36]. This allometric evidence is consistent with reports that more than 50% of a tree stem’s volume typically derives from the outer 30% of its annual rings [39], and its average radiocarbon age is likely to be approximately a third of its overall lifespan [10] (Fig. 1), while the destruction of old wood during trunk hollow formation [40] and replacement of older branches [41] is likely to sharpen carbon distributions in mature trees still further. Providing the assemblage is representative of the

woodland source, therefore, ecological parameters suggest most wood-charcoal samples are likely to calibrate to dates which are equal to or only slightly earlier than their date of deposition [13, 17, 42].

Quantifying the relationship between these radiocarbon determinations and the constructional date of the building from which they were removed is particularly important in historic contexts where wider political, cultural, and environmental processes are understood with reasonably high chronological precision. That the IA of a wood-charcoal fragment is contingent on its botanical character has long been recognised, and half a century ago Tjalling Waterbolk (1971) suggested samples could be usefully divided into three groups whereby: Group A materials deriving from twigs and outermost tree rings would present a radiocarbon ‘time difference’ which was negligible (< c. 20 years); Group B materials deriving from short-lifespan wood species would present time differences measurable in decades (20–100 years); while Group C materials deriving from longer lifespan species might result in time differences of over a century [10. See also 11].¹ Waterbolk (1971) also acknowledged that the archaeological context from which a sample was recovered might suggest an association with a lower IA Group, and proposed that charcoal fragments from hearths or ovens were likely to be narrowly distributed since ‘firewood for daily consumption would have consisted mostly of very young wood’ [10],² although the historiography of MERLF materials research reveals contrasting approaches to this issue. Rainer Berger’s (1992; 1995) analysis of materials from various pre-Romanesque chapel sites in Ireland, for example, began from a premise that short-lived wood was deliberately selected for lime-burning fuel and the calibrated radiocarbon determinations returned by single (probably bulk) MERLF samples were thereby reported as direct standalone constructional estimates [43, 44]. In clear contrast, a re-interpretation of large radiocarbon datasets from masonry buildings in Africa and Asia began from a premise that storage age and re-use in individual wood-charcoal fragments were ‘indeterminable’ chronological factors, whose interpretation required analysis of multiple samples from each phase [17, 12, 45].^{3,4} Notably, this latter assertion followed an article by Patrick Ashmore (1999) which highlighted the dangers of bulking multiple charcoal fragments in a single sample and the challenges of establishing charcoal residence times on archaeological

¹ See [10] p. 16.

² See [10] p. 22.

³ See [17] p. 83.

⁴ See [12] p. 15.

sites [18]. But in both instances highlighted above, the radiocarbon distribution of each sample assemblage is not expected to reflect the ecology of a natural woodland source (both are essentially defined by anthropological or technical processes), and there is a concomitant lack of botanical information on the character of the materials under consideration (see also [46–48]).

Ultimately, where the radiocarbon determination returned by a MERLF sample might be associated with significant IA, then circumscription of the chronological period within which the constructional event took place requires a comparative approach. Indeed, multidisciplinary approaches to MERLF radiocarbon data can very usefully bracket the period of building construction where historical or archaeological evidence post-dating that event is also available, since these are effective *terminus post quem* (TPQ) and *terminus ante quem* (TAQ) dates, and where the constructional date is already known with some precision then the IA of the MERLF sample or assemblage can be closely quantified [49]. Where multiple radiocarbon determinations are available, however, then Bayesian and other statistical techniques can be used to generate a comparative ‘standalone’ constructional estimate from the radiocarbon and phasing evidence alone - complete with upper limits which are independent of historical evidence [7]. Once again, such statistical interpretations are generally predicated on a binary distinction between short or long-lived organic materials, although that is most often defined by the distribution of the determinations within the radiocarbon dataset, rather than the botanical character of the samples within the charcoal assemblage. Where samples deposited in a single event have returned determinations so narrowly distributed that a chi-square type test suggests the dataset is statistically consistent at 5% significance, then the samples can be regarded as effectively contemporaneous, and a more precise Combine average can be generated which is assumed to directly represent their date of deposition [50]. Where determinations from a particular depositional context are not statistically consistent at 5% significance, however, then a higher level of IA must be suspected, and a different approach is required. In the OxCal calibration programme used throughout this paper, measurements from datasets subject to IA can be grouped into model phases framed by probability distributions known as Start and End Boundaries; and the position of this latter event at the end of the phase (or between phases in a multiphase scenario) may be accepted as a reasonable estimate for the completion of the constructional event [51]. Generating a Last distribution will also provide a probability estimate for the last determination within the series, however, and these measurements can be further constrained to reflect our

prior belief that the dataset should be exponentially distributed—in line with allometric data. OxCal offers two main methods by which this might be achieved: a Tau Start Boundary can be selected to impose an exponential ‘prior’ distribution on the whole phase; or each individual determination can be tagged with an Outlier Probability linked to a separate exponentially distributed Charcoal Outlier Model [13]. The default Charcoal Outlier Model in OxCal is specified with a 1000 year time-constant to encompass the mean lifespan of an extremely long-lived assemblage, but the logarithmic scale of the model is defined by the actual distribution of the radiocarbon determinations in each dataset and, providing sufficient independent determinations are available, the lowest IA materials are expected to be steeply distributed very close to the exponential asymptote [13, 17].

The assumptions which underpin these interpretive schemes and their general application for MERLF analysis are open to challenge. Ashmore’s [18] thesis demonstrated that very short-lived charcoal materials retrieved from various excavated contexts have sometimes returned problematically early radiocarbon determinations, but the storage age potential of MERLF materials is likely to be more limited where wood (rather than charcoal) has routinely been used as a limekiln fuel, and long residence times are largely irrelevant in a mortared masonry context where intrusion is effectively precluded. Recent studies have reported evidence that bark evidence does occasionally survive on wood-charcoal MERLF fragments, and some of the assemblages associated with these fragments have also returned radiocarbon determinations which are statistically consistent at 5% significance [52], but historical, archaeological, and radiocarbon evidence from across northern Europe and elsewhere suggests that limekilns were often charged with mixtures of different wood taxa which can return statistically inconsistent radiocarbon datasets [7]. In an important piece of work evaluating the accuracy and precision of ‘standalone’ constructional estimates generated using Bayesian techniques in OxCal, Michael Dee and Christopher Bronk Ramsey (2014) concluded that the Charcoal Outlier Model approach generates the most consistently accurate End Boundary estimates from wood-charcoal datasets, whilst the exponential prior approach generated more precise but occasionally inaccurate distributions [17]. Where the number of determinations from a particular phase is more limited, however, then the Charcoal Outlier approach tends to generate very broad positively skewed End Boundary distributions, which can seem incongruous against the comparatively low mean lifespans of most temperate woodland taxa. The TPQ role

performed by wood-charcoal MERLF radiocarbon determinations can be of huge value for multidisciplinary interpretation and the effect of model selection on upper limits may be much less important where an early and convincing TAQ is available to truncate these distributions (Fig. 2a–f). Standalone estimate precision, however, is vital for increased interdisciplinary (rather than multidisciplinary) discourse. And while there is also some evidence that reducing the exponential time-constant of the Charcoal Outlier Model to reflect the more limited source material lifespans can constrain End Boundary distributions [49], persistent contrasts in precision with estimates using the exponential prior approach and binary approaches to statistical consistency do not appear to reflect a continuous spectrum of potential IAs predicated on variation in woodland ecologies. Importantly for this paper, however, the accuracy and precision of constructional estimates generated using different Bayesian approaches can also be evaluated using simulated datasets in theoretical models, without initial reference to architectural or historical evidence.

This paper describes a re-evaluation of these Bayesian frameworks, with a concern to further characterise statistical relationships which might pertain between the different limekiln fuel resources exploited during the construction of medieval masonry buildings, and the archaeological potential of any surviving MERLF materials. Following the approach developed by Dee and Bronk Ramsey [17], this work is predicated on Bayesian analysis of simulated and actual radiocarbon datasets subject to varying levels of IA, although a broader range of simulated single-phase datasets, model specifications and generated estimates are considered here. Indeed, two theoretical studies centred on a single date in the medieval period will demonstrate how a chronologically continuous spectrum of distributions can be generated from radiocarbon datasets of varying lifespans and sizes, and different Bayesian model specifications can therefore be employed to maximise constructional estimate precision whilst retaining accuracy. These theoretical results will then inform the modelling approaches applied to the published radiocarbon datasets from six culturally important Scottish medieval buildings (CS1–6), each of which is associated with a MERLF assemblage of contrasting botanical character. Highlighting remarkable levels of consistency between the radiocarbon, historical and ecological data, the paper will conclude that the age range of an in-situ MERLF assemblage does often appear to be constrained by the taxa-specific and environmentally contingent lifespans and post-mortem durabilities of the limekiln fuel source.

Method

The methodologies presented below detail the processes by which data were generated in two theoretical studies and six case studies. Following previous authors [17], the theoretical studies are essentially circular and pragmatic. Exponentially distributed sets of calibrated radiocarbon dates associated with different IA mean lifespans (hereafter IA τ) have been simulated from a particular ‘true event’ calendar date, and these datasets have then been constrained within various single-phase Bayesian models to assess how the accuracy and precision of newly generated distributions are affected by model specification. In contrast to that previous work, however, a calendar date of 1250 AD has been selected for the true event in each theoretical study, since this correlates with a relatively monotonic section of the radiocarbon calibration curve and occupies a central chronological position relative to the case studies presented later in the paper. The error margin of ± 35 years on each simulated date was also selected to more closely reflect the data associated with these case studies. An increased range of dataset IA τ and model specifications has also been employed, while End Boundary and Last distributions are evaluated for constructional estimate accuracy and precision. All datasets and models have been generated using OxCal 4.4 [51] and are calibrated with the IntCal20 atmospheric calibration curve [53].

Theoretical studies

In Theoretical Study 1 (TS1), multiple sets of twenty simulated calibrated dates subject to varying levels of IA were generated from a theoretical true event date of 700 BP ± 35 years (1250 AD). Twenty independent datasets were generated in TS1, with four separate datasets each subject to IA τ specified at 10, 50, 100, 200 and 500 years. The number of dates in each dataset which included the true event date has been counted, dataset age ranges have been estimated using the OxCal Difference function to compare the earliest and latest simulated dates [51], and the actual mean lifespan of each dataset has been calculated by finding the sum of the mean values from each individual simulated date. Each dataset has then been situated in a single-phase Bayesian model framed by Start and End Boundaries and subject to a range of different specifications. Run at default Oxcal settings to allow a reasonably fast turnaround of results, these include: (i) a Combine model; (ii) an exponential prior/no outlier model; (iii) an exponential prior/modified Charcoal Outlier Model (with a time-constant modified to the same scale as the IA τ specified for the simulated dataset); (iv) an exponential prior/default Charcoal Outlier Model; (v) a uniform prior/no outlier model; (vi) a uniform prior/

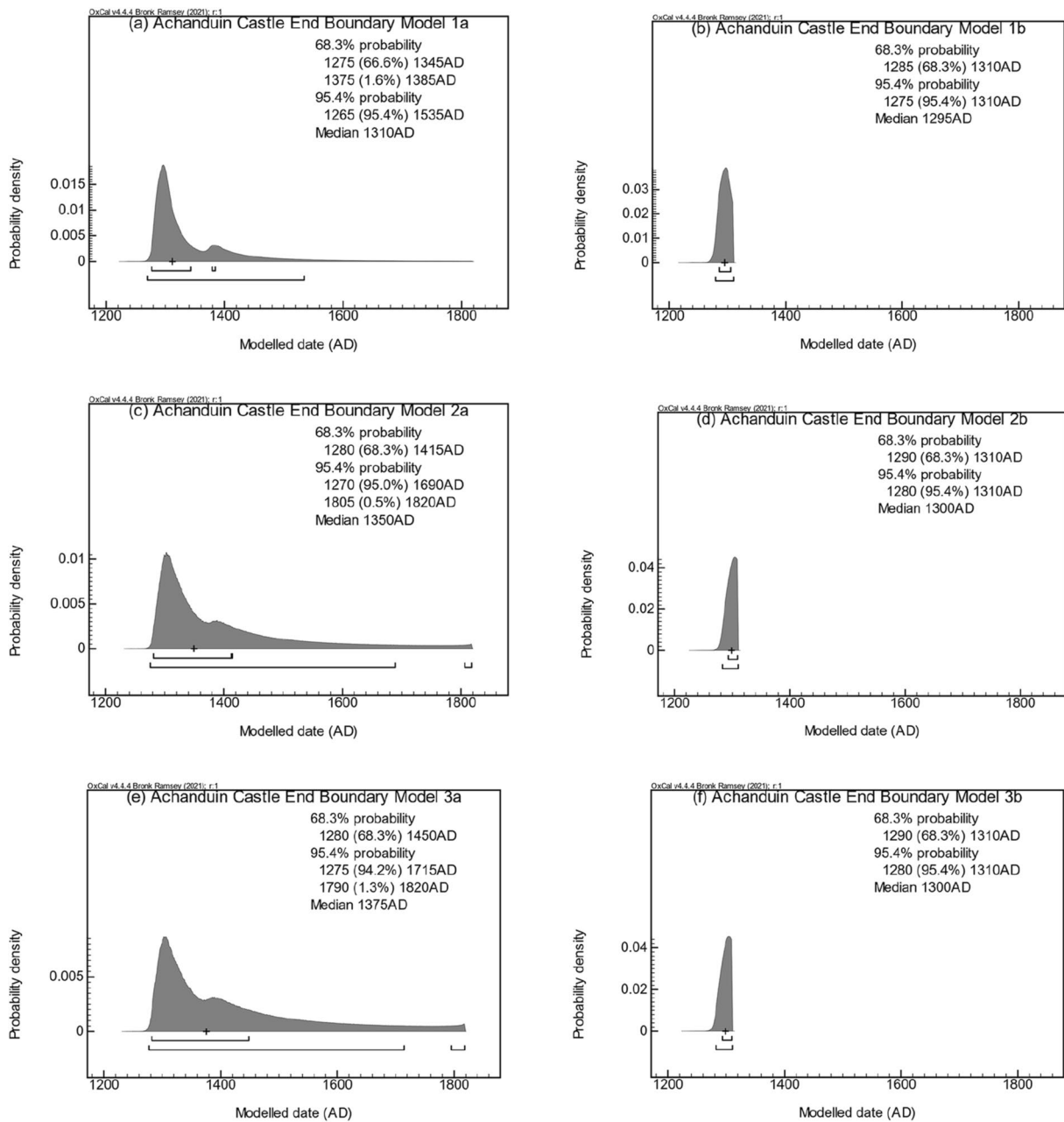


Fig. 2 a–f Comparative End Boundary distributions generated from single-phase MERLF radiocarbon data associated with a recent study of Achanduin Castle [49] highlighting the effect of different outlier models on standalone and multidisciplinary constructional estimate precision. In standalone model 1a, an exponential prior was applied, and all three available radiocarbon determinations were tagged with a 5% Outlier Probability in the default OxCal General Outlier Model (subfigure a); in standalone model 2a, a uniform prior was applied, and all three available radiocarbon determinations were tagged with a 100% Outlier Probability in a Charcoal Outlier Model with a time-constant modified to 100 years (subfigure c); and in standalone model 3a, a uniform prior was applied, and all three radiocarbon determinations were tagged with a 100% Outlier Probability in the default Charcoal Outlier Model (subfigure e). Multidisciplinary models 1b, 2b and 3b are a development from 1a, 2a and 3a, and each includes a 1310 AD documentary *TAQ* (subfigures **b**, **d** and **f**). All models have been updated using OxCal v4.4 [51] and the IntCal20 atmospheric curve [53], with results rounded out to 5 years. X axis scales in these plots have been standardised to facilitate visual comparison, but note also the different y-axis probability density scales, as well as the contrasting End Boundary distributions and medians

modified Charcoal Outlier Model (with a time-constant modified to the same scale as the specified $IA\tau$ of the simulated dataset); and (vii) a uniform prior/default Charcoal Outlier Model. In the third and fourth run of each dataset/modelling approach combination, a Last distribution was also generated. All models associated with TS1 are presented in Additional file 1.

In Theoretical Study 2 (TS2), multiple simulated datasets of varying size and subject to varying levels of IA were generated from a theoretical true event date of $700BP \pm 35$ years. Forty-five independent datasets were generated in TS2 with three separate datasets associated with an $IA\tau$ specified to 10, 50, 100, 200 and 500 years and including fifteen, ten and five simulated dates. As in TS1, the number of dates in each TS2 dataset which included the true event date has been counted, the age range has been estimated using the OxCal Difference function to compare the earliest and latest simulated dates, and the actual mean lifespan of each dataset has been calculated by finding the sum of the mean values from each simulated date. These datasets were included in single-phase models framed by Start and End Boundaries and subject to three model specifications including: (i) an exponential prior/no outlier model, (ii) an exponential prior/modified Charcoal Outlier Model (with a time-constant modified to match the $IA\tau$ specified for the simulated dataset), and (iii) a uniform prior/default Charcoal Outlier Model. All these TS2 models have been run at default settings to allow a reasonably fast turnaround of results, and all include a Last distribution. All models associated with TS2 are presented in Additional file 2.

In Case Studies 1-6 (CS1-6), the radiocarbon data from six Scottish medieval buildings with wood-charcoal MERLF assemblages comprised of contrasting taxa are re-evaluated. This includes Castle Fincharn main block (CS1), Aros Castle north-west block (CS2), Castle Roy enclosure and tower (CS3), Lochindorb Castle primary enclosure (CS4), Achanduin castle enclosure and hall (CS5), and Lismore Cathedral nave (CS6). The MERLF assemblages associated with the first five of these studies are dominated by charcoal fragments which displayed no surviving terminal ring, bark, or sapwood boundary evidence, and each has been published elsewhere in some detail. Full details of CS6 await publication but is included here since the MERLF assemblage included a *Corylus* sp. fragment with some terminal ring evidence. The distributions of each of these radiocarbon datasets was investigated using the Ward and Wilson (1978) chi-square type test [50], and an age range was calculated using the Difference function to compare the earliest and latest dates available [51]. The data from each site were then included in a series of single-phase Bayesian models. Run at 1 year resolution and 20,000 Iterations, these

include: a Combine model; an exponential prior/no outlier model; an exponential prior/modified Charcoal Outlier Model; an exponential prior/default Charcoal Outlier Model; and a uniform prior/default Charcoal Outlier Model. The modified Charcoal Outlier Model IA time-constants specified in CS1-6 have been estimated from published data regarding tree mean lifespan and wood post-mortem resilience data (Table 1). Mean lifespans are rarely reported so working values have been calculated at 33% of reported maximum lifespans, in line with allometric data, added to which an estimate of post-mortem resilience has been derived from the resistance to wood-destroying fungi according to the (1–5) durability scale applied by British and European Standards [54] and other published reports (Table 1). Where the datasets returned by mixed-taxa assemblages are statistically consistent at 5% significance (CS5) then these are tagged to a single Charcoal Outlier Model with a time-constant modified to reflect the lowest $IA\tau$ samples, and where these datasets are not statistically consistent at 5% significance (CS2 and CS6) then the highest $IA\tau$ data is used. A Last distribution has been generated in all case study models, and the Last and End Boundary distributions compared with various potential *TPQ* and *TAQ* dates (from other types of historical, archaeological or architectural evidence) using the Order function [51]. All models associated with these case studies are presented in Additional file 3. In the interest of brevity, presentation of wider evidence relating to these buildings is kept to a minimum, and readers are encouraged to follow the cited references for more detailed information.

Calibrated date ranges in each theoretical and case study radiocarbon dataset are expressed as cal AD or cal BC at 95% and 68% confidence using upright text and have been rounded out to 10 years [12].⁵ Modelled age range, End Boundary, and Last distributions are reported as Highest Posterior Density (HPD) interval date ranges at both 68% and 95% probability with median values, and these estimates have been rounded out to 5 years and are presented in italics. Generated date ranges in both theoretical studies are regarded as accurate when they include the true event date from which each simulated dataset was generated (i.e. 1250 cal AD). The agreement indices returned by each model are considered [51, 55], but individual measurements which fall below the accepted 60% threshold of compatibility have not been removed from theoretical models since to do so would bias results [56].

⁵ See [12] pp. 42 and 49.

Table 1 Ecological data from UK and Scotland relating to tree taxa from case studies

Maximum lifespan	Taxa	Habit	Life cycle	Post-mortem resilience	Working IA τ	References
50 Years	<i>Corylus avellana</i>	Shrub	'self-coppicing' cycles of ≤ 30 –50 year old stems in UK. ≤ 12 –15 year old stems on some thin Scottish Atlantic soils	Not included in BSI standards	20 years	[30, 33]
100 Years	<i>Betula pubescens</i>	Shrub/Small Tree	Matures 50–60 with lifespan ≤ 100 years in UK. 'Shortest-lived common tree [in UK] after Aspen.'	5—Not Durable. Dies rapidly and rots quickly. Life expectancy in ground contact 'less than 5 years'	50 years	[30–32, 54, 57–59]
200 Years	<i>Betula pendula</i>	Tree	≤ 100 years in UK generally ≤ 180 years in Central Scotland	5—Not Durable. As per <i>Betula pubescens</i>	100 years	[30, 31, 54, 58, 60]
600 Years	<i>Pinus sylvestris</i>	Tree	Generally aged ≤ 300 years. Lifespan ≤ 550 years in NW Scotland	3–4 moderate-slightly durable	300 years	[54, 61, 62]
	<i>Quercus robur</i> and <i>petraea</i>	Tree	General ages ≤ 300 years in UK woodlands. Scottish medieval timber ≤ 418 years Darnaway (NE Scotland)	2—Durable. Sapwood ≤ 20 years, heartwood over 50 years	300 years	[30, 54, 63–65] ^a

^a See [41] p. 130

Results (theoretical studies)

Theoretical Study 1 (TS1)

The twenty simulated datasets generated in TS1 are all exponentially distributed (e.g. Figure 3). There is relatively little variation between the latest simulated date in each dataset, and all include the 1250 AD true event at 95% confidence (Table 2). Increased dataset IA τ is associated with some decrease in latest date age, however, and with a decrease in the number of dates containing the true event at 95% confidence (from all 20 dates in 10 years IA τ dataset M1a run 1, to only a single date in 500 years IA τ dataset M1e run 4). An average of 19 simulated dates include the true event in 10 year IA τ datasets, 13 in 50 year IA τ datasets, 11.5 in 100 year IA τ datasets, 5 in 200 year IA τ datasets (M1d), and 2.5 in 500 year IA τ datasets.

Age range variation in the TS1 datasets is mostly predicated on variation in the earliest simulated dates within each dataset (Table 2). Increased IA τ is generally associated with an increase in earliest date age, an increase in date range, and an increase in date range variation. The earliest calibrated dates in all the datasets specified with 10 years IA τ are situated in the second millennium AD and age range variation in this group is limited to between -35 – 225 years (M1a run 1) and 20 – 250 years (M1a run 2). This 10 years IA τ group includes the only dataset in TS1 which falls into minus values, and this is the same dataset in which all simulated dates include the 1250 AD true event. In contrast, all earliest dates in the datasets specified with 500 years IA τ are situated in the

cal BC period, with age range variation between 1315 – 1640 years (M1e run 3) and 3205 – 3465 years (M1e run 1). Dataset age ranges in these two lowest and highest IA τ groups are distinctive, and the datasets throughout the study are generally consistent with this trend, but there is considerable overlap between individual datasets in adjacent 50, 100 and 200 years IA τ groups.

All dataset mean lifespans are earlier than the 1250 AD true event date in TS1 and these values also generally increase in age and variation with increased IA τ specification (Table 2). The mean lifespans of the datasets specified with 10 years IA τ are narrowly distributed between 1224 and 1242 cal AD, whilst the datasets specified with 500 years IA τ present mean lifespans situated in the first millennium AD between 491 and 780 cal AD. The average lifespans within each group are all consistent with this trend and close to expected values—1229 cal AD (10 years IA τ specified), 1183 cal AD (50 years IA τ specified), 1156 cal AD (100 years IA τ specified), 1039 cal AD (200 years IA τ specified), and 670 cal AD (500 years IA τ specified)—although there is some overlap in the lifespans of individual datasets in adjacent groups specified to 50, 100 and 200 years IA τ .

There is a clear relationship between the IA τ specified, the distribution of simulated dates, and the date range of each dataset generated in TS1. All four datasets in the 10 years IA τ group (M1a runs 1–4) pass the Ward and Wilson (1978) chi-square type test and have generated accurate Combined dates, although three of these models contain four individual dates with low agreement indices

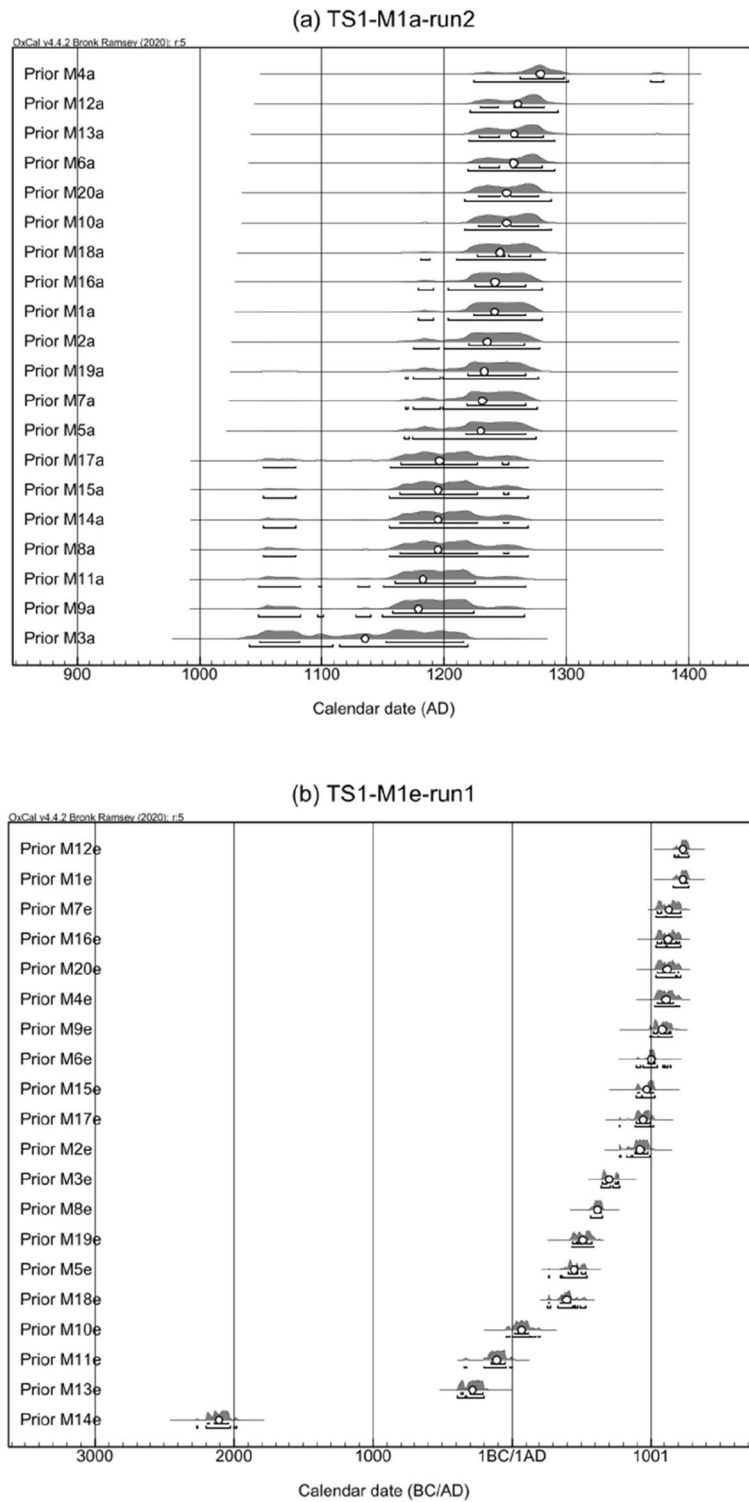


Fig. 3 Selected multiple plots from TS1, illustrating exponentially distributed simulated datasets with specified IAt of 10 years and 500 years. Subfigure **a** presents distribution plots from a dataset specified with 10 years IAt (M1a run 2) with simulated dates ranging from 1040–1220 cal AD (M3a) to 1220–1380 cal AD (M4a) at 95% confidence, nineteen of which include the true event date of 1250 AD at 95% confidence. Subfigure **b** presents distribution plots from a dataset specified with 500 years IAt (M1e run 1), with simulated dates ranging from 2270 to 1980 cal BC (M14e) to 1160–1280 cal AD (M12e) at 95% confidence, two of which include the 1250 AD true event date at 95% confidence. Small circles represent the mean average of each distribution

Table 2 Selected features of the datasets from TS1. Age range values have been rounded out to 5 years

Specified dataset IA τ and code	Run	Earliest simulated date (95% confidence)	Latest simulated date (95% confidence)	Accurate dates	Dataset range (95% probability)	Mean lifespan
10 years IA τ M1a	1	1050–1280 cal AD (M9a)	1220–1380 cal AD (M4a)	20	– 35–225 years	1242 cal AD
	2	1040–1220 cal AD (M3a)	1220–1380 cal AD (M4a)	19	20–250 years	1224 cal AD
	3	1040–1230 cal AD (M12a)	1220–1300 (M15a)	18	15–235 years	1225 cal AD
	4	1040–1230 cal AD (M14a)	1210–1290 cal AD (M16a)	19	10–230 years	1224 cal AD
Mean Average 10 years IA τ				19	5–235 years	1229 cal AD
50 years IA τ M1b	1	990–1160 cal AD (M9b)	1220–1300 cal AD (M14b)	11	85–290 years	1180 cal AD
	2	970–1160 cal AD (M14b)	1220–1390 cal AD (M15b)	13	120–385 years	1181 cal AD
	3	1020–1210 cal AD (M11b)	1220–1300 cal AD (M9b)	16	55–250 years	1193 cal AD
	4	890–1120 cal AD (M14b)	1210–1290 cal AD (M13b)	13	160–380 years	1177 cal AD
Mean Average 50 years IA τ				13	105–325 years	1183 cal AD
100 years IA τ M1c	1	990–1160 cal AD (M4c)	1220–1380 cal AD (M16c)	16	80–280 years	1199 cal AD
	2	680–950 cal AD (M4c)	1210–1290 cal AD (M9c)	9	310–570 years	1145 cal AD
	3	410–570 cal AD (M3c)	1180–1290 cal AD (M18c)	10	670–845 years	1127 cal AD
	4	770–980 cal AD (M17c)	1210–1290 cal AD (M3c)	11	260–500 years	1151 cal AD
Mean average 100 years IA τ				11.5	330–550 years	1156 cal AD
200 years IA τ M1d	1	400–560 cal AD (M3d)	1210–1290 cal AD (M18d)	6	680–865 years	982 cal AD
	2	670–880 cal AD (M2d)	1160–1280 cal AD (M7d)	4	315–575 years	1062 cal AD
	3	560–660 cal AD (M6d)	1180–1290 cal AD (M12d)	5	570–710 years	1025 cal AD
	4	680–950 cal AD (M5d)	1170–1290 cal AD (M18d)	5	300–560 years	1086 cal AD
Mean Average 200 years IA τ				5	465–680 years	1039 cal AD
500 years IA τ M1e	1	2270–1980 cal BC (M14e)	1160–1280 cal AD (M12e)	2	3205–3465 years	606 cal AD
	2	1270–1010 cal BC (M10e)	1160–1280 cal AD (M11e)	4	2245–2520 years	762 cal AD
	3	360–40 cal BC (M14e)	1220–1390 cal AD (M5e)	3	1315–1640 years	780 cal AD
	4	1950–1740 cal BC (M1e)	1150–1280 cal AD (M10e)	1	2920–3190 years	491 cal AD
Mean Average 500 years IA τ				2.5	2420–2705 years	670 cal AD

($A_i \leq 60\%$) and present low overall Combined Agreement Indices (A_{comb}) (Table 3). The exception is the 10 years IA τ dataset in which all 20 simulated dates include the true event date (M1a run 1), which has a mean lifespan of 1242 cal AD (the highest in the study and very close to the 1250 AD true event) and has only returned one low A_i . All sixteen simulated datasets specified with 50, 100, 200 and 500 years IA τ fail the Ward and Wilson (1978) test. The four datasets specified to 50 years IA τ (M1b runs 1–4) and one specified to 100 years IA τ (M1c run 1) have generated Combined date ranges, although these are all too early. The three remaining models associated with datasets specified to 100 years IA τ (M1c runs 2–4) and all models specified with 200 and 500 years IA τ datasets have failed to generate a Combined distribution at all.

Out-with the Combine models, all TS1 models except one present overall agreement indices which are above the 60% threshold (Table 4). The exception is associated with a uniform prior/no outlier modelling approach to a 50-year IA τ dataset (M1b, run 4), which presents an Overall Agreement Index of 58.9%. The number of

individual dates with low Agreement Indices decreases with increasing IA τ , and with models employing an exponential prior specification. All three uniform prior approaches generate higher numbers of individual low Agreement Index distributions than their exponential counterparts from 10 and 50 years IA τ datasets. The uniform prior/no outlier approach contains the most low Agreement Index distributions in TS1, with a maximum of three presented from a 10 year IA τ dataset (M1a run 3). Individual low Agreement Indices are limited to a single dates in all exponential prior modelling approaches (Table 4).

98% of all TS1 models (118/120) have generated End Boundary HPD intervals which are accurate at 95% probability, and 85% (102/120) are also accurate at 68% probability (Table 5). Consistency of End Boundary accuracy at 68% probability is inversely proportional to dataset IA τ ; decreasing from 96% of models associated with datasets specified with 10 years IA τ to 58% of models associated with datasets specified with 500 years IA τ . Consistency of End Boundary accuracy also varies with model specification and a broad correlation with prior distribution

Table 3 Combine distributions and agreement indices in TS1

Dataset		Combine date ranges/cal AD				Agreement indices		
Specified IAT and code	Run	68%	95%	median	mean	χ^2 test	Acomb	Ai \leq 60%
10 years IAT; M1a	1	1230–1270	1225–1270	1245	1250	Pass	112	1
	2	1220–1260	1220–1265	1245	1240	Pass	23.3	4
	3	1220–1260	1220–1265	1245	1240	Pass	26.9	4
	4	1220–1260	1220–1265	1245	1240	Pass	36.7	4
50 years IAT; M1b	1	1175–1220	1175–1220	1190	1195	Fail	0.2	10
	2	1175–1220	1175–1220	1190	1195	Fail	0.4	9
	3	1210–1225	1175–1225	1215	1210	Fail	10.5	7
	4	1175–1220	1175–1220	1190	1195	Fail	0.4	9
100 years IAT; M1c	1	1215–1225	1180–1225	1220	1220	Fail	2.3	8
	2	No range	No range	-	-	Fail	-	-
	3	No range	No range	-	-	Fail	-	-
	4	No range	No range	-	-	Fail	-	-
200 years IAT; M1d	1	No range	No range	-	-	Fail	-	-
	2	No range	No range	-	-	Fail	-	-
	3	No range	No range	-	-	Fail	-	-
	4	No range	No range	-	-	Fail	-	-
500 years IAT; M1e	1	No range	No range	-	-	Fail	-	-
	2	No range	No range	-	-	Fail	-	-
	3	No range	No range	-	-	Fail	-	-
	4	No range	No range	-	-	Fail	-	-

Date ranges and median dates are rounded out to 5 years. Inaccurate date ranges (not including the 1250 AD true event) are reported in bold emphasis

is evident; with 85–90% of models with exponential priors generating accurate End Boundary estimates at 68% probability, reducing to 70–85% of models with uniform prior distributions. Overall, the uniform prior/default Charcoal Outlier Model approach has generated the least consistently accurate estimates, with 70% (14/20) of all End Boundary HPD intervals associated with this specification including the true event date at 68% probability; ranging from 75% (3/4) of datasets specified to 10 years IAT, to 50% (2/4) of datasets specified to 100 years and 500 years IAT. The two End Boundary estimates in this study which are inaccurate at 95% probability are also associated with the same 500 years IAT dataset (M1e run 3) and with uniform prior/Charcoal Outlier Model approaches. The exponential prior/Charcoal Outlier Model approaches have generated the most consistently accurate End Boundary distributions in TS1; with this specification generating accurate End Boundaries at 68% probability from 90% of all datasets, and accurate End Boundaries at 95% probability from all datasets (100%). Notably, all models employing an exponential prior have generated accurate End Boundary HPD intervals at both 95% and 68% probability from all datasets specified with 10, 50 and 100 years IAT (Table 5).

Inaccurate End Boundary distributions at 68% probability in TS1 can be either earlier or later than the true

event (Table 4). All inaccurate estimates generated by uniform prior models are late, including both of those which are inaccurate at 95% probability, whilst exponential prior models have generated End Boundary HPD intervals which are both too early and too late at 68% probability. The exponential prior/no outlier modelling approach to 50 years IAT and 200 years IAT datasets are the only two modelling-dataset combinations in TS1 which have generated End Boundary average medians that are earlier than the true event date of 1250 AD.

All Last HPD intervals generated in TS1 are accurate at 95% probability (Table 6), although this would not have been the case had Last distributions been generated in runs 1 and 2. Last HPD interval accuracy at 68% probability is inversely proportional to the specified dataset IAT; and falls sharply from 100% accuracy in models associated with 10 years and 50 years IAT datasets, to 58% accuracy in those generated from datasets specified to 500 years IAT. Most model specifications have generated accurate Last HPD intervals at 68% probability from 90% of all datasets. This is reduced to 80% for the uniform prior/default Charcoal Outlier Model approach, although this difference relates to one extra inaccurate date only.

End Boundary precision in TS1 is inversely proportional to specified dataset IAT for all modelling approaches (Table 7). Overall, End Boundary median

Table 4 Last and End Boundary HPD intervals in TS1

Dataset and model specification		Last HPD intervals and medians/ cal AD			End Boundary HPD intervals and medians/cal AD			Agreement Indices		
10yrs IAT (M1a)	Run	68%	95%	Median	68%	95%	Median	Amodel	Aoverall	Ai ≤ 60%
Exponential prior; No Outlier Model	1	-	-	-	1235–1275	1230–1280	1265	127.1	124	0
	2	-	-	-	1240–1275	1225–1280	1255	80.2	69	1
	3	1240–1270	1225–1275	1255	1240–1270	1225–1280	1255	100.9	91.5	0
	4	1240–1270	1225–1275	1255	1240–1270	1225–1275	1255	107.8	97.6	0
Exponential prior; 10-year Charcoal	1	-	-	-	1240–1280	1235–1285	1265	130.6	126.8	0
	2	-	-	-	1245–1275	1230–1285	1260	81.3	71.7	1
	3	1245–1275	1230–1280	1260	1245–1275	1230–1280	1260	101.8	94.1	0
	4	1240–1270	1230–1280	1255	1240–1275	1230–1280	1255	108.3	99.9	0
Exponential prior; Default Charcoal	1	-	-	-	1240–1280	1235–1285	1270	132.1	128.1	0
	2	-	-	-	1245–1280	1230–1285	1260	84.7	75.6	1
	3	1245–1275	1230–1285	1260	1245–1275	1230–1285	1260	104.7	98.2	0
	4	1245–1275	1230–1280	1260	1245–1275	1230–1285	1260	111.2	104.3	0
Uniform prior; No Outlier Model	1	-	-	-	1235–1280	1230–1285	1265	129.9	125.2	0
	2	-	-	-	1240–1280	1225–1285	1260	86.4	61.8	2
	3	1240–1275	1225–1280	1255	1240–1275	1225–1285	1260	94	72.7	3
	4	1240–1270	1225–1280	1255	1240–1275	1225–1280	1255	97.8	78	2
Uniform prior; 10-year Charcoal	1	-	-	-	1240–1285	1235–1290	1270	131.1	126.4	0
	2	-	-	-	1245–1280	1230–1290	1260	87.1	67.9	2
	3	1240–1275	1230–1285	1260	1240–1275	1230–1285	1260	91.3	76	2
	4	1240–1275	1225–1280	1255	1240–1275	1225–1285	1260	97.3	83	2
Uniform prior; Default Charcoal	1	-	-	-	1255–1285	1235–1290	1270	134	129.1	0
	2	-	-	-	1245–1285	1230–1295	1265	90.8	75.4	1
	3	1245–1280	1230–1290	1265	1245–1280	1230–1295	1265	100.1	89.2	0
	4	1245–1275	1230–1285	1260	1245–1280	1230–1290	1260	105.8	95.3	0
50yrs IAT (M1b)	Run	68%	95%	Median	68%	95%	Median	Amodel	Aoverall	Ai ≤ 60%
Exponential prior; No Outlier Model	1	-	-	-	1240–1275	1230–1285	1255	92.5	91	0
	2	-	-	-	1230–1265	1225–1285	1250	73.6	73.7	1
	3	1220–1250	1220–1270	1240	1220–1255	1220–1275	1240	94.5	91.2	0
	4	1235–1265	1225–1275	1250	1235–1270	1225–1280	1250	115.2	114.3	0
Exponential prior; 50-year Charcoal	1	-	-	-	1245–1285	1235–1300	1265	92.9	91.2	0
	2	-	-	-	1235–1275	1230–1295	1260	78.5	78	1
	3	1225–1260	1220–1280	1245	1225–1260	1220–1280	1245	96	93.8	0
	4	1240–1270	1230–1285	1255	1240–1275	1230–1290	1260	113.8	112.9	0
Exponential prior; Default Charcoal	1	-	-	-	1245–1285	1235–1300	1265	93.2	91.7	0
	2	-	-	-	1240–1280	1230–1300	1260	80.2	79.8	1
	3	1225–1260	1220–1280	1245	1225–1265	1220–1280	1250	96.5	94.5	0
	4	1240–1275	1230–1290	1260	1240–1280	1230–1290	1260	114.2	113.5	0
Uniform prior; No Outlier Model	1	-	-	-	1255–1290	1235–1305	1270	89.7	88.5	0
	2	-	-	-	1245–1290	1230–1305	1270	76.5	75.2	2
	3	1225–1260	1220–1275	1245	1225–1265	1220–1285	1250	83.6	79.2	2
	4	1240–1270	1230–1280	1255	1240–1275	1230–1290	1260	57.7	58.9	1
Uniform prior; 50-year Charcoal	1	-	-	-	1255–1295	1235–1315	1275	89.1	87.8	0
	2	-	-	-	1250–1300	1235–1320	1275	81.6	80.6	2
	3	1230–1270	1220–1285	1250	1230–1270	1220–1290	1255	88.8	85.5	2
	4	1245–1280	1230–1295	1265	1245–1285	1230–1305	1265	93	92.1	1
Uniform prior; Default Charcoal	1	-	-	-	1255–1295	1240–1320	1280	90.6	89.4	0

Table 4 (continued)

50yrs IAτ (M1b)										
	Run	68%	95%	Median	68%	95%	Median	Amodel	Aoverall	Ai ≤ 60%
	2	-	-	-	1250–1300	1235–1320	1280	84.3	83.6	2
	3	1230–1270	1220–1285	1250	1230–1270	1225–1290	1255	88.6	85.5	2
	4	1245–1285	1230–1305	1265	1250–1290	1235–1315	1270	102.2	101.5	1
100yrs IAτ (M1c)										
	Run	68%	95%	Median	68%	95%	Median	Amodel	Aoverall	Ai ≤ 60%
Exponential prior; No Outlier Model	1	-	-	-	1240–1275	1230–1280	1255	99.1	98	0
	2	-	-	-	1235–1270	1225–1285	1255	108.8	108.5	0
	3	1240–1270	1225–1275	1255	1245–1275	1225–1290	1260	107.6	107.4	0
	4	1230–1265	1220–1275	1245	1235–1270	1225–1280	1250	98.2	97	0
Exponential prior; 100-year Charcoal	1	-	-	-	1245–1280	1230–1295	1265	101.1	99.7	0
	2	-	-	-	1240–1280	1230–1300	1260	108.9	108.4	0
	3	1245–1275	1225–1295	1260	1245–1285	1230–1305	1265	106.7	106.6	0
	4	1235–1275	1225–1290	1260	1240–1280	1225–1300	1260	97.6	96.4	0
Exponential prior; Default Charcoal	1	-	-	-	1245–1280	1235–1290	1265	100.9	99.8	0
	2	-	-	-	1245–1280	1230–1300	1265	108.9	108.8	0
	3	1245–1275	1225–1295	1260	1245–1285	1230–1305	1265	106.8	106.6	0
	4	1240–1275	1225–1295	1260	1240–1280	1225–1300	1265	97.7	96.7	0
Uniform prior; No Outlier Model	1	-	-	-	1240–1285	1225–1295	1260	82.6	70.4	2
	2	-	-	-	1250–1290	1235–1320	1275	69.3	70	1
	3	1250–1275	1240–1280	1265	1255–1315	1240–1385	1285	94.8	94.8	0
	4	1245–1275	1230–1280	1260	1250–1290	1230–1315	1270	85.2	85	1
Uniform prior; 100-year Charcoal	1	-	-	-	1250–1290	1235–1310	1270	96.5	92.9	0
	2	-	-	-	1245–1295	1230–1330	1275	107.9	107.2	0
	3	1250–1290	1235–1320	1270	1250–1295	1230–1325	1275	104.3	103.8	0
	4	1245–1290	1230–1320	1270	1250–1300	1230–1335	1275	93.3	92.3	0
Uniform prior; Default Charcoal	1	-	-	-	1250–1290	1235–1310	1270	96.3	92.5	0
	2	-	-	-	1250–1300	1235–1335	1280	108.1	107.8	0
	3	1255–1305	1240–1345	1285	1255–1310	1240–1350	1285	105	104.8	0
	4	1250–1300	1230–1330	1280	1255–1310	1235–1345	1285	95	94.1	0
200yrs IAτ (M1d)										
	Run	68%	95%	Median	68%	95%	Median	Amodel	Aoverall	Ai ≤ 60%
Exponential prior; no Outlier Model	1	-	-	-	1220–1270	1190–1300	1245	96.5	96.7	0
	2	-	-	-	1175–1220	1155–1250	1200	97.8	95.6	0
	3	1220–1260	1200–1275	1235	1225–1270	1200–1300	1250	98.3	97.3	0
	4	1185–1230	1170–1250	1210	1190–1235	1175–1260	1215	83.9	84.3	1
Exponential prior; 200-year Charcoal	1	-	-	-	1225–1285	1195–1330	1255	97.5	97	0
	2	-	-	-	1180–1240	1160–1285	1210	97.9	95.7	0
	3	1225–1275	1200–1320	1255	1230–1290	1210–1335	1265	98.9	98.3	0
	4	1200–1260	1180–1280	1225	1200–1260	1185–1285	1235	89.8	89.8	1
Exponential prior; default Charcoal	1	-	-	-	1230–1295	1200–1340	1265	97.5	97.6	0
	2	-	-	-	1185–1240	1165–1285	1215	98.2	96.3	0
	3	1225–1270	1210–1300	1250	1230–1285	1215–1320	1260	99.2	98.8	0
	4	1195–1255	1180–1285	1230	1200–1260	1180–1290	1235	90	90.1	1
Uniform prior; No Outlier Model	1	-	-	-	1230–1300	1205–1370	1270	97.9	98.1	0
	2	-	-	-	1190–1250	1170–1290	1225	91.6	90.3	0
	3	1230–1270	1215–1280	1250	1235–1300	1215–1365	1270	102.3	102	0
	4	1205–1255	1180–1270	1225	1210–1270	1180–1300	1240	76.4	76	1
Uniform prior; 200-year Charcoal	1	-	-	-	1245–1350	1220–1450	1305	97.4	97.3	0
	2	-	-	-	1190–1265	1170–1315	1235	95.8	94.5	0
	3	1235–1300	1215–1375	1270	1245–1335	1225–1420	1295	100	99.6	0

Table 4 (continued)

200yrs IAτ (M1d)	Run	68%	95%	Median	68%	95%	Median Amodel	Aoverall	Ai ≤ 60%	
Uniform prior; default Charcoal	4	1220–1280	1190–1320	1250	1225–1295	1195–1345	1265	91.7	92.1	0
	1	-	-	-	1250–1355	1225–1425	1305	98.3	98.3	0
	2	-	-	-	1205–1275	1175–1335	1240	92.4	91.4	0
500yrs IAτ (M1e)	Run	68%	95%	Median	68%	95%	Median Amodel	Aoverall	Ai ≤ 60%	
exponential prior; no Outlier Model	1	-	-	-	1225–1300	1190–1370	1265	98	97.4	0
	2	-	-	-	1225–1290	1195–1345	1260	99.2	98.8	0
	3	1230–1295	1225–1300	1270	1255–1325	1225–1375	1290	97.4	97.2	0
	4	1160–1230	1120–1265	1190	1170–1275	1120–1355	1225	95.4	95.9	0
Exponential prior; 500-year Charcoal	1	-	-	-	1235–1325	1200–1405	1285	98.4	97.9	0
	2	-	-	-	1230–1310	1205–1375	1275	99	98.7	0
	3	1255–1335	1225–1405	1295	1270–1365	1235–1440	1320	98.8	98.7	0
	4	1165–1255	1110–1350	1210	1180–1300	1135–1420	1250	96.6	97.2	0
Exponential prior; default Charcoal	1	-	-	-	1235–1325	1200–1400	1280	98.1	97.8	0
	2	-	-	-	1230–1315	1205–1395	1280	99	98.7	0
	3	1245–1335	1225–1415	1295	1270–1365	1235–1450	1320	98.6	98.6	0
	4	1165–1260	1115–1345	1215	1180–1305	1140–1420	1250	96.6	97.1	0
Uniform prior; No Outlier Model	1	-	-	-	1230–1430	1205–1740	1345	99.2	99.1	0
	2	-	-	-	1235–1380	1205–1605	1315	96.9	96.8	0
	3	1260–1295	1225–1305	1275	1265–1370	1230–1500	1320	98	98.1	0
	4	1170–1255	1150–1275	1210	1185–1385	1150–1665	1300	98.8	99	0
Uniform prior; 500-year Charcoal	1	-	-	-	1260–1585	1220–1870	1450	99.6	99.5	0
	2	-	-	-	1270–1460	1240–1685	1375	98.1	98	0
	3	1270–1405	1235–1535	1350	1300–1455	1265–1605	1390	99.6	99.7	0
	4	1170–1285	1145–1490	1245	1215–1495	1170–1795	1375	99.8	99.8	0
Uniform prior; default Charcoal	1	-	-	-	1245–1470	1215–1790	1375	99.4	99.4	0
	2	-	-	-	1265–1485	1230–1685	1405	97.5	97.6	0
	3	1270–1410	1235–1535	1350	1295–1460	1265–1605	1395	99.5	99.5	0
	4	1165–1350	1140–1625	1260	1220–1540	1175–1905	1405	99.6	99.8	0

HPD intervals and median dates are rounded out to 5 years. Inaccurate HPD intervals (not including the 1250 AD true event date) and agreement indices less than 60% are reported in bold emphasis

Table 5 Accuracy of End Boundary HPD intervals in TS1 (summarised from Table 4)

Specified dataset IAτ	Accuracy of End Boundary HPD intervals							All models	
	Exp. prior; no Outlier	Exp. prior; modified Charcoal	Exp. prior; default Charcoal	Uniform prior; no Outlier	Uniform prior; modified Charcoal	Uniform prior; default Charcoal	68%	95%	
	68% (95%)	68% (95%)	68% (95%)	68% (95%)	68% (95%)	68% (95%)	68%	95%	
10 years	4/4 (4/4)	4/4 (4/4)	4/4 (4/4)	4/4 (4/4)	4/4 (4/4)	3/4 (4/4)	96%	100%	
50 years	4/4 (4/4)	4/4 (4/4)	4/4 (4/4)	3/4 (4/4)	3/4 (4/4)	3/4 (4/4)	88%	100%	
100 years	4/4 (4/4)	4/4 (4/4)	4/4 (4/4)	3/4 (4/4)	4/4 (4/4)	2/4 (4/4)	88%	100%	
200 years	2/4 (4/4)	3/4 (4/4)	3/4 (4/4)	4/4 (4/4)	4/4 (4/4)	4/4 (4/4)	83%	100%	
500 years	3/4 (4/4)	3/4 (4/4)	3/4 (4/4)	3/4 (4/4)	1/4 (3/4)	2/4 (3/4)	58%	92%	
All Datasets	85% (100%)	90% (100%)	90% (100%)	85% (100%)	80% (95%)	70% (95%)	85%	98%	

age is also inversely proportional to dataset IAτ across the study, although that trend is much clearer in models with uniform priors (Table 8). End Boundary precision

and median age also vary with model specification; such that the imposition of an exponential prior distribution generally increases relative End Boundary precision and

Table 6 Accuracy of Last HPD intervals in TS1 (summarised from Table 4)

Specified dataset IAT	Accuracy of Last HPD intervals								
	Exp. prior; no Outlier	Exp. prior; modified Charcoal	Exp. prior; default Charcoal	Uniform prior; no Outlier	Uniform prior; modified Charcoal	Uniform prior; default Charcoal	All models		
	68% (95%)	68% (95%)	68% (95%)	68% (95%)	68% (95%)	68% (95%)	68%	95%	
10 years	2/2 (2/2)	2/2 (2/2)	2/2 (2/2)	2/2 (2/2)	2/2 (2/2)	2/2 (2/2)	100%	100%	
50 years	2/2 (2/2)	2/2 (2/2)	2/2 (2/2)	2/2 (2/2)	2/2 (2/2)	2/2 (2/2)	100%	100%	
100 years	2/2 (2/2)	2/2 (2/2)	2/2 (2/2)	2/2 (2/2)	2/2 (2/2)	1/2 (2/2)	92%	100%	
200 years	1/2 (2/2)	2/2 (2/2)	2/2 (2/2)	2/2 (2/2)	2/2 (2/2)	2/2 (2/2)	92%	100%	
500 years	2/2 (2/2)	1/2 (2/2)	1/2 (2/2)	1/2 (2/2)	1/2 (2/2)	1/2 (2/2)	58%	100%	
All Datasets	90% (100%)	90% (100%)	90% (100%)	90% (100%)	90% (100%)	80% (100%)	88%	100%	

Table 7 Precision of End Boundary HPD intervals in TS1 (summarised from Table 4)

Specified dataset IAT	Average precision of End Boundary HPD intervals/years					
	Exp. prior; no Outlier Model	Exp. prior; modified Charcoal	Exp. prior; default Charcoal	Uniform prior; no Outlier	Uniform prior; mod. Charcoal	Uniform prior; def. Charcoal
	68% (95%)	68% (95%)	68% (95%)	68% (95%)	68% (95%)	68% (95%)
10 years	34 (53)	34 (53)	34 (51)	39 (58)	38 (63)	35 (65)
50 years	35 (56)	38 (63)	40 (64)	39 (68)	43 (78)	43 (78)
100 years	34 (58)	39 (71)	38 (69)	46 (96)	46 (94)	50 (99)
200 years	46 (96)	58 (120)	58 (116)	66 (153)	86 (154)	89 (178)
500 years	79 (179)	96 (216)	99 (221)	163 (430)	238 (515)	233 (525)

Table 8 Average End Boundary median values in TS1 (summarised from Table 4)

Specified dataset IAT	Average median of End Boundary HPD intervals/cal AD					
	Exp. prior; no Outlier Model	Exp. prior; modified Charcoal	Exp. prior; default Charcoal	Uniform prior; no Outlier	Uniform prior; modified Charcoal	Uniform prior; default Charcoal
10 years	1258	1260	1263	1260	1258	1263
50 years	1249	1258	1259	1263	1268	1271
100 years	1255	1263	1265	1273	1274	1280
200 years	1241	1258	1256	1266	1290	1290
500 years	1260	1283	1283	1320	1398	1395

median age (whether or not a Charcoal Outlier Model is also used), whilst the introduction of a Charcoal Outlier Model generally decreases relative End Boundary precision and median age (whatever prior distribution is employed) (Tables 7 and 8). Decreasing the Charcoal Outlier Model time-constant has generally increased End Boundary median age in lower IAT TS1 datasets (whatever the priors) and slightly increased End Boundary

precision in models associated with uniform priors (Tables 7 and 8). These effects are cumulative; such that variation in model specification has a much more significant on End Boundary precision and median age when associated with higher IAT datasets.

Last HPD interval precision in TS1 is also inversely proportional to dataset IAT for all modelling approaches (Table 9). Last precision also varies according to model

Table 9 Precision of Last HPD intervals in TS1 (summarised from Table 4)

Specified dataset IA τ	Average precision of Last HPD intervals/years					
	Exp. prior; no Outlier Model	Exp. prior; modified Charcoal	Exp. prior; default Charcoal	Uniform prior; no Outlier	Uniform prior; mod. Charcoal	Uniform prior; default Charcoal
	68% (95%)	68% (95%)	68% (95%)	68% (95%)	68% (95%)	68% (95%)
10 years	30 (50)	30 (50)	30 (53)	33 (55)	35 (55)	33 (58)
50 years	30 (50)	33 (58)	35 (60)	33 (58)	38 (65)	40 (70)
100 years	33 (53)	35 (68)	33 (70)	28 (45)	43 (88)	50 (103)
200 years	43 (78)	55 (110)	53 (98)	45 (78)	63 (145)	58 (110)
500 years	68 (110)	80 (210)	93 (210)	60 (103)	125 (323)	163 (393)

Table 10 Average Last median values in TS1 (summarised from Table 4)

Specified dataset IA τ	Average medians of Last HPD intervals/cal AD					
	Exp. prior; no Outlier Model	Exp. prior; modified Charcoal	Exp. prior; default Charcoal	Uniform prior; no Outlier	Uniform prior; modified Charcoal	Uniform prior; default Charcoal
10 years	1255	1258	1260	1255	1258	1263
50 years	1245	1250	1253	1250	1258	1258
100 years	1250	1260	1260	1263	1270	1283
200 years	1223	1240	1240	1238	1260	1258
500 years	1230	1253	1245	1243	1298	1305

specification: decreasing on association with a Charcoal Outlier Model (whichever prior distribution is used) and increasing on association with exponential priors and lower IA τ datasets. In general, these two factors have a cumulative effect, although the Last distributions generated by the uniform prior/no outlier model approach display a lower decrease in precision with increased dataset IA τ than other modelling approaches and are thereby associated much greater comparative precision at higher datasets IA τ s. Modifying outlier model time-constant has no clear effect on Last precision and there is no clear relationship between Last median ages and dataset IA τ . Importantly, all model-dataset combinations in TS1 have generated Last distributions which are more precise and have earlier median values than their corresponding End Boundaries, and this contrast is also more significant with increasing dataset IA τ (Tables 7, 8, 9 and 10). 37% (11/30) of the model-dataset combinations in TS1 have returned Last distributions with average medians of 1250 AD or earlier (Table 10).

Theoretical Study 2 (TS2)

Most TS2 datasets present convincingly exponential distributions, and 91% (41/45) contain at least one simulated date which includes the true event (Table 11). Increased

IA τ specification in this study has generally resulted in datasets with earlier latest dates, a decreased number of dates which include the true event, increased age ranges, increased age range variation, earlier earliest dates, and earlier mean lifespans. No latest dates in TS2 are later than the true event at 95% probability. Decreased dataset size has also resulted in earlier latest dates, however, and at very high IA τ this can result in no true dates at all. There is no clear correlation between dataset size and percentage of true dates or mean lifespans for a given IA τ across the study, but earliest dates tend to decrease in age with decreased dataset size and thereby age range and age variation also decrease (since this is mostly driven by the early dates) (Fig. 4a–c).

The inverse correlation between dataset IA τ and the age of the latest date is exaggerated by dataset size. There is a strong correlation in TS2 between the specified IA τ and the number of accurate dates in each dataset, with 94–98% of all determinations including the true event date at 95% confidence in datasets specified with 10 years IA τ , and 67% (6/9) of these 10 years IA τ datasets are completely dominated by such accurate simulated dates in all three dataset sizes. At the other end of the IA τ spectrum, only 6–13% of datasets specified with 500 years IA τ are dates which include the true event at

Table 11 Selected features of the TS2 datasets

Dataset IAt	Dataset Size	Dataset Code	Run	Earliest date (95% confidence)	Latest date (95% confidence)	Accurate dates (95%)	Age range (95% probability)	Mean lifespan		
10 Years	15 dates	MR1a	1	1040–1230 (MR15a)	1220–1300 (MR11a)	14	15–230 years	1226 cal AD		
			2	1040–1270 (MR13a)	1220–1380 (MR4a and M14a)	15	10–240 years	1234 cal AD		
			3	1040–1270 (MR12a)	1220–1390 (MR7a)	15	10–245 years	1232 cal AD		
	Average of 15 date/10 years IAt datasets						14.7/15 (98%)	10–240 years	1231 cal AD	
	10 dates	MRR1a	1	1040–1230 (MRR6a)	1220–1300 (MRR10a)	9	15–230 years	1218 cal AD		
			2	1050–1280 (MRR5a)	1210–1290 (MRR10a)	10	– 45–210 years	1238 cal AD		
			3	1040–1270 (MRR10a)	1220–1300 (MRR7a)	10	0–230 years	1229 cal AD		
		Average of 10 date/10 years IAt datasets						9.7/10 (97%)	– 10–225 years	1228 cal AD
		5 dates	MRRR1a	1	1040–1270 (MRRR1a)	1210–1290 (MRRR4a)	5	– 20–225 years	1219 cal AD	
				2	1040–1270 (MRRR5a)	1220–1300 (MRRR2a)	5	5–230 years	1219 cal AD	
	3			1040–1230 (MRRR5a)	1180–1290 (MRRR2a)	4	5–220 years	1194 cal AD		
	Average of 5 date/10 years IAt datasets						4.7/5 (94%)	– 5–225 years	1211 cal AD	
	50 Years	15 dates	MR1b	1	990–1160 (MR7b)	1210–1290 (MR15b)	10	80–275 years	1192 cal AD	
				2	990–1160 (MR10b)	1220–1300 (MR13b)	10	85–290 years	1183 cal AD	
				3	990–1170 (MR1b)	1220–1380 (MR7b)	8	70–280 years	1181 cal AD	
Average of 15 date/50 years IAt datasets						9.3/15 (62%)	75–285 years	1185 cal AD		
10 dates		MRR1b	1	990–1160 (MRR1b)	1170–1290 (MRR9b)	9	70–265 years	1206 cal AD		
			2	1030–1210 (MRR3b)	1220–1380 (MRR9b)	8	50–260 years	1216 cal AD		
			3	900–1160 (MRR5b)	1180–1290 (MRR3b)	6	75–285 years	1177 cal AD		
		Average of 10 date/50 years IAt datasets						7.7/10 (77%)	65–270 years	1199 cal AD
		5 dates	MRRR1b	1	990–1160 (MRRR2b)	1220–1300 (MRRR3b)	3	85–290 years	1182 cal AD	
				2	1040–1230 (MRRR2b)	1219–1290 (MRRR1b)	4	10–225 years	1194 cal AD	
3				1020–1200 (MRRR2b)	1170–1280 (MRRR3b)	3	40–235 years	1188 cal AD		
Average of 5 date/50 years IAt datasets						3.3/5 (66%)	45–250 years	1188 cal AD		

Table 11 (continued)

Dataset IAt	Dataset Size	Dataset Code	Run	Earliest date (95% confidence)	Latest date (95% confidence)	Accurate dates (95%)	Age range (95% probability)	Mean lifespan	
100 Years	15 dates	MR1c	1	990–1160 (MR8c)	1210–1290 (MR14c)	9	75–270 years	1178 cal AD	
			2	650–800 (MR4c)	1220–1300 (MR9c)	6	450–625 years	1087 cal AD	
			3	990–1160 (MR10c)	1170–1290 (MR6c)	7	65–265 years	1143 cal AD	
	Average of 15 date/100 years IAt datasets						7.3/15 (49%)	195–390 years	1136 cal AD
	10 dates	MRR1c	1	770–1000 (MRR8c)	1170–1280 (MRR9c)	3	215–460 years	1113 cal AD	
			2	770–1000 (MRR3c)	1180–1290 (MRR10c)	3	235–480 years	1128 cal AD	
			3	890–1150 (MRR6c)	1170–1280 (MRR7c)	6	110–355 years	1168 cal AD	
	Average of 10 date/100 years IAt datasets						4/10 (40%)	185–435 years	1136 cal AD
	5 dates	MRRR1c	1	1030–1210 (MRRR1c)	1160–1280 (MRRR2c)	3	10–225 years	1163 cal AD	
			2	1020–1210 (MRRR3c)	1150–1280 (MRRR5c)	4	– 10–225 years	1180 cal AD	
			3	680–950 (MRRR3c)	1220–1380 (MRRR1c)	3	335–595 years	1109 cal AD	
	Average of 5 date/100 years IAt datasets						3.3/5 (66%)	110–350 years	1150 cal AD
	200 Years	15 dates	MR1d	1	700–980 (MR5d)	1160–1280 (MR15d)	1	230–525 years	1048 cal AD
				2	640–780 (MR2d)	1220–1380 (MR13d)	10	460–710 years	1108 cal AD
				3	60–240 (MR13d)	1170–1290 (MR4d)	4	990–1200 years	985 cal AD
Average of 15 date/200 years IAt datasets						5/15 (33%)	560–815 years	1047 cal AD	
10 dates		MRR1d	1	770–1000 (MRR1d)	1040–1270 (MRR3d)	2	85–405 years	1098 cal AD	
			2	670–890 (MRR7d)	1170–1280 (MRR8d)	4	320–575 years	1097 cal AD	
			3	550–650 (MRR4d)	1170–1280 (MRR7d)	4	550–710 years	1035 cal AD	
Average of 10 date/200 years IAt datasets						3.3/10 (33%)	315–565 years	1076 cal AD	
5 dates		MRRR1d	1	440–650 (MRRR4d)	1150–1280 (MRRR5d)	1	525–770 years	999 cal AD	
			2	670–890 (MRRR2d)	1210–1290 (MRRR3d)	2	360–590 years	1085 cal AD	
			3	650–780 (MRRR4d)	990–1160 (MRRR5d)	0	245–485 years	916 cal AD	
Average of 5 date/200 years IAt datasets						1/5 (20%)	375–615 years	1000 cal AD	

Table 11 (continued)

Dataset IA τ	Dataset Size	Dataset Code	Run	Earliest date (95% confidence)	Latest date (95% confidence)	Accurate dates (95%)	Age range (95% probability)	Mean lifespan
500 years	15 dates	MR1e	1	– 1020–830 (MR13e)	1050–1270 (MR8e)	1	1975–2255 years	765 cal AD
			2	– 1410–1220 (MR9e)	1210–1290 (MR6e)	1	2470–2685 years	612 cal AD
			3	– 1280–1020 (MR1e)	1160–1280 (MR9e)	2	2240–2525 years	719 cal AD
			Average of 15 date/500 years IA τ datasets					1.3/15 (8.7%)
	10 dates	MRR1e	1	– 1120–910 (MRR10e)	1030–1220 (MRR3e)	0	1980–2290 years	773 cal AD
			2	– 90–120 (MRR2e)	1050–1270 (MRR5e)	2	1045–1310 years	795 cal AD
			3	– 170–60 (MRR10e)	1050–1270 (MRR8e)	2	1100–1400 years	803 cal AD
			Average of 10 date/500 years IA τ datasets					1.3/10 (13%)
	5 dates	MRRR1e	1	– 380–160 (MRRR1e)	1040–1270 (MRRR5e)	1	1265–1590 years	516 cal AD
			2	– 380–150 (MRRR2e)	1040–1230 (MRRR5e)	0	1245–1570 years	652 cal AD
			3	250–430 (MRRR4e)	1020–1180 (MRRR3e)	0	620–885 years	817 cal AD
			Average of 5 date/500 years IA τ datasets					0.3/5 (6%)

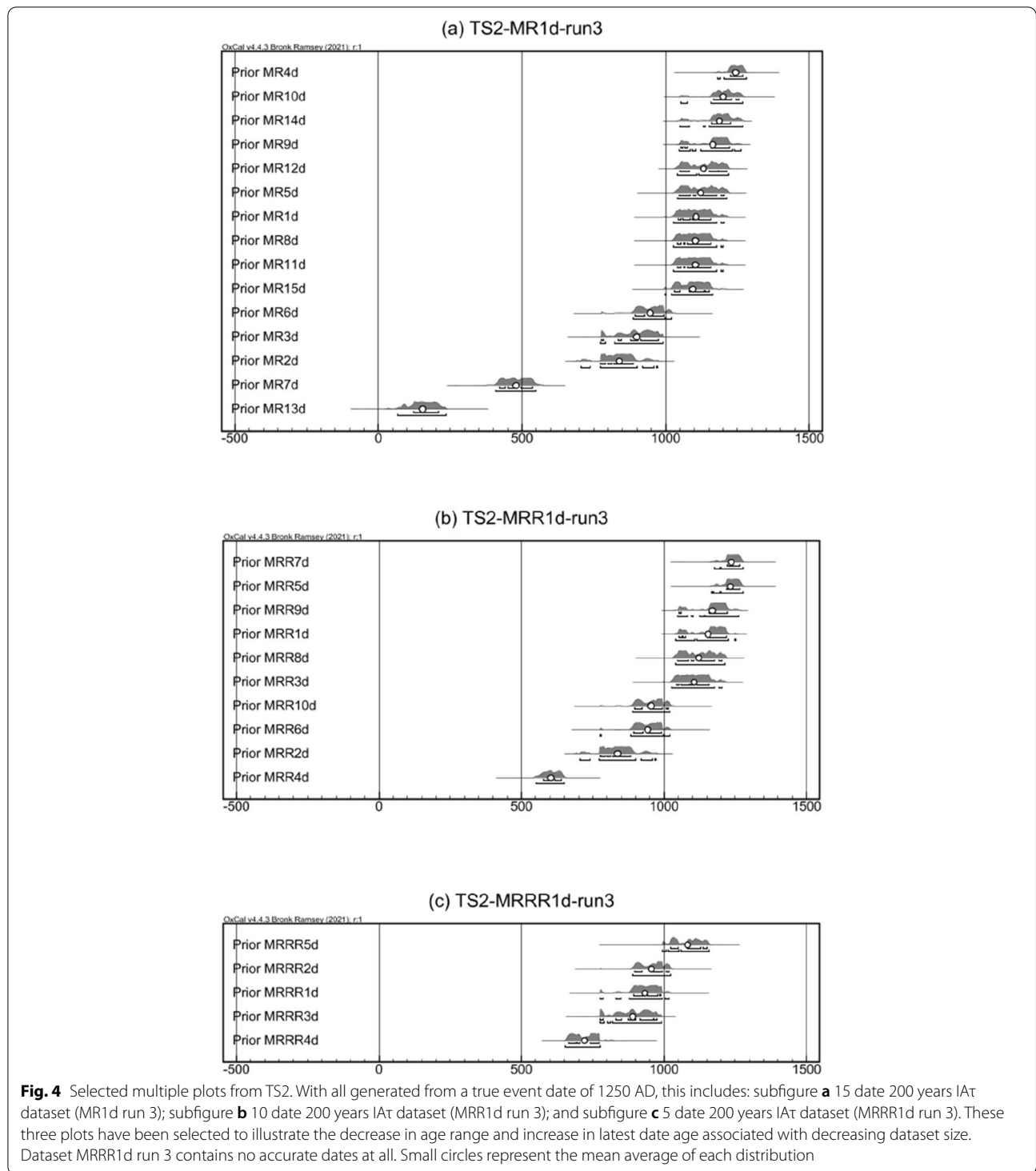
Age range values have been rounded out to 5 years. Inaccurate latest dates are in bold emphasis. Averages are mean values calculated from all three datasets in each group

95% confidence and four datasets in the study do not contain any accurate simulated dates at all (MRRR1d run 3; MRR1e run 1; MRRR1e runs 2 and 3). Although there is no clear relationship between number of true dates and dataset size for each IA τ specified, the earliest latest dates in all five IA τ groups are presented by five date datasets, and the latest latest dates have been generated within a 15 date dataset in four of the five IA τ groups. Three of the four datasets which do not contain an accurate date are limited to 5 dates (the other is a 10 dater) and three of the four are 500 years IA τ .

Age range and age range variation across TS2 generally increases with increased IA τ , and with dataset size within each IA τ group (Table 11). Narrowly distributed averages of – 5–225 years (MRRR1a) to 10–240 years (MR1a) are presented in datasets specified to 10 years IA τ , and much more widely distributed averages of 1040–1350 years (MRRR1e) to 2225–2490 years (MR1e) are presented in datasets specified to 500 years IA τ . The average age ranges presented by the 50, 100 and 200 years IA τ datasets are consistent with this trend, although there is some overlap between individual datasets from all these adjacent groups. The 5 date 100 years IA τ group

is particularly notable since this contains two datasets with extraordinarily narrow age ranges of – 10–225 years (MRRR1c run 2) and 10–225 years (MRRR1c run 1), but also extends up to 450–625 years (MR1c run 2). The narrowest age ranges are presented by 5 date datasets in four of the five IA τ groups, whilst the widest age ranges are presented by 15 date datasets in three of the five IA τ groups. Age range variation is mostly predicated on the earliest simulated date in each dataset, which generally increase in age with increased IA τ specification and dataset size; varying from 1053–1273 cal AD in the 10 years IA τ dataset (MRR1a, run 2), to 1416–1224 cal BC in the 500 years IA τ dataset (MR1e, run 2). Where datasets include very low numbers of dates, and few which include the true event date, then the exponential distribution becomes less visible and more sigmoidal distributions are apparent (Fig. 4a–c).

Mean lifespans are all earlier than the true event date and generally increase in age with the increased IA τ specification and age range in TS2 (Table 11). Without rounding out these are all close to expected values. Depending on dataset size, the study presents average mean lifespans of: 1211–1231 cal AD in the group specified with 10 years



IA τ (average 1223 rather than 1240 AD); 1185–1199 cal AD in the group specified with 50 years IA τ (1191 rather than 1200 AD); 1136–1150 cal AD in the group specified with 100 years IA τ (1141 rather than 1150 AD); 1000–1076 cal AD in the group specified with 200 years IA τ

(1041 rather than 1050 AD); and 699–790 cal AD in the group specified with 500 years IA τ (717 rather than 750 AD). Average mean lifespans for each level of specified IA τ are all distinct from adjacent groups although, apart from the 500 years IA τ , there is some overlap between

the mean lifespans of individual datasets with those of all other adjacent groups.

All TS2 models have returned Overall Agreement Indices that are above the 60% threshold (Table 12). 12% (16/135) of these models contain at least one simulated date with a low Agreement Index (A_i) and 4% (6/135) contain more than one such date. Individual dates with low Agreement Indices are more strongly associated with lower IA_τ and larger datasets, with no instances in the 500 years IA_τ or 5 date dataset groups. All six models associated with more than a single low A_i date are associated with two 15 date datasets specified with 10 years IA_τ (MR1a, runs 2 and 3, all three model specifications).

99% of all models in TS2 (133/135) have generated accurate End Boundary HPD intervals at 95% probability, and 84% (113/135) are also accurate at 68% probability (Table 13). Consistency of End Boundary accuracy varies across the study with dataset IA_τ , model specification, and dataset size although these relationships are not straightforward. The lowest IA_τ datasets have produced the most consistently accurate estimates at both 95% and 68%, but there is no clear overall trend in the relationship between these variables in the rest of the study: all End Boundary HPD intervals generated from datasets specified with 10 years IA_τ are accurate at both 68% and 95% probability; all models associated with the 50 year IA_τ datasets are also accurate at 95% probability, but only 70% of these estimates are accurate at 68% probability; 78% of models associated with the 100 years and 200 years IA_τ groups have returned accurate estimates at 68% probability, but accuracy at 95% probability is down to 96% in both cases; while the 500 years IA_τ group has returned 100% accuracy at 95% probability and 93% accuracy at 68% probability. The exponential prior/modified Charcoal Outlier Model approach has presented the most consistently accurate End Boundary HPD intervals across the study, with all models (45/45) generating accurate estimates at 95% probability and 87% (39/45) generating accurate estimates at 68% probability; the uniform prior/default Charcoal Outlier Model approach is also 100% accurate at 95% probability, and 80% (36/45) of these models are accurate at 68% probability; the exponential prior/no outlier approach has presented accurate estimates in 84% of models at 68% probability but is the only approach to present inaccurate End Boundary HPD intervals at 95% probability. Overall consistency of End Boundary accuracy in TS2 is inversely proportional to dataset size: 100% (45/45) of all modelled End Boundaries associated with 5 date datasets are accurate at 95%, and 89% (40/45) are also accurate at 68% probability; 98% (44/45) of all modelled End Boundaries associated with 10 date datasets are also accurate at 95%, and 84%

(38/45) are also accurate at 68% probability; and 98% (44/45) of all modelled End Boundaries associated with 15 date datasets are accurate at 95%, and 78% (35/45) are also accurate at 68% probability.

95% of all models in TS2 (128/135) have generated accurate Last distributions at 95% probability, and 81% (109/135) are also accurate at 68% probability (Table 13). Consistency of Last distribution accuracy varies across the study with dataset IA_τ , model specification, and dataset size although these relationships are not straightforward. The lowest IA_τ datasets have produced the most consistently accurate estimates at both 95% and 68%, but there is no clear overall trend in the relationship between these variables in the rest of the study. All Last distributions generated from datasets specified with 10 years.

IA_τ are accurate at both 68% and 95% probability; all models associated with the 50-year and 100-year IA_τ datasets are also accurate at 95% probability, but accuracy at 68% probability decreases to 81% and 89% respectively. 81% of the 200 years IA_τ groups have returned accurate estimates at 95% probability, and 75% of these distributions are also accurate at 68%. 93% of the Last distributions generated from the 500-year IA_τ datasets are accurate at 95% probability, but only 59% of this group remains accurate at 68%. The uniform prior/default Charcoal Outlier Model approach has generated the most consistently accurate Last distributions across TS2 and is the only model specification to generate accurate Last distributions for all (45/45) TS2 datasets at 95% probability. 87% (39/45) of these estimates are also accurate at 68% probability. Consistent accuracy is slightly lower for distributions generated using the exponential prior/modified Charcoal Outlier Model approach, with 96% of Last distributions accurate at 95% probability and 82% (37/45) at 68% probability; whilst the exponential prior/no Outlier approach has generated the least consistently accurate Last distributions overall, with 82% (37/45) of models at 95% probability and 73% (33/45) at 68% probability. In direct contrast with the End Boundary data, overall consistency of Last Distribution accuracy in TS2 is proportional to dataset size: with 98% (44/45) of all generated Last distributions generated from 15 date datasets are accurate at 95%, and 78% (35/45) also accurate at 68% probability; and 96% (43/45) of all modelled End Boundaries associated with 10 date datasets are accurate at 95%, and 78% (35/45) are also accurate at 68% probability; and 91% (41/45) of all modelled End Boundaries associated with 5 date datasets are accurate at 95%, and 80% (36/45) are also accurate at 68% probability.

End Boundary precision in TS2 relates strongly to dataset IA_τ , dataset size and model specification (Table 14). End Boundary precision is inversely proportional to dataset IA_τ , and the continuous spectra presented by all

Table 12 Last and End Boundary HPD intervals in TS2

Dataset and model specifications		Last HPD intervals and medians/cal AD			End Boundary HPD intervals and medians/cal AD			Agreement Indices		
10yrs IAT /15 dates (MR1a)	Run	68%	95%	median	68%	95%	median	Amodel	Aoverall	Ai < 60%
Exponential prior; no Outlier Model	1	1240–1270	1230–1280	1255	1240–1275	1225–1280	1255	104.1	97.8	0
	2	1240–1275	1230–1280	1255	1240–1275	1225–1280	1255	72.3	68.7	3
	3	1240–1270	1225–1275	1255	1240–1270	1225–1275	1255	95.9	99.1	2
Exponential prior; 10-year Charcoal Outlier Model	1	1245–1275	1230–1280	1260	1245–1275	1230–1285	1260	104.5	99.5	0
	2	1245–1275	1230–1285	1260	1245–1280	1230–1285	1260	76.3	73.1	3
	3	1245–1270	1230–1280	1255	1245–1275	1230–1280	1260	98.1	101.5	2
Uniform prior; default Charcoal Outlier Model	1	1245–1280	1230–1290	1260	1245–1280	1230–1295	1265	96.8	89.9	1
	2	1250–1285	1230–1295	1265	1250–1285	1230–1300	1270	85.5	80	3
	3	1245–1275	1230–1285	1260	1245–1280	1230–1290	1260	100.1	104.2	2
10yrs IAT /10 dates (MRR1a)	Run	68%	95%	median	68%	95%	median	Amodel	Aoverall	Ai < 60%
Exponential prior; no Outlier Model	1	1235–1270	1220–1275	1250	1235–1275	1220–1280	1255	101.8	100.6	0
	2	1240–1275	1230–1280	1255	1240–1275	1230–1280	1260	129.8	130.7	0
	3	1240–1270	1225–1280	1255	1240–1275	1225–1285	1255	92.8	93	0
Exponential prior; 10-year Charcoal Outlier Model	1	1240–1275	1225–1280	1255	1240–1275	1225–1285	1255	102.8	101.9	0
	2	1245–1275	1230–1280	1260	1245–1280	1230–1285	1260	128.7	129.4	0
	3	1245–1275	1230–1285	1260	1245–1280	1230–1285	1260	94.9	95.3	0
Uniform prior; default Charcoal Outlier Model	1	1240–1280	1225–1290	1260	1240–1285	1225–1305	1265	103.2	101.9	0
	2	1245–1280	1230–1285	1265	1245–1280	1230–1295	1265	129.3	129.9	0
	3	1245–1280	1230–1290	1260	1245–1285	1230–1300	1265	91.7	92.2	1
10yrs IAT /5 dates (MRRR1a)	Run	68%	95%	median	68%	95%	median	Amodel	Aoverall	Ai < 60%
Exponential prior; no Outlier Model	1	1235–1275	1220–1280	1255	1235–1285	1220–1315	1260	95.5	95	0
	2	1235–1275	1220–1285	1255	1235–1285	1220–1320	1260	93.8	94.6	0
	3	1220–1260	1185–1280	1240	1220–1275	1180–1325	1250	104.1	104	0
Exponential prior; 10-year Charcoal Outlier Model	1	1240–1280	1225–1285	1260	1240–1285	1220–1320	1265	96.5	96.2	0
	2	1240–1280	1225–1290	1260	1240–1285	1220–1325	1265	95	95.8	0
	3	1220–1265	1190–1285	1245	1225–1280	1180–1330	1255	104.6	104.6	0
Uniform prior; default Charcoal Outlier Model	1	1240–1285	1220–1310	1265	1235–1295	1220–1355	1275	97	96.3	0
	2	1240–1285	1220–1315	1265	1240–1300	1220–1365	1275	97.3	97.7	0
	3	1225–1275	1185–1315	1250	1225–1300	1185–1385	1270	109.4	108.7	0

Table 12 (continued)

Dataset and model specifications		Last HPD intervals and medians/ <i>cal</i> /AD				End Boundary HPD intervals and medians/ <i>cal</i> /AD				Agreement indices	
Run	50yrs IAT /15 dates (MR1b)	68%	95%	median	68%	95%	median	Amodel	Aoverall	Ai <60%	
1	Exponential prior; no Outlier Model	1230-1265	1220-1275	1250	1235-1270	1225-1285	1255	104.5	104.2	0	
2		1250-1280	1235-1285	1270	1255-1285	1235-1295	1270	100.8	99.4	0	
3		1235-1285	1230-1285	1265	1240-1290	1230-1300	1270	90.9	85.2	0	
1	Exponential prior; 50-year Charcoal Outlier Model	1240-1275	1225-1290	1255	1240-1280	1225-1295	1260	103.9	103.4	0	
2		1255-1285	1240-1300	1270	1260-1295	1240-1310	1275	99.8	99.7	0	
3		1245-1290	1230-1305	1270	1250-1295	1235-1310	1275	90.9	85.9	0	
1	Uniform prior; default Charcoal Outlier Model	1245-1285	1230-1310	1265	1250-1295	1230-1330	1275	99.6	99.1	0	
2		1260-1295	1245-1325	1280	1265-1310	1245-1350	1290	98.7	97.9	0	
3		1260-1300	1235-1320	1280	1265-1310	1240-1340	1285	95.2	91.4	0	
Run	50yrs IAT /10 dates (MRR1b)	68%	95%	median	68%	95%	median	Amodel	Aoverall	Ai <60%	
1	Exponential prior; no Outlier Model	1240-1270	1225-1275	1255	1245-1275	1225-1285	1260	121.1	121.3	0	
2		1260-1285	1235-1290	1270	1260-1290	1235-1300	1275	98.6	92.7	0	
3		1245-1275	1230-1280	1260	1250-1285	1230-1305	1265	92.7	92.1	0	
1	Exponential prior; 50-year Charcoal Outlier Model	1245-1275	1225-1285	1260	1245-1280	1225-1295	1265	118.9	118.9	0	
2		1260-1295	1235-1305	1275	1260-1300	1240-1315	1280	96.8	92.3	0	
3		1250-1280	1235-1295	1265	1250-1290	1235-1315	1275	91.5	90.8	0	
1	Uniform prior; default Charcoal Outlier Model	1245-1285	1225-1305	1265	1245-1290	1225-1320	1270	108.6	108.7	0	
2		1260-1300	1235-1320	1280	1260-1310	1235-1340	1285	85.1	80.4	1	
3		1250-1295	1235-1340	1275	1255-1315	1240-1380	1290	81.6	79.1	0	
Run	50yrs IAT /5 dates (MRRR1b)	68%	95%	median	68%	95%	median	Amodel	Aoverall	Ai <60%	
1	Exponential prior; no Outlier Model	1235-1280	1225-1290	1260	1240-1305	1225-1395	1280	96.5	96.5	0	
2		1225-1270	1215-1285	1245	1225-1285	1205-1350	1260	103.2	102.8	0	
3		1225-1270	1190-1280	1245	1225-1285	1180-1345	1260	100.9	98.3	0	
1	Exponential prior; 50-year Charcoal Outlier Model	1245-1290	1225-1315	1270	1245-1320	1225-1410	1290	97	97.1	0	
2		1230-1280	1215-1305	1255	1230-1295	1215-1365	1270	105	104.9	0	
3		1230-1275	1200-1305	1255	1230-1295	1185-1360	1265	100.8	99.1	0	
1	Uniform Prior/default Charcoal Outlier Model	1240-1305	1225-1395	1280	1250-1360	1225-1535	1315	94.6	94.9	0	
2		1230-1280	1215-1325	1260	1230-1305	1210-1400	1275	110	108.9	0	
3		1225-1280	1185-1340	1260	1225-1320	1185-1435	1280	92.4	91.3	0	

Dataset and model specifications		Last HPD intervals and medians/ <i>cal</i> /AD				End Boundary HPD intervals and medians/ <i>cal</i> /AD				Agreement indices	
Run	100yrs IAT /15 dates (MR1c)	68%	95%	median	68%	95%	median	Amodel	Aoverall	Ai <60%	
1	Exponential Prior/no Outlier Model	1245-1265	1230-1280	1260	1245-1280	1230-1290	1265	100.4	99.9	0	
2		1225-1260	1215-1280	1245	1230-1275	1220-1305	1255	102.6	103.2	0	
3		1180-1225	1165-1240	1200	1180-1225	1165-1245	1205	85.7	85.4	1	

Table 12 (continued)

Dataset and model specifications		Last HPD intervals and medians/ ca/AD			End Boundary HPD intervals and medians/ca/AD			Agreement indices		
100yrs IAT /15 dates (MR1c)	Run	68%	95%	median	68%	95%	median	Amodel	Aoverall	Ai < 60%
Exponential Prior/100-year Charcoal Outlier Model	1	1250–1285	1235–1295	1265	1250–1290	1235–1305	1270	99.8	99.4	0
	2	1230–1280	1220–1310	1255	1240–1290	1225–1330	1270	102.9	103.3	0
	3	1185–1235	1170–1260	1215	1190–1240	1170–1265	1215	91.5	91.3	1
Uniform Prior/default Charcoal Outlier Model	1	1255–1290	1235–1315	1275	1260–1300	1240–1335	1280	99.7	99	0
	2	1245–1325	1225–1400	1290	1255–1345	1235–1435	1310	100.2	100.2	0
	3	1195–1250	1175–1280	1225	1200–1260	1175–1295	1235	99.1	99.2	1
100yrs IAT /10 dates (MRR1c)	Run	68%	95%	median	68%	95%	median	Amodel	Aoverall	Ai < 60%
Exponential Prior/no Outlier Model	1	1220–1260	1195–1280	1240	1225–1280	1190–1315	1255	101.4	100.3	0
	2	1205–1250	1180–1270	1225	1210–1265	1180–1290	1235	94.6	96.5	0
	3	1225–1265	1215–1280	1245	1230–1270	1210–1300	1250	100.6	98.3	0
Exponential Prior/100-year Charcoal Outlier Model	1	1225–1275	1200–1310	1250	1230–1295	1205–1340	1265	101.8	100.9	0
	2	1215–1270	1185–1295	1240	1220–1280	1190–1315	1250	97.4	98.8	0
	3	1230–1275	1215–1300	1255	1235–1280	1215–1315	1260	99.9	98.1	0
Uniform Prior/default Charcoal Outlier Model	1	1230–1295	1210–1370	1270	1240–1330	1215–1425	1290	102.1	101.6	0
	2	1225–1290	1195–1345	1260	1230–1310	1195–1385	1275	99.6	100.3	0
	3	1235–1285	1215–1330	1265	1240–1300	1215–1365	1275	84.4	84.1	1
100yrs IAT /5 dates (MRRR1c)	Run	68%	95%	median	68%	95%	median	Amodel	Aoverall	Ai < 60%
Exponential Prior/no Outlier Model	1	1180–1235	1170–1265	1215	1185–1260	1165–1320	1225	86.6	86.4	0
	2	1185–1260	1175–1270	1220	1190–1265	1170–1315	1230	97.9	98.2	0
	3	1230–1295	1220–1305	1275	1240–1360	1225–1550	1310	100.1	100.4	0
Exponential Prior/100-year Charcoal Outlier Model	1	1195–1260	1170–1295	1225	1190–1275	1165–1350	1240	90.6	90.8	0
	2	1205–1270	1175–1295	1235	1205–1285	1175–1340	1245	99.9	100.2	0
	3	1235–1310	1220–1385	1285	1255–1385	1230–1570	1330	100.6	100.9	0
Uniform Prior/default Charcoal Outlier Model	1	1190–1260	1165–1310	1225	1190–1285	1165–1400	1245	87.8	87.3	0
	2	1200–1270	1170–1315	1235	1195–1290	1170–1405	1255	93.1	94.6	0
	3	1250–1380	1220–1520	1305	1270–1485	1235–1855	1390	99.5	99.6	0
Dataset and model specifications		Last HPD intervals and medians/ ca/AD			End Boundary HPD intervals and medians/ca/AD			Agreement indices		
200yrs IAT /15 dates (MR1d)	Run	68%	95%	median	68%	95%	median	Amodel	Aoverall	Ai < 60%
Exponential Prior/no Outlier Model	1	1070–1220	1060–1230	1175	1075–1235	1065–1250	1185	76.2	76.3	1
	2	1220–1260	1215–1280	1245	1225–1275	1220–1300	1255	100.3	102.9	1
	3	1215–1260	1190–1275	1235	1220–1280	1185–1315	1250	98.6	99.3	0

Table 12 (continued)

Dataset and model specifications		Last HPD intervals and medians/ ca/AD			End Boundary HPD intervals and medians/ca/AD			Agreement indices		
200yrs IAT /15 dates (MR1d)	Run	68%	95%	median	68%	95%	median	Amodel	Aoverall	Ai < 60%
Exponential Prior/200-year Charcoal Outlier Model	1	1095–1255	1070–1270	1195	1090–1265	1070–1285	1205	80.3	80.1	1
	2	1230–1280	1220–1310	1255	1235–1290	1225–1325	1265	103.1	105.3	0
	3	1220–1270	1190–1300	1245	1225–1290	1200–1340	1260	99.8	100.2	0
Uniform Prior/default Charcoal Outlier Model	1	1175–1255	1115–1305	1215	1185–1280	1110–1340	1235	84.5	83.1	0
	2	1245–1315	1230–1370	1285	1245–1320	1230–1385	1290	108.3	109.8	0
	3	1245–1360	1215–1490	1310	1245–1385	1215–1545	1325	100.7	100.8	0
200yrs IAT /10 dates (MRR1d)	Run	68%	95%	median	68%	95%	median	Amodel	Aoverall	Ai < 60%
Exponential Prior/no Outlier Model	1	1075–1220	1070–1220	1165	1075–1225	1065–1235	1175	92	90.4	0
	2	1220–1260	1195–1275	1240	1220–1280	1190–1320	1255	98.8	97.9	0
	3	1220–1265	1200–1280	1240	1225–1290	1190–1355	1265	99.6	98.7	0
Exponential Prior/200-year Charcoal Outlier Model	1	1135–1230	1070–1245	1180	1135–1240	1070–1260	1185	93.8	92.4	0
	2	1220–1275	1195–1325	1255	1230–1300	1205–1350	1270	99.2	98.6	0
	3	1225–1280	1195–1330	1255	1235–1310	1205–1385	1275	99.4	98.8	0
Uniform Prior/default Charcoal Outlier Model	1	1145–1245	1075–1275	1195	1150–1270	1075–1310	1205	92.4	91.2	0
	2	1235–1315	1205–1395	1275	1245–1340	1210–1445	1295	97.8	97.4	0
	3	1225–1285	1205–1360	1260	1245–1365	1215–1520	1315	99.5	99.3	0
200yrs IAT /5 dates (MRRR1d)	Run	68%	95%	median	68%	95%	median	Amodel	Aoverall	Ai < 60%
Exponential Prior/no Outlier Model	1	1175–1255	1160–1270	1210	1185–1335	1125–1605	1270	99.6	99.3	0
	2	1220–1275	1200–1285	1245	1225–1330	1190–1525	1290	96.2	96.4	0
	3	990–1095	990–1150	1035	1000–1135	990–1325	1080	98.9	99	0
Exponential Prior/200-year Charcoal Outlier Model	1	1180–1270	1155–1400	1235	1200–1370	1160–1650	1300	99.7	99.5	0
	2	1225–1290	1200–1395	1265	1235–1370	1205–1560	1310	97.2	97.3	0
	3	995–1115	990–1200	1060	1015–1175	995–1345	1105	99.6	99.7	0
Uniform Prior/default Charcoal Outlier Model	1	1180–1335	1155–1620	1245	1210–1520	1165–2050	1385	99	98.8	0
	2	1225–1320	1210–1455	1285	1245–1425	1210–1740	1345	96.8	96.9	0
	3	1020–1150	990–1265	1085	1030–1230	995–1545	1155	98.4	98.5	0
Dataset and model specifications		Last HPD intervals and medians/ ca/AD			End Boundary HPD intervals and medians/ca/AD			Agreement indices		
500yrs IAT /15 dates (MR1e)	Run	68%	95%	median	68%	95%	median	Amodel	Aoverall	Ai < 60%
Exponential Prior/no Outlier Model	1	1155–1220	1070–1235	1180	1160–1260	1080–1315	1205	95.6	96.1	0
	2	1220–1280	1180–1290	1245	1230–1325	1210–1445	1285	97.6	97.7	0
	3	1180–1245	1165–1270	1250	1195–1285	1170–1370	1250	97.3	97.2	0

Table 12 (continued)

Dataset and model specifications		Last HPD intervals and medians/ ca/ AD			End Boundary HPD intervals and medians/ ca/ AD			Agreement indices		
500yrs IAT /15 dates (MR1e)	Run	68%	95%	median	68%	95%	median	Amodel	Aoverall	Ai < 60%
Exponential Prior/500-year Charcoal Outlier Model	1	1155–1240	1085–1285	1195	1170–1280	1100–1355	1225	96.3	96.8	0
	2	1225–1305	1205–1435	1275	1240–1375	1220–1510	1320	98.5	98.5	0
	3	1190–1270	1160–1340	1235	1205–1315	1175–1420	1270	97.7	97.7	0
Uniform Prior/default Charcoal Outlier Model	1	1190–1375	1130–1560	1295	1210–1440	1125–1655	1335	97.6	97.7	0
	2	1225–1460	1215–1730	1365	1280–1610	1235–1955	1475	99.2	99.1	0
	3	1195–1290	1170–1430	1255	1230–1500	1185–1815	1385	98.1	98.1	0
500yrs IAT /10 dates (MRR1e)	Run	68%	95%	median	68%	95%	median	Amodel	Aoverall	Ai < 60%
Exponential Prior/no Outlier Model	1	1075–1180	1060–1215	1135	1105–1230	1060–1330	1175	105	104.8	0
	2	1175–1255	1165–1265	1215	1195–1300	1165–1435	1255	101.8	101.6	0
	3	1170–1230	1130–1275	1205	1185–1295	1095–1430	1245	100	99.2	0
Exponential Prior/500-year Charcoal Outlier Model	1	1100–1210	1055–1275	1160	1115–1265	1070–1385	1200	104.5	104.3	0
	2	1190–1265	1165–1330	1230	1205–1330	1170–1470	1275	101.6	101.4	0
	3	1175–1270	1075–1420	1230	1195–1345	1145–1515	1275	99.6	99	0
Uniform Prior/default Charcoal Outlier Model	1	1120–1230	1065–1370	1180	1150–1500	1090–1980	1350	101.4	101.4	0
	2	1180–1295	1160–1525	1250	1215–1490	1180–1870	1375	99.1	99.1	0
	3	1180–1285	1160–1405	1245	1215–1440	1170–1735	1350	99.8	99.6	0
500yrs IAT /5 dates (MRRR1e)	Run	68%	95%	median	68%	95%	median	Amodel	Aoverall	Ai < 60%
Exponential Prior/no Outlier Model	1	1050–1225	1040–1265	1180	1075–1495	1050–2100	1325	97.1	97.1	0
	2	1155–1220	1060–1230	1180	1150–1455	1065–1985	1305	98.5	98.4	0
	3	1080–1155	1030–1170	1115	1080–1280	1035–1605	1190	100.3	100.2	0
Exponential Prior/500-year Charcoal Outlier Model	1	1055–1260	1045–1370	1200	1140–1555	1055–2115	1365	97.4	97.4	0
	2	1135–1260	1055–1430	1205	1165–1515	1080–2050	1355	98.7	98.6	0
	3	1075–1190	1030–1325	1140	1100–1330	1045–1660	1230	100.1	100.1	0
Uniform Prior/default Charcoal Outlier Model	1	1055–1285	1040–1505	1210	1160–1790	1070–3010	1505	97.6	97.6	0
	2	1130–1345	1060–1650	1230	1180–1805	1125–2990	1535	98.5	98.5	0
	3	1075–1220	1030–1420	1155	1110–1465	1050–2025	1310	99.8	99.8	0

All HPD intervals and medians are rounded out to 5 years. Inaccurate date ranges (not including the true event date of 1250 AD) are presented in bold emphasis

Table 13 Accuracy of Last and End Boundary HPD intervals in TS2 (summarised from Table 12)

Dataset specification	Last HPD interval accuracy				End Boundary HPD interval accuracy			
	Exp. prior/ no outlier model	Exp. prior/ modified Charcoal	Uniform prior/ default Charcoal	Dataset size subtotals	Exp. prior/ no outlier model	Exp. prior/ modified Charcoal	Uniform prior/ default Charcoal	Dataset size subtotals
10 years IAT	68% (95%)	68% (95%)	68% (95%)	68%	68% (95%)	68% (95%)	68% (95%)	68%
15 dates	3/3 (3/3)	3/3 (3/3)	3/3 (3/3)	9/9	3/3 (3/3)	3/3 (3/3)	3/3 (3/3)	9/9
10 dates	3/3 (3/3)	3/3 (3/3)	3/3 (3/3)	9/9	3/3 (3/3)	3/3 (3/3)	3/3 (3/3)	9/9
5 dates	3/3 (3/3)	3/3 (3/3)	3/3 (3/3)	9/9	3/3 (3/3)	3/3 (3/3)	3/3 (3/3)	9/9
subtotals	9/9 (9/9)	9/9 (9/9)	9/9 (9/9)	100%	9/9 (9/9)	9/9 (9/9)	9/9 (9/9)	100%
50 years IAT	68% (95%)	68% (95%)	68% (95%)	68%	68% (95%)	68% (95%)	68% (95%)	68%
15 dates	3/3 (3/3)	2/3 (3/3)	2/3 (3/3)	7/9	2/3 (3/3)	2/3 (3/3)	1/3 (3/3)	5/9
10 dates	2/3 (3/3)	2/3 (3/3)	2/3 (3/3)	6/9	2/3 (3/3)	2/3 (3/3)	1/3 (3/3)	5/9
5 dates	3/3 (3/3)	3/3 (3/3)	3/3 (3/3)	9/9	3/3 (3/3)	3/3 (3/3)	3/3 (3/3)	9/9
subtotals	8/9 (9/9)	7/9 (9/9)	7/9 (9/9)	81%	7/9 (9/9)	7/9 (9/9)	5/9 (9/9)	70%
100 years IAT	68% (95%)	68% (95%)	68% (95%)	68%	68% (95%)	68% (95%)	68% (95%)	68%
15 dates	2/3 (2/3)	2/3 (3/3)	3/3 (3/3)	7/9	2/3 (2/3)	2/3 (3/3)	1/3 (3/3)	5/9
10 dates	3/3 (3/3)	3/3 (3/3)	3/3 (3/3)	9/9	3/3 (3/3)	3/3 (3/3)	3/3 (3/3)	9/9
5 dates	2/3 (3/3)	3/3 (3/3)	3/3 (3/3)	8/9	3/3 (3/3)	2/3 (3/3)	2/3 (3/3)	7/9
subtotals	7/9 (8/9)	8/9 (9/9)	9/9 (9/9)	89%	7/9 (9/9)	7/9 (9/9)	6/9 (9/9)	78%
200 years IAT	68% (95%)	68% (95%)	68% (95%)	68%	68% (95%)	68% (95%)	68% (95%)	68%
15 dates	2/3 (2/3)	3/3 (3/3)	3/3 (3/3)	8/9	2/3 (3/3)	3/3 (3/3)	3/3 (3/3)	8/9
10 dates	2/3 (2/3)	2/3 (2/3)	2/3 (3/3)	6/9	2/3 (2/3)	2/3 (3/3)	3/3 (3/3)	7/9
5 dates	2/3 (2/3)	2/3 (2/3)	2/3 (3/3)	6/9	2/3 (2/3)	2/3 (3/3)	2/3 (3/3)	6/9
subtotals	6/9 (6/9)	7/9 (7/9)	7/9 (9/9)	75%	6/9 (8/9)	7/9 (9/9)	8/9 (9/9)	78%
500 years IAT	68% (95%)	68% (95%)	68% (95%)	68%	68% (95%)	68% (95%)	68% (95%)	68%
15 dates	2/3 (2/3)	2/3 (3/3)	3/3 (3/3)	7/9	3/3 (3/3)	3/3 (3/3)	2/3 (3/3)	8/9
10 dates	1/3 (2/3)	2/3 (3/3)	2/3 (3/3)	5/9	2/3 (3/3)	3/3 (3/3)	3/3 (3/3)	8/9
5 dates	0/3 (1/3)	2/3 (3/3)	2/3 (3/3)	4/9	3/3 (3/3)	3/3 (3/3)	3/3 (3/3)	9/9
subtotals	3/9 (5/9)	6/9 (9/9)	7/9 (9/9)	59%	8/9 (9/9)	9/9 (9/9)	8/9 (9/9)	93%
All Datasets	68% (95%)	68% (95%)	68% (95%)	68%	68% (95%)	68% (95%)	68% (95%)	68%
Total	73% (82%)	82% (96%)	87% (100%)	81%	84% (96%)	87% (100%)	80% (100%)	84%
All Datasets	68% (95%)	68% (95%)	68% (95%)	68%	68% (95%)	68% (95%)	68% (95%)	68%
Total	73% (82%)	82% (96%)	87% (100%)	81%	84% (96%)	87% (100%)	80% (100%)	84%

Table 14 Average precision of Last and End Boundary HPD intervals in TS2 (summarised from Table 12)

Specified dataset IAt and model specification	Average precision of Last HPD intervals /years			Average precision of End Boundary HPD intervals/years		
	15 dates	10 dates	5 dates	15 dates	10 dates	5 dates
10 years IAt	68% (95%)	68% (95%)	68% (95%)	68% (95%)	68% (95%)	68% (95%)
Exp. Prior/no Outlier Model	32 (50)	33 (53)	40 (73)	33 (53)	37 (57)	52 (113)
Exp. Prior/10-year Charcoal	28 (52)	32 (53)	42 (73)	32 (53)	35 (57)	48 (118)
Uniform Prior/default Charcoal	33 (60)	37 (60)	47 (105)	35 (65)	40 (72)	65 (160)
50 years IAt	68% (95%)	68% (95%)	68% (95%)	68% (95%)	68% (95%)	68% (95%)
Exp. Prior/no Outlier Model	32 (52)	28 (52)	45 (75)	38 (63)	32 (67)	62 (160)
Exp. Prior/50-year Charcoal	37 (67)	32 (63)	47 (92)	40 (72)	38 (75)	68 (170)
Uniform Prior/default Charcoal	38 (82)	42 (90)	57 (145)	45 (102)	52 (113)	93 (250)
100 years IAt	68% (95%)	68% (95%)	68% (95%)	68% (95%)	68% (95%)	68% (95%)
Exp. Prior/no Outlier Model	33 (63)	42 (83)	65 (92)	42 (75)	50 (108)	90 (208)
Exp. Prior/100-year Charcoal	45 (80)	50 (102)	68 (137)	47 (90)	57 (120)	98 (230)
Uniform Prior/default Charcoal	57 (120)	60 (142)	90 (197)	63 (140)	77 (183)	135 (363)
200 years IAt	68% (95%)	68% (95%)	68% (95%)	68% (95%)	68% (95%)	68% (95%)
Exp. Prior/no Outlier Model	78 (107)	77 (103)	80 (118)	90 (132)	92 (155)	130 (383)
Exp. Prior/200-year Charcoal	87 (133)	68 (147)	92 (217)	98 (152)	83 (172)	155 (398)
Uniform Prior/default Charcoal	88 (202)	80 (182)	127 (328)	103 (238)	112 (258)	230 (655)
500 years IAt	68% (95%)	68% (95%)	68% (95%)	68% (95%)	68% (95%)	68% (95%)
Exp. Prior/no Outlier Model	63 (127)	82 (133)	105 (178)	95 (223)	113 (292)	308 (847)
Exp. Prior/500-year Charcoal	82 (203)	93 (243)	148 (332)	118 (263)	142 (328)	331 (882)
Uniform Prior/default Charcoal	172 (402)	110 (305)	197 (482)	277 (627)	283 (715)	537 (1593)

three dataset sizes for this parameter is notable. In the 15 date models there is a continuous spectrum in End Boundary distributions at 68% probability from 33 years (10 years IAt) to 277 years (500 years IAt), and at 95% probability from 53 years (10 years IAt) to 627 years (500 years IAt). In the 5 date models there is a continuous spectrum at 68% probability from 52 years (10 years IAt) to 537 years (500 years IAt), and at 95% probability from 113 years (10 years IAt) to 1593 years (500 years IAt). End Boundary precision in TS2 is proportional dataset size; and reducing datasets from 15 to 5 dates more than doubles the age range of End Boundary HPD intervals in all models at 95% probability (whatever the specified dataset IAt), although the contrast between 10 and 5 date datasets accounts for much of this increase. End Boundary precision also varies according to model specification; with the exponential prior/no outlier approach almost invariably presenting the most precise End Boundary HPD intervals at both 68% and 95% probabilities (the exception here being the models generated from 10-year IAt datasets) and the uniform prior/default Charcoal Outlier Model approach has always presented the least precise End Boundary date ranges from each dataset. The exponential prior/modified Charcoal Outlier Model approach is generally situated between these two ranges, but closer to the other more precise exponential

modelling approach. Each of these effects is cumulative, such that the effects of decreased dataset size and broader model specification on End Boundary precision increases with dataset IAt.

Last distribution precision in TS2 relates strongly to dataset IAt, dataset size and model specification (Table 14). Last distribution precision is inversely proportional to dataset IAt (generally at least doubling between 10-year and 200-year IAt datasets at both 68% and 95% probability), and directly proportional to dataset size (Last distributions generated from 5 date datasets are generally 1.5 times broader than 15 date datasets). Again, the difference in Last distribution precision between 10 and 5 dates is considerable and accounts for much of this overall contrast. In general, exponential prior approaches are associated with increased relative precision and Charcoal Outlier Model approaches with decreased precision. All three of these parameters have a cumulative effect on Last distribution precision, such that the 15 date 10 years IAt datasets modelled using the exponential prior/no outlier approach have generated Last distributions with an average precision of 50 years at 95% probability and 30 years at 68% probability; whilst the 5 date 500 years IAt datasets modelled with using the uniform prior/default Charcoal Outlier Model approach have

generated Last distributions with an average precision of 1593 years at 95% probability and 537 years at 68% probability.

Average End Boundary median values in TS2 vary from 1213 cal AD (MRRR1d; exponential prior/no outlier) to 1450 cal AD (MRRR1e; uniform prior/default Charcoal Outlier). End Boundary median values relate directly to model specification; whereby exponential prior distributions are associated with increased median age and the Charcoal Outlier Model approaches are associated with decreased median age (Table 15). End Boundary median values generally decrease in age, and variability increases, with reduced dataset size and increasing IA τ .

Average Last distribution median values in TS2 vary from 1158 cal AD (MRRR1e; exponential prior/no outlier) to 1305 cal AD (MR1e; uniform prior/default Charcoal Outlier) (Table 15). These median values relate directly to model specification; whereby exponential prior distributions are generally associated with higher median ages and the Charcoal Outlier Model approaches with lower median ages. Last median values generally increase in age with reduced dataset size, however, and (although more complex) with increasing dataset IA τ . This is clearest in the smaller datasets.

Case Study 1 (CS1)—Castle Fincharn main block.

Documentary evidence suggests some kind of secular building was constructed in the Mid-Argyll settlement of Fincharn between 1240 and 1296 AD, or more certainly 1240–1308 AD [7, 66, 67]. Castle Fincharn has never been excavated, however, and architectural interpretations of the upstanding but fragmentary 2–3 storey structure surviving on the site have varied from the 13th to the sixteenth century. An assemblage of MERLF fragments removed from this building included *Quercus* sp., *Betula* sp. and *Corylus* sp., consistent with regional vegetational histories, and radiocarbon analysis of five widely spaced single entity *Corylus* sp. samples returned determinations which calibrate to dates ranging from 1050–1270 cal AD (95% confidence; SUERC-54793) to 1220–1380 cal AD (95% confidence; SUERC-54796) (Table 16; Fig. 5).

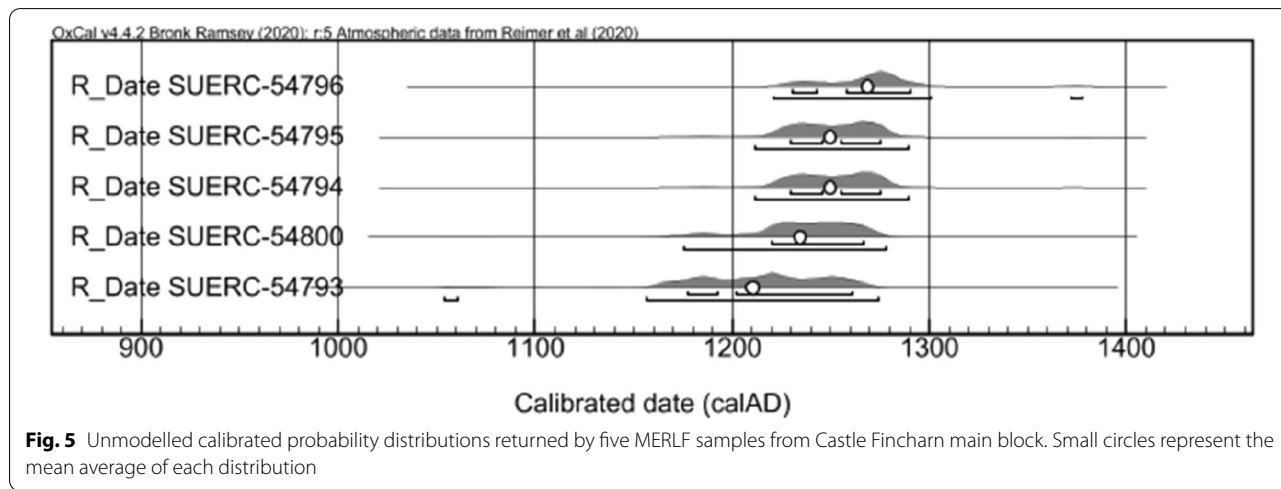
This 5 date MERLF radiocarbon dataset is statistically consistent at 5% significance level ($T' = 3.5$, $T'(5\%) = 9.5$, $v = 4$); generating a Combine distribution of 1220–1275 cal AD (95% probability; *Fincharn Castle*; Additional file 3: Sect. 3.2) and an age range Difference of – 40 to 220 years (95% probability; *Fincharn Range*; Additional file 3: Sect. 3.1) (Table 16). The Last and End Boundary distributions generated from the dataset range vary between 1230–1285 cal AD (95% probability) probably

Table 15 Average medians in Last and End Boundary HPD intervals in TS2 (summarised from Table 12)

Specified dataset IA τ and model specification	Last HPD interval average median/cal AD			End Boundary HPD interval average median/cal AD		
	15 dates	10 dates	5 dates	15 dates	10 dates	5 dates
10 years IA τ						
Exponential prior/no outlier model	1255	1253	1250	1255	1257	1257
Exponential prior/10-year Charcoal Outlier Model	1258	1258	1255	1260	1258	1252
Uniform prior/default Charcoal Outlier Model	1262	1262	1260	1265	1265	1273
50 years IA τ						
Exponential prior/no outlier model	1262	1262	1250	1265	1267	1267
Exponential prior/50-year Charcoal Outlier Model	1265	1267	1260	1270	1273	1275
Uniform prior/default Charcoal Outlier Model	1275	1273	1267	1283	1282	1290
100 years IA τ						
Exponential prior/no outlier model	1235	1237	1236	1242	1247	1255
Exponential prior/100-year Charcoal Outlier Model	1245	1248	1248	1252	1265	1272
Uniform prior/default Charcoal Outlier Model	1263	1265	1255	1275	1280	1297
200 years IA τ						
Exponential prior/no outlier model	1218	1215	1163	1230	1232	1213
Exponential prior/200-year Charcoal Outlier Model	1232	1230	1187	1243	1243	1238
Uniform prior/default Charcoal Outlier Model	1270	1243	1205	1283	1272	1295
500 years IA τ						
Exponential prior/no outlier model	1225	1185	1158	1247	1225	1273
Exponential prior/500-year Charcoal Outlier Model	1235	1207	1182	1272	1250	1317
Uniform prior/default Charcoal Outlier Model	1305	1225	1198	1398	1358	1450

Table 16 Radiocarbon results, dataset age ranges and Combine distributions associated with Castle Fincham main block (CS1)

Castle Fincham	Radiocarbon results					Modelled distributions	
Laboratory code	SUERC-54793	SUERC-54800	SUERC-54794	SUERC-54795	SUERC-54796	Dataset age range (years)	Combine range (cal AD)
Sample taxon	<i>Corylus</i>	<i>Corylus</i>	<i>Corylus</i>	<i>Corylus</i>	<i>Corylus</i>		
δ ¹³ C (‰)	− 26.6	− 26.9	− 28.7	− 27.5	26.4		
¹⁴ C age (BP)	837 ± 36	808 ± 36	777 ± 36	777 ± 36	744 ± 36		
Calibrated date 68% probability (cal AD)	1160–1250	1210–1270	1220–1280	1220–1280	1230–1290	5 to 95	1225–1270
Calibrated date 95% probability (cal AD)	1050–1270	1160–1280	1190–1290	1190–1290	1220–1380	− 40 to 220	1220–1275



1245–1280 cal AD (68% probability; *Fincham Lowest IA MERLF 1*; Additional file 3: Sect. 3.3), and 1230–1335 cal AD (95% probability) probably 1245–1295 cal AD (68% probability; *Castle Fincham Construction Completed 4*; Additional file 3: Sect. 3.6) (Table 17). This includes an exponential prior/modified Charcoal Outlier Model approach specified with a 20 year time-constant consistent with the *Corylus*-dominated character of the analysed MERLF assemblage (Table 1) and character of the local woodland (Additional file 3: Sect. 3.4).

The upper end of the Combine distribution generated from this Castle Fincham dataset is not inconconsistent with the historical evidence relating to the site but is relatively early. All Last and End Boundary distributions are also consistent with historical evidence—ranging from: 90% after TPQ and 100% before TAQ (*Fincham Lowest IA MERLF 1*; Additional file 3: Sect. 3.3) to 96% after TPQ and 89% before TAQ (*Castle Fincham Construction Completed 4*; Additional file 3: Sect. 3.6). There is little variation in lower limits of all these End Boundary and Last ranges but decreased upper limit ages in End Boundary HPD intervals generated by models which include Charcoal Outlier Models at 95% probability reduces precision and consistency with historical evidence. All Last ranges are more precise than the latest calibrated date

(SUERC-54796) and, with an estimate-TPQ/TAQ probability sum of 195%, the Last distribution generated by the exponential prior/modified Charcoal Outlier Model approach is the most consistent with currently available historical evidence (Table 17; Fig. 6).

Case Study 2 (CS2)—Aros Castle north-west block

Documentary evidence suggests some kind of castle building was constructed on the *Dun Aros* site before 1385, and current art-historical typologies suggest the bar traceried arcuate windows in the upstanding 2–3 storey north-west block first emerged in Scotland at Elgin Cathedral after 1270 AD [68]. The site has never been excavated and the relationship between the north-west-block and the adjacent enclosure is currently unknown, but architectural comparanda also suggests a late 13th–14th date for this former building is likely. An assemblage of MERLF samples removed from this structure during a wider programme of buildings and materials analysis included fragments of *Betula* sp., *Corylus* sp., *Fraxinus* sp. and *Quercus* sp. These taxa are consistent with regional vegetational histories, and radiocarbon analysis of five widely spaced single entity *Betula* and *Corylus* samples returned determinations which calibrate to dates

Table 17 Last and End Boundary distributions generated by different Bayesian models from the 5 date Castle Fincham MERLF radiocarbon dataset, with TPQ and TAQ probabilities

Model specification	Last HPD intervals/cal AD				End Boundary HPD intervals/cal AD				Agreement indices				
	68%	95%	Median	After TPQ	Before TAQ	68%	95%	Median	After TPQ	Before TAQ	Amodel	Aoverall	Ai
exponential prior; no outlier	1245–1280	1230–1285	1265	90%	100%	1240–1285	1225–1305	1270	92%	97%	81.1	82.2	0
exponential prior; modified Charcoal	1250–1285	1230–1295	1270	95%	100%	1250–1290	1230–1315	1275	96%	95%	83.4	84.2	0
exponential prior; default Charcoal	1250–1290	1230–1305	1270	96%	97%	1250–1295	1230–1325	1275	97%	92%	83.1	83.9	0
uniform prior; default Charcoal	1250–1290	1230–1305	1270	95%	98%	1245–1295	1230–1335	1275	96%	89%	83.1	83.9	0

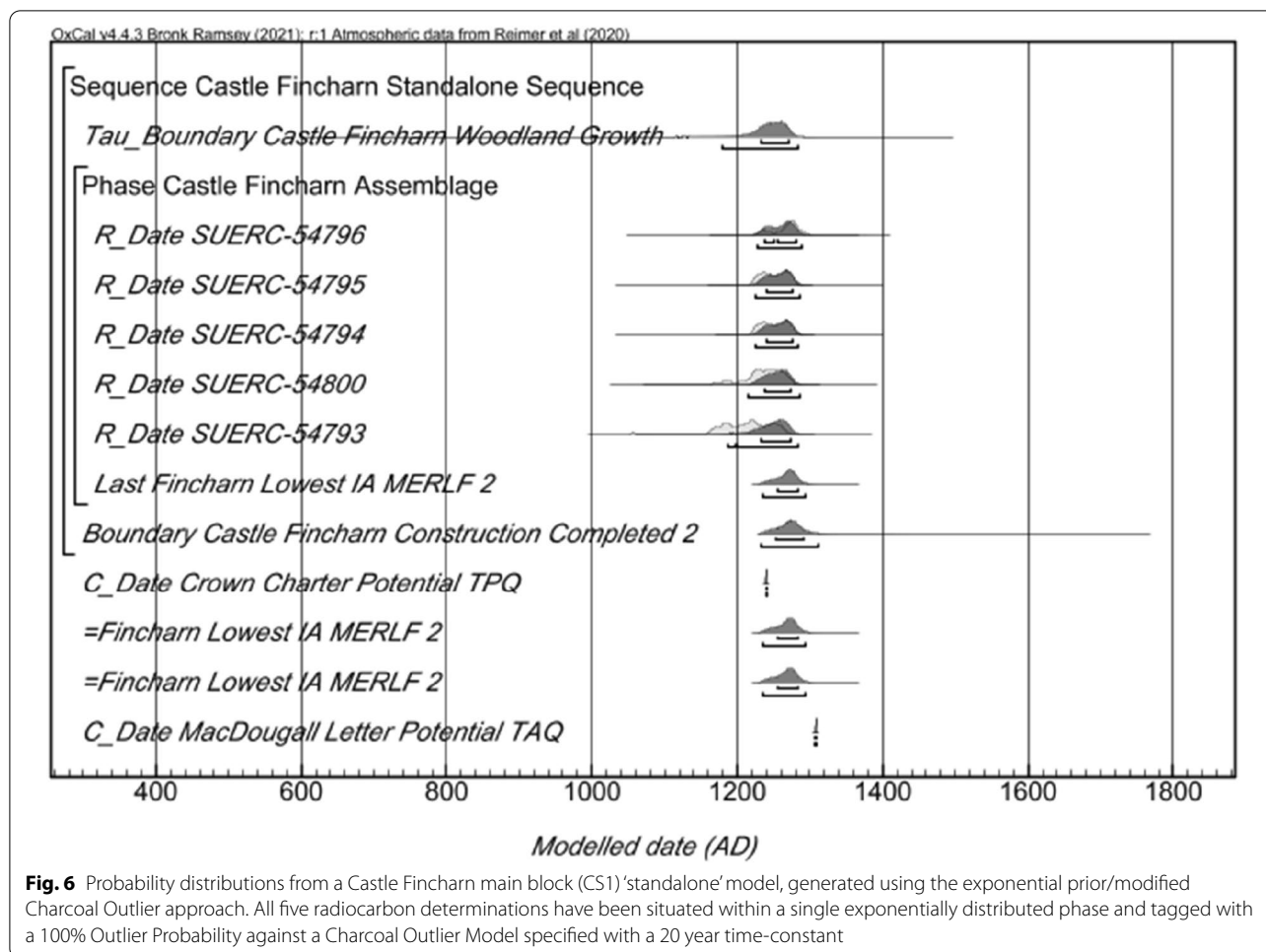


Fig. 6 Probability distributions from a Castle Fincham main block (CS1) 'standalone' model, generated using the exponential prior/modified Charcoal Outlier approach. All five radiocarbon determinations have been situated within a single exponentially distributed phase and tagged with a 100% Outlier Probability against a Charcoal Outlier Model specified with a 20 year time-constant

Table 18 Radiocarbon results, dataset age ranges and Combine distributions associated with Aros Castle NW block (CS2)

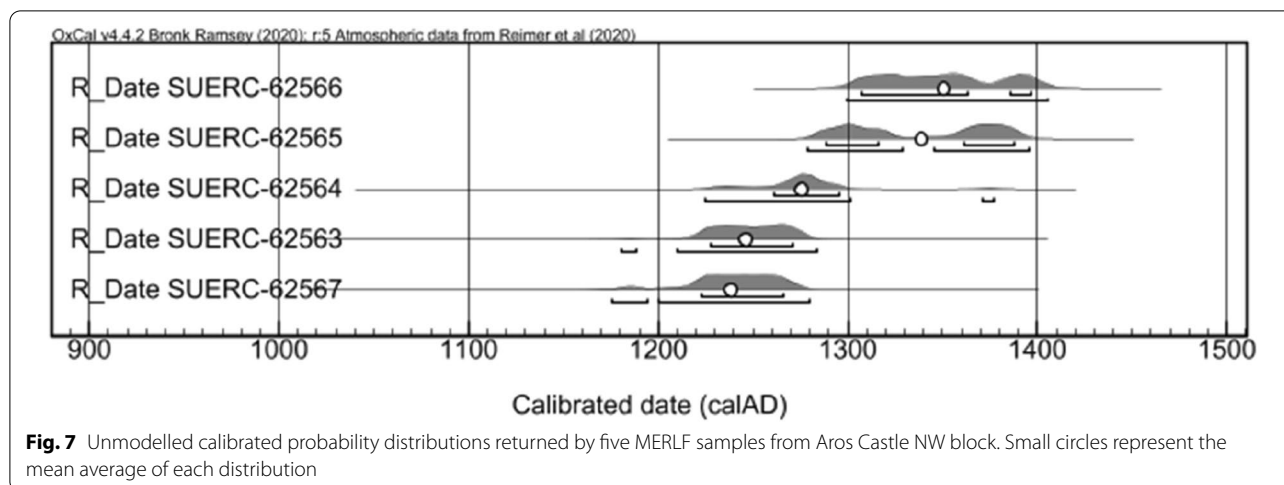
Aros Castle NW block	Radiocarbon results					Modelled distributions	
Laboratory code	SUERC-62567	SUERC-62563	SUERC-62564	SUERC-62565	SUERC-62566	Dataset age range (years)	Combine range (cal AD)
Sample taxon	<i>Betula</i>	<i>Betula</i>	<i>Betula</i>	<i>Corylus</i>	<i>Betula</i>		
δ ¹³ C (‰)	- 26.6	- 25.8	- 26.9	- 26.3	- 25.4		
¹⁴ C age (BP)	804 ± 34	787 ± 34	736 ± 34	657 ± 34	607 ± 34		
Calibrated date 68% probability (cal AD)	1220–1270	1220–1280	1260–1300	1289–1390	1300–1400	65 to 150	1275–1285
Calibrated date 95% probability (cal AD)	1170–1280	1180–1290	1220–1380	1270–1400	1290–1410	35 to 190	1270–1295

Combined ranges are highlighted in bolditalic emphasis as these show poor agreement

ranging between 1170 and 1280 cal AD (95% confidence; SUERC-82567) and 1290–1410 cal AD (95% confidence; SUERC-62566) (Table 18; Fig. 7).

The current 5 date dataset associated with this building is not statistically consistent at 5% significance level ($T' = 22.3$, $T'(5\%) = 9.5$, $v = 4$), but generated a Combine distribution of 1270–1295 cal AD (95% probability; Aros Castle; Additional file 3: Sect. 3.8) and an age range of 35 to 190 years (95% probability;

Aros Range; Additional file 3: Sect. 3.7) (Table 18). The End Boundary and Last distributions generated from the dataset range between 1290–1395 cal AD (95% probability) probably 1295–1380 cal AD (68% probability; Aros NW Lowest IA MERLF 1; Additional file 3: Sect. 3.9), and 1290–1595 cal AD (95% probability) probably 1310–1425 cal AD (68% probability; Aros NW Block Construction Completed 4; Additional file 3: Sect. 3.12) (Table 19). This includes an



exponential prior/modified Charcoal Outlier Model approach specified with a time-constant of 50 years (Additional file 3: Sect. 3.10) consistent with the longest-lived fragments of *Betula* sp. (here probably *B. pubescens*) (Table 19; Fig. 8).

All estimates generated from this dataset are consistent with the art-historical, architectural, and documentary evidence relating to the building and site, although the Combine distribution is very early. Variation in the lower limit of all other generated distributions is limited to five years at 95% probability (1295–1300 cal AD), and hence all are 100% after TPQ. Decreases in the upper limit age (and median) of these Last and End Boundary ranges decreases precision and consistency with historical evidence. With an estimate-TPQ/TAQ probability sum of 193%, the Last distribution generated using the exponential prior/no Outlier approach is most consistent with the available art-historical and historical evidence, presenting a date range very similar to latest dataset date (SUERC-62566; 1290–1410 cal AD at 95% probability) (Table 19; Fig. 8).

Case Study 3 (CS3)—Castle Roy enclosure and tower

The Speyside lordship of Abernethy emerges into the surviving documentary record in 1226 AD and the castle enclosure currently surviving on the site of the *Castle of Abernethy* (now known as Castle Roy) displays an arcuate entrance which is unlikely to have been constructed before 1150 AD [69]. Excavation suggests this substantially upstanding masonry structure is the earliest building on the site, and an extensive assemblage of *in-situ* MERLF fragments removed from the upstanding castle enclosure included *Quercus* sp., *Betula* sp. and *Pinus* sp. This is broadly

consistent with the vegetational history of the region and five widely distributed single entity fragments of *Betula* and *Pinus* returned radiocarbon determinations which calibrate to dates ranging between 990 and 1160 cal AD (95% confidence; SUERC-75745) and 1040–1260 cal AD (95% confidence; SUERC-75746) (Table 20; Fig. 9).

This 5 date dataset is statistically consistent at 5% significance ($T' = 7.2$, $T'(5\%) = 9.5$, $v = 4$), but generates a Combine distribution with poor agreement of 1040–1170 cal AD (95% probability; *Castle Roy*; Additional file 3: Sect. 3.14) and an age range of – 75 to 210 years (95% probability; *Roy Range*; Additional file 3: Sect. 3.13) (Table 20). The Last and End Boundary distributions generated from the dataset during this study range between: 1050–1225 cal AD (95% probability) probably 1155–1220 cal AD (68% probability; *Roy Lowest IA MERLF 1*; Additional file 3: Sect. 3.15); and 1055–1415 cal AD (95% probability) probably 1080–1290 cal AD (68% probability; *Castle Roy Construction Completed 4*; Additional file 3: Sect. 3.18) (Table 21), and this includes an exponential prior/modified Charcoal Outlier Model specified with a time-constant of 100 years (Additional file 3: Sect. 3.16), consistent with the shortest-lived fragments of *Betula* sp. (here probably *B. pendula*; Table 1).

The extreme upper end of the Combine distribution is consistent with the architectural evidence but is very early. Variation in the lower limits of the generated End Boundary and Last distributions is limited to five years between 1050 and 1055 cal AD at 95% probability, and all End Boundary and Last distributions are consistent with the available architectural and historical evidence relating to the building and site.

Table 19 Last and End Boundary distributions generated by different Bayesian models from the 5 date Aros Castle NW block MERLF radiocarbon dataset, with TPQ and TAQ probabilities

Model specification	Last HPD intervals/cal AD			End Boundary HPD intervals/cal AD			Agreement indices						
	68%	95%	Median	After TPQ	before TAQ	68%	95%	Median	After TPQ	Before TAQ	Amodel	Aoverall	Ai
exponential prior; no outlier	1295–1380	1290–1395	1320	100%	93%	1300–1385	1285–1460	1340	100%	76%	77.7	78	0
exponential prior; modified Charcoal	1300–1380	1290–1410	1335	100%	86%	1305–1390	1290–1470	1350	100%	71%	79.6	79.8	0
exponential prior; default Charcoal	1300–1390	1285–1450	1340	100%	79%	1305–1400	1285–1505	1360	100%	64%	79.7	79.8	0
uniform prior; default Charcoal	1305–1390	1290–1445	1350	100%	76%	1310–1425	1290–1595	1380	100%	52%	81.3	81.3	0

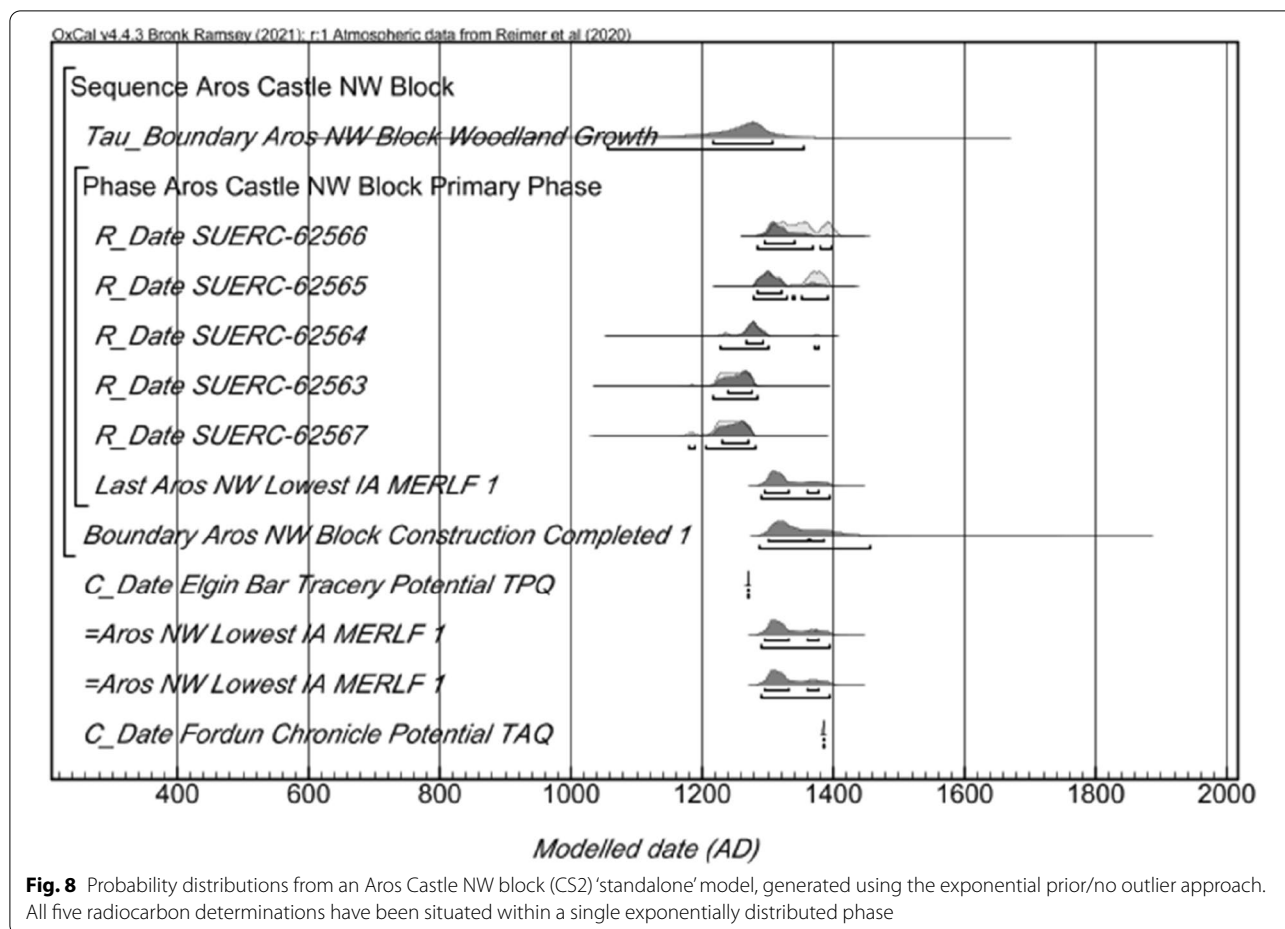


Fig. 8 Probability distributions from an Aros Castle NW block (CS2) 'standalone' model, generated using the exponential prior/no outlier approach. All five radiocarbon determinations have been situated within a single exponentially distributed phase

Table 20 MERLF Radiocarbon results, assemblage age ranges and Combine distributions for Castle Roy (CS3)

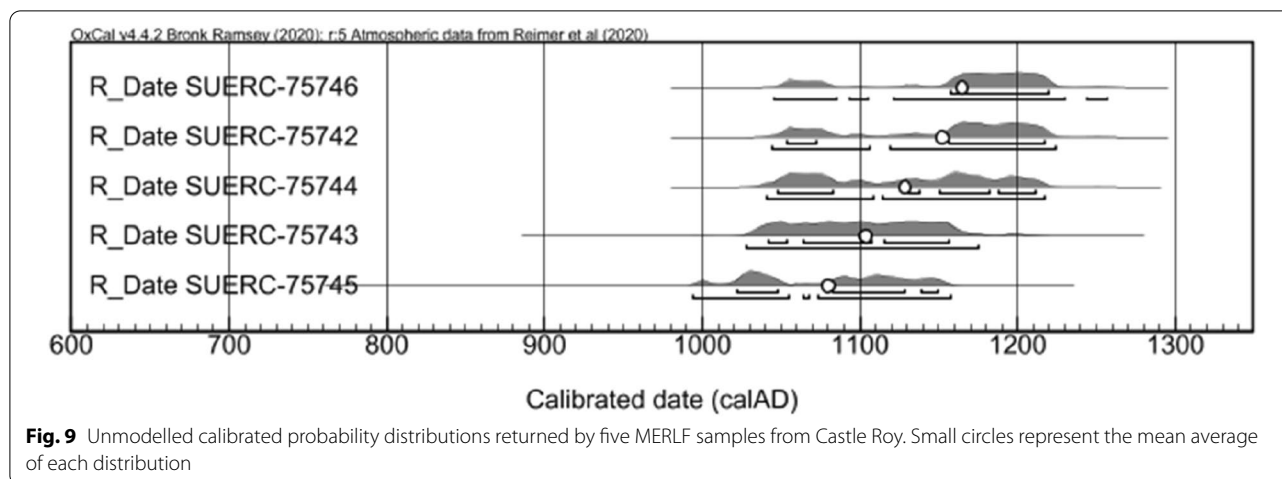
Castle Roy	Radiocarbon results					Modelled distributions	
Laboratory code	SUERC-75745	SUERC-75743	SUERC-75744	SUERC-75742	SUERC-75746	Dataset age range (years)	Combine range (cal AD)
Sample taxon	<i>Pinus</i>	<i>Betula</i>	<i>Pinus</i>	<i>Betula</i>	<i>Betula</i>		
δ ¹³ C (‰)	- 25.3	- 26.5	- 25.7	- 27.0	- 25.8		
¹⁴ C age (BP)	985 ± 31	939 ± 31	905 ± 31	887 ± 31	878 ± 31		
Calibrated date 68% probability (cal AD)	1020–1150	1040–1160	1040–1220	1050–1220	1150–1220	30 to 175	1050–1165
Calibrated date 95% probability (cal AD)	990–1160	1020–1180	1040–1220	1040–1230	1040–1260	- 75 to 210	1040–1170

The Combined distribution is highlighted in bolditalic emphasis as this displayed poor agreement

With an estimate-TPQ/TAQ probability sum of 173%, the Last distribution generated using the exponential prior/no outlier approach is most consistent with this evidence, presenting a date range very similar to latest date (SUERC-75746) at 68% probability, but considerably more precise at 95% probability (Table 21; Fig. 10).

Case Study 4 (CS4)—Lochindorb Castle enclosure

A very narrow 1258–1279 AD constructional date has been widely accepted for initial construction of the upland Moray castle of Lochindorb on the basis that the building was constructed by John Comyn before a 1279 reference to 'Robert of Lochindorb' [7,



70]. A limited assemblage of *in-situ* MERLF samples removed from the earliest upstanding phase of the enclosure was completely dominated by fragments of *Quercus* sp., although this genus is not consistent with relict semi-natural woodland populations of *Pinus-Betula* surviving locally. Five widely spaced single entity *Quercus* sp. samples with no terminal ring evidence were selected from this phase for radiocarbon analysis, and these returned a wide distribution of calibrated dates ranging between 550 and 380 cal BC (95% confidence; SUERC-75752) and 1160–1270 cal AD (95% confidence; SUERC-75747) (Table 22; Fig. 11).

This 5 date dataset is not statistically consistent at 5% significance ($T' = 2014$, $T'(5\%) = 9.5$, $v = 4$), generating an age range of 1555 to 1925 years (95% probability; *Lochindorb Range*; Additional file 3: Sect. 3.19) and failing to generate a Combine distribution (Additional file 3: Sect. 3.20) (Table 22). The Last and End Boundary distributions generated from this dataset range between 1175–1270 cal AD (95% probability) probably 1195–1260 cal AD (68% probability; *Lochindorb Lowest IA MERLF 1*; Additional file 3: Sect. 3.21), and 1200–3010 cal AD (95% probability) probably 1235–1890 cal AD (68% probability; *Construction Lochindorb Castle 4*; Additional file 3: Sect. 3.24) (Table 23). This includes an exponential prior/modified Charcoal Outlier Model specified with a time-constant of 300 years (Additional file 3: Sect. 3.22) consistent with the *Quercus* sp. dominated character of the MERLF assemblage (Table 1).

All generated Last and End Boundary estimates are consistent with the available historical evidence. With an estimate-TPQ/TAQ probability sum of 114%, the Last distribution generated using the exponential prior/modified Charcoal Outlier Model approach is

the most consistent with this other evidence, and this distribution is later and somewhat broader than the latest dataset date (SUERC-75747) (Table 23; Fig. 12).

Case Study 5 (CS5)—Achanduin Castle enclosure and hall

Surviving charter evidence suggests the upstanding castle at Achanduin on Lismore was constructed between 1240 and 1310 AD, whilst a Balliol coin recovered during excavation beneath the castle courtyard has been highlighted to suggest this constructional period may be constrained to a very narrow 1292–1310 AD period [49, 71]. A very limited assemblage of *in-situ* MERLF fragments removed from the upstanding essentially single-phase building was comprised of *Quercus* sp. and *Betula* sp., consistent with regional vegetational histories, and radiocarbon analysis of one *Quercus* and two *Betula* fragments returned determinations which calibrate to between 1180–1290 cal AD (SUERC-62547) and 1260–1390 cal AD (SUERC-62546) at 95% confidence (Table 24; Fig. 13).

This 3 date dataset is statistically consistent at the 5% significance level ($T' = 4.0$, $T'(5\%) = 6.0$, $v = 2$), generating a Combine distribution of 1265–1295 cal AD (95% probability; *Achanduin Castle*; Additional file 3: Sect. 3.26) and an age range of 0 to 155 years (95% probability; *Achanduin Range*; Additional file 3: Sect. 3.25) (Table 24). The Last and End Boundary distributions generated from the dataset range between 1270–1385 cal AD (95% probability) probably 1275–1305 cal AD (68% probability; *Achanduin Lowest IA MERLF 1*; Additional file 3: Sect. 3.27), and 1275–1820 cal AD (95% probability) probably 1280–1450 cal AD (68% probability; *Achanduin Castle Construction Completed 4*; Additional file 3: Sect. 3.30) (Table 25), and this includes an exponential prior/modified Charcoal Outlier Model specified

Table 21 Last and End Boundary distributions generated by different Bayesian models from the 5 date Castle Roy MERLF radiocarbon dataset, with TPQ and TAQ probabilities

Model specification	Last HPD intervals/ cal AD				End Boundary HPD intervals/cal AD				Agreement indices				
	68%	95%	Median	After TPQ	Before TAQ	68%	95%	Median	After TPQ	Before TAQ	Amodel	Aoverall	Ai
Exponential prior; no Outlier	1155–1220	1050–1225	1175	74%	99%	1070–1235	1050–1270	1185	77%	85%	73.2	71.9	0
Exponential prior; modified Charcoal	1155–1230	1060–1255	1185	80%	89%	1155–1255	1055–1300	1200	82%	73%	75.5	74.6	0
Exponential prior; default Charcoal	1155–1235	1055–1270	1190	81%	86%	1155–1260	1055–1320	1200	83%	71%	75.4	74.8	0
Uniform prior; default Charcoal	1080–1240	1055–1280	1190	80%	84%	1080–1290	1055–1415	1215	84%	58%	74	73.3	0

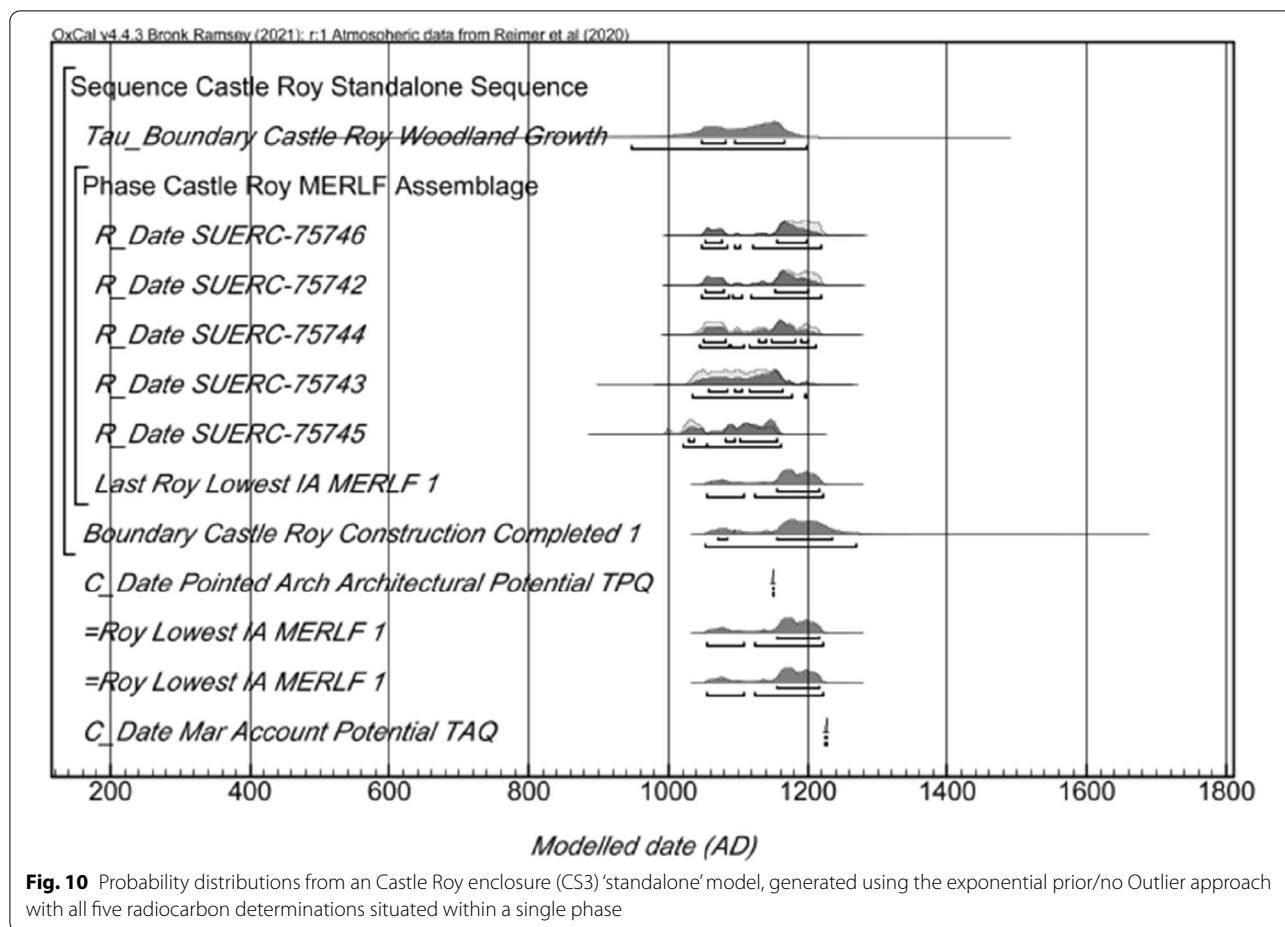


Fig. 10 Probability distributions from an Castle Roy enclosure (CS3) ‘standalone’ model, generated using the exponential prior/no Outlier approach with all five radiocarbon determinations situated within a single phase

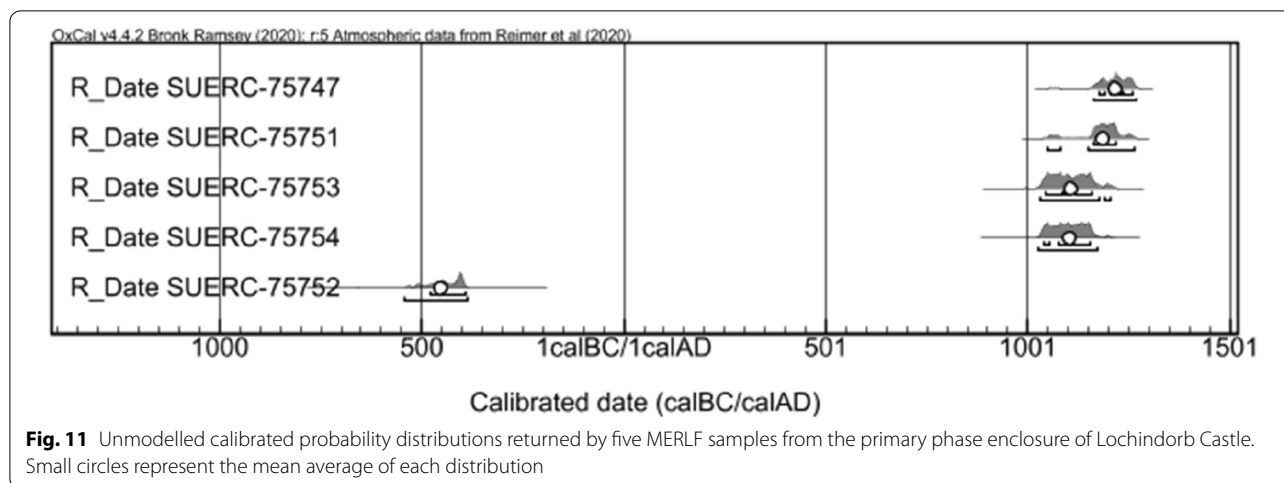
Table 22 MERLF Radiocarbon Determinations, calibrated dates, assemblage age range and Combine distributions for CS4 Lochindorb Castle primary phase enclosure

Lochindorb Castle	Radiocarbon results					Modelled distributions	
Laboratory code	SUERC-75752	SUERC-75754	SUERC-75753	SUERC-75751	SUERC-75747	Dataset age range (years)	Combine range (cal AD)
Sample taxon	<i>Quercus</i>	<i>Quercus</i>	<i>Quercus</i>	<i>Quercus</i>	<i>Quercus</i>		
δ ¹³ C (‰)	− 26.7	− 26.1	− 24.7	− 25.3	− 26.5		
¹⁴ C age (BP)	2368 ± 31	940 ± 31	932 ± 31	862 ± 31	835 ± 31		
Calibrated date 68% probability (cal AD)	− 480 to − 390	1040–1160	1040–1160	1160–1220	1170–1260	1600 to 1720	Failed
Calibrated date 95% probability (cal AD)	− 550 to − 380	1020–1180	1030–1210	1050–1270	1160–1270	1555 to 1925	Failed

with a time-constant of 50 years (Additional file 3: Sect. 3.28), consistent with the shortest-lived *Betula* fraction of the MERLF assemblage (Table 1).

The generated Combine distribution is not consistent with the archaeological evidence at 68% probability. All Last and End Boundary distributions generated are consistent with the available archaeological and historical evidence, with lower limits varying from

1265 to 1275 cal AD and precision and median age decreasing with uniform prior and Charcoal Outlier Model specifications (Table 25). With an estimate-TPQ/TAQ probability sum of 141%, the Last distribution generated using the exponential prior/modified Charcoal Outlier Model approach is the most consistent with this other evidence, and this distribution is similar to the latest dataset date (SUERC-62546) at



95% probability but much more precise at 68% probability (Table 25; Fig. 14).

Case Study 6 (CS6)—Lismore Cathedral nave

The earliest surviving contemporary reference to a church building which can be reasonably related to the site of Lismore cathedral dates to 1314 AD, although other historical evidence suggests the diocese was formally erected between 1192 and 1214 AD [72–74]. An upstanding medieval church chancel on the site has been ascribed to a range of 13th to fourteenth century dates and highlighted to illustrate the challenges faced by architectural historians in ascribing more precise dates to western Scottish masonry buildings of this period [75]. An assemblage of MERLF samples removed during excavation of the more fragmentary nave and western tower included fragments of *Alnus* sp., *Betula* sp., *Corylus* sp. and *Quercus* sp. consistent with local vegetational histories, and 3 samples of *Corylus* and *Quercus* from the earlier nave returned a range of radiocarbon determinations calibrating to between 1030–1219 cal AD (95% confidence; SUERC-75732) and 1290–1400 (95% confidence; SUERC-75727) (Table 26; Fig. 15). The *Corylus* MERLF sample (SUERC-75727) within this small assemblage retained some probable terminal ring evidence.

This 3 date dataset is not statistically consistent at 5% significance ($T' = 48.9$, $T'(5\%) = 6.0$, $v = 2$) but has generated a Combine distribution with poor agreement of 1250–1275 cal AD (95% probability; *Lismore Cathedral Nave*; Additional file 3: Sect. 3.32), and an age range of 125 to 345 years (95% probability; *Lismore Range*; 4.31) (Table 26). The Last and End Boundary distributions generated from the data range between 1295–1400 cal AD (95% probability) probably 1300–1395 cal AD (68% probability; *Lismore Nave Lowest*

IA MERLF 1; Additional file 3: Sect. 3.33), and 1320–1905 cal AD (95% probability) probably 1325–1905 cal AD (68% probability; *Lismore Cathedral Nave Complete 4*; Additional file 3: Sect. 3.36). This includes an exponential prior/modified Charcoal Outlier Model specified with a time-constant of 300 years (Additional file 3: Sect. 3.34), consistent with the longest-lived *Quercus* fraction of the assemblage (Table 1).

The late 13th-century Combine date is consistent with available historical evidence. All Last and End Boundary distributions are later than the historical TPQ (100% probability), but the extent to which these distributions pre-date the documentary TAQ varies between 24% (*Lismore Nave Lowest IA MERLF 1*; Additional file 3: Sect. 3.33) and 0% (*Lismore Cathedral Nave Complete 4*; Additional file 3: Sect. 3.36). With an estimate-TPQ/TAQ probability sum of 124%, the Last distribution generated using the exponential prior/no outlier approach is the most consistent with this other evidence, and is very similar to the latest dataset date (SUERC-75727) (Table 27; Fig. 16).

Discussion

The theoretical studies

Variation in the datasets generated from the same model parameters during these theoretical studies highlights that radiocarbon date simulation is a random probabilistic process, and multiple datasets are therefore required to examine how this variability affects the estimates generated using different modelling approaches. Sixty-five exponentially distributed datasets of between five and twenty simulated dates were randomly generated from a true event of 1250 AD for the two main theoretical studies considered in this paper—TS1 and TS2.

Table 23 Last and End Boundary distributions generated by different Bayesian models from the 5 date Lochindorb Castle MERLF radiocarbon dataset, with TPQ and TAQ probabilities

Model specification	Last HPD intervals/cal AD				End Boundary HPD intervals/cal AD				Agreement indices				
	68%	95%	Median	After TPQ	Before TAQ	68%	95%	Median	After TPQ	Before TAQ	Amodel	Aoverall	Ai
Lochindorb Castle all data													
Exponential prior;	1195–1260	1175–1270	1220	8%	100%	1200–1420	1170–1895	1325	77%	33%	78.1	78.1	0
No outlier													
Exponential prior; modified Charcoal	1185–1280	1160–1485	1245	39%	75%	1210–1485	1175–2005	1370	86%	21%	79.4	79.4	0
Exponential prior; default Charcoal	1180–1295	1160–1685	1250	46%	67%	1210–1520	1175–2125	1385	88%	19%	79.3	79.3	0
Uniform prior; default Charcoal	1180–1465	1165–1990	1335	70%	38%	1235–1890	1200–3010	1620	97%	5%	79.5	79.5	0

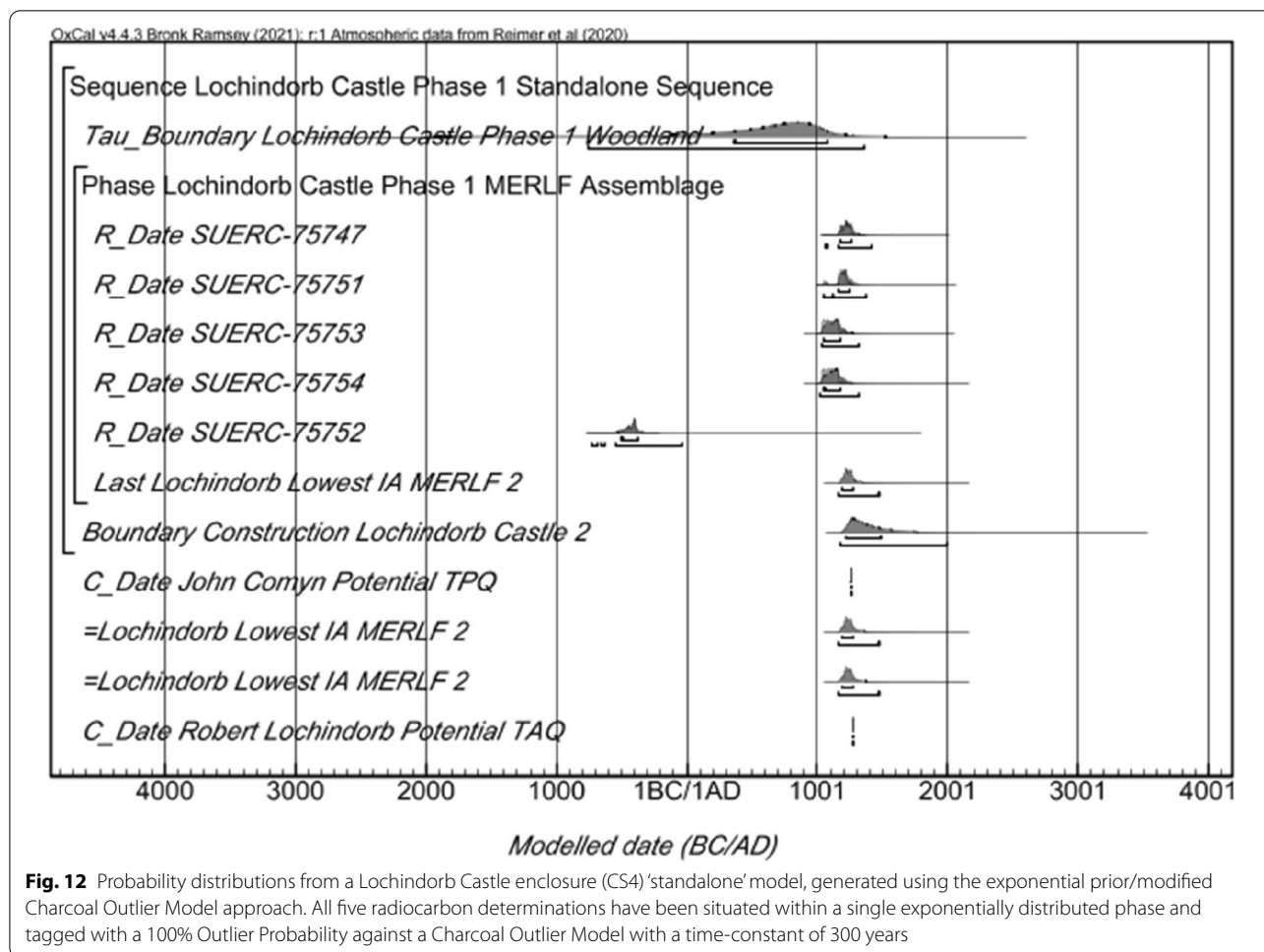


Fig. 12 Probability distributions from a Lochindorb Castle enclosure (CS4) ‘standalone’ model, generated using the exponential prior/modified Charcoal Outlier Model approach. All five radiocarbon determinations have been situated within a single exponentially distributed phase and tagged with a 100% Outlier Probability against a Charcoal Outlier Model with a time-constant of 300 years

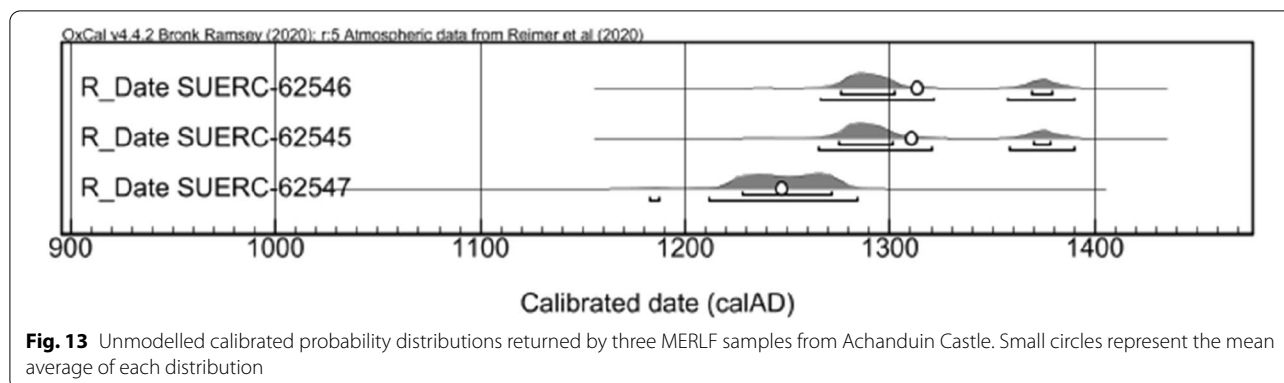
Table 24 MERLF Radiocarbon results, assemblage age ranges and Combine distributions for Achanduin Castle (CS5)

Achanduin Castle	Radiocarbon results			Modelled distributions	
Laboratory code	SUERC-62547	SUERC-62545	SUERC-62546	Dataset age range (years)	Combine range (cal AD)
Sample taxon	<i>Betula</i>	<i>Betula</i>	<i>Quercus</i>		
$\delta^{13}\text{C}$ (‰)	- 25.0	- 26.9	- 25.7		
^{14}C age (BP)	785 ± 34	701 ± 34	698 ± 34		
Calibrated date 68% probability (cal AD)	1220–1280	1270–1380	1270–1380	5–125	1270–1285
Calibrated date 95% probability (cal AD)	1180–1290	1260–1390	1260–1390	0–155	1265–1295

None of these TS1 or TS2 datasets contain dates which are later than the true event at 95% probability, and the number of dates in a single dataset which contain the true event at 95% probability varies from twenty to zero (Tables 2 and 11). Almost all datasets contain at least one date which includes the true event, and this includes all 15 date and 20 date datasets and all datasets with a specified $\text{IA}\tau$ of 100 years or less. Increasing dataset $\text{IA}\tau$ has increased the age of the latest date in both studies and

thereby resulted in datasets with a lower fraction of dates which include the true event (Table 28). There is no convincing relationship between fraction of accurate dates and dataset size in these studies, although a drop off is apparent between 10 and 5 date datasets (Table 28) and some small very high $\text{IA}\tau$ datasets are completely dominated by inaccurately early dates (Table 11).

Dataset age ranges in these studies are proportional to $\text{IA}\tau$ and size (Table 29). The only 20 date dataset to



present an age range with minus values was a 10 years IA τ dataset in which all simulated dates contained the true event (TS1 M1a run 1), but three smaller datasets also present minus age range values, including a 5 date 100 years IA τ dataset (TS2 MRRR1c run 2) within which four dates include the true event (Tables 2 and 11). With some dataset age ranges ranging across thousands of years, it is clear that single determinations from theoretical assemblages subject to IA τ do not always directly represent the true event, while the inaccuracy of all Combine distributions generated from 20 date datasets of 50 years IA τ or more illustrates that the unweighted averaging of datasets subject to considerable IA does not directly represent this event either. It is salient, however, that the Combine approach can generate accurate distributions from datasets specified with 10 years IA τ , at least (Table 3).

251 (98%) of the 255 models in TS1 and TS2 have generated accurate End Boundary HPD intervals at 95% probability, and 215 (84%) of these are also accurate at 68% probability (Table 30). Accurate End Boundary estimates have been generated with almost identical consistency in TS1 and TS2, and by the three main models included in both studies (Table 31). End Boundary and Last distributions generated from datasets with very low IA lifespans (10 years IA τ) are more consistently accurate in both studies, but no general relationship between accuracy and dataset IA or dataset size was noted elsewhere (Tables 13, 31 and 32). The most consistently accurate End Boundary estimates in both theoretical studies were generated by models specified with both exponential priors and Charcoal Outlier Models (Table 32). This was the only model specification to generate accurate End Boundary HPD intervals at 95% probability from all datasets in both studies, and in both studies 87–90% of these estimates were also accurate at 68% probability. No change in End Boundary accuracy resulted from

modifying the Charcoal Outlier Model time-constant (to match that of the specified dataset lifespan) in 20 date models with exponential priors, but an increase in accuracy is evident in the less precise uniform prior approaches (Table 5).

All Last distributions are slightly earlier than the End Boundaries generated from the same datasets in both theoretical studies. These contrasts are more marked in 95% probability distributions and increase with increasing dataset IA τ , decreasing dataset size, and uniform prior and Charcoal Outlier Model specifications. The Last distributions generated in the 5 date to 15 date datasets of TS2 are slightly less consistently accurate than the corresponding End Boundaries (Table 30) and, in further contrast, there is some minor evidence that Last accuracy is proportional to dataset size. Overall, the most consistently accurate Last distributions in TS2 were generated by the uniform prior/default Charcoal Outlier Model approach; and this was the only model specification to generate accurate Last distributions at 95% probability from all TS2 datasets, with 87% of these also accurate at 68% probability (Table 13). That these accuracy percentages are identical to those reported for exponential prior/Charcoal Outlier Model End Boundary distributions is salient and will be returned to below.

Relative precision in End Boundary and Last distributions across both theoretical studies consistently decreases with increasing dataset IA τ , decreasing dataset size, and the imposition of a uniform prior distribution or Charcoal Outlier Model, and each of these factors has a cumulative effect. This is illustrated by the average precision of Last and End Boundary distributions generated using the exponential Prior/modified Charcoal Outlier Model approach in TS1 and TS2 where increasing dataset IA τ above 100 years or reducing dataset size below 10 dates has considerable impact, even though these datasets

Table 25 Last and End Boundary distributions generated by different Bayesian models from the 3 date Achauduin Castle MERLF radiocarbon dataset, with TPQ and TAQ probabilities

Model specification	Last HPD intervals/cal AD				End Boundary HPD Intervals/cal AD				Agreement indices				
	68%	95%	Median	After TPQ	Before TAQ	68%	95%	Median	After TPQ	Before TAQ	Amodel	Aoverall	Ai
Exponential prior; no outlier	1275–1305	1270–1385	1295	55%	81%	1275–1385	1265–1535	1310	81%	48%	82.8	82.2	0
Exponential prior; modified Charcoal	1280–1320	1270–1405	1300	78%	63%	1280–1395	1270–1550	1325	91%	35%	84	83.6	0
Exponential prior; default Charcoal	1275–1385	1270–1460	1305	81%	54%	1280–1410	1270–1610	1335	92%	30%	83.1	82.7	0
uniform prior; default Charcoal	1280–1390	1270–1480	1310	83%	50%	1280–1450	1275–1820	1375	95%	19%	81.7	81.5	0

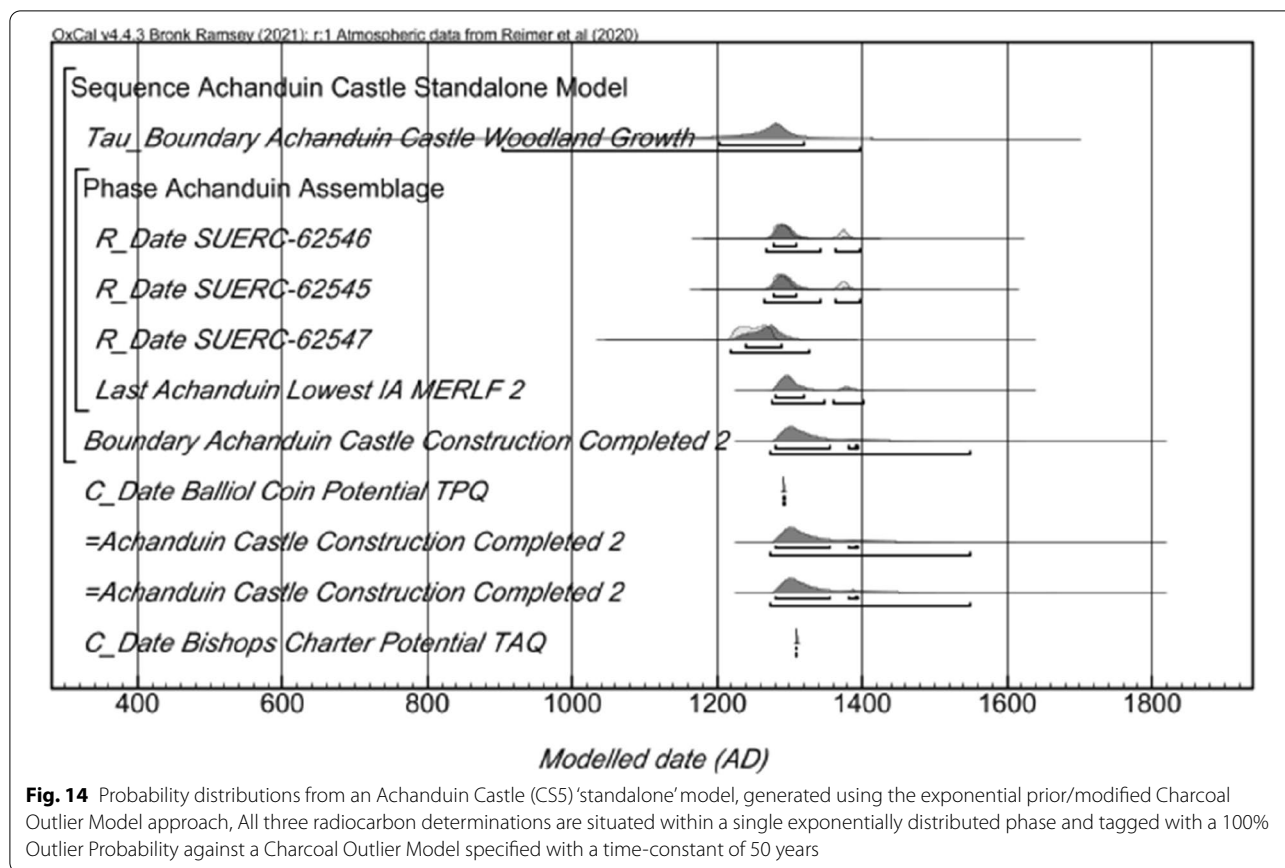


Table 26 Radiocarbon results, dataset age ranges and Combine distributions associated with the MERLF assemblage from Lismore Cathedral nave (CS6)

Lismore Cathedral nave	Radiocarbon results			Modelled distributions	
Laboratory code	SUERC-75732	SUERC-75726	SUERC-75727	Dataset age range (years)	Combine range (cal AD)
Sample taxon	<i>Quercus</i>	<i>Quercus</i>	<i>Corylus</i>		
$\delta^{13}C$ (‰)	- 23.9‰	- 25.5‰	- 29.6‰		
^{14}C age (BP)	921 ± 30	843 ± 30	616 ± 30		
Calibrated date 68% probability (cal AD)	1040–1170	1170–1260	1300–1400	175–300	1250–1265
Calibrated date 95% probability (cal AD)	1030–1210	1160–1270	1290–1400	125–345	1250–1275

Combine distributions have been highlighted in bolditalic emphasis as this model presented poor agreement and the dataset failed a chi-square type test

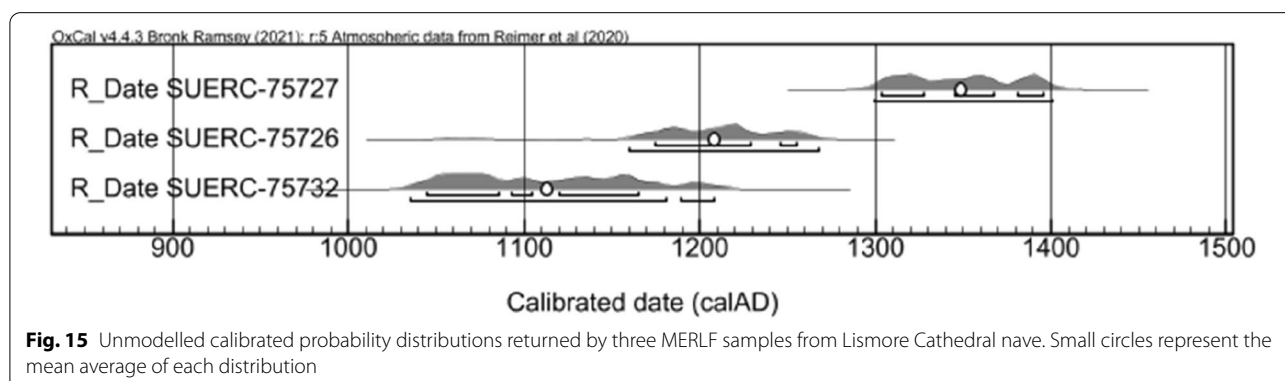


Table 27 Last and End Boundary distributions generated by different Bayesian models from the 3 date Lismore Cathedral nave MERLF radiocarbon dataset, with TPQ and TAQ probabilities

Model specification	Last HPD intervals/cal AD				End Boundary HPD intervals/cal AD				Agreement indices				
	68%	95%	Median	After TPQ	Before TAQ	68%	95%	Median	After TPQ	Before TAQ	Amodel	Aoverall	Ai
Exponential prior; no Outlier	1300–1395	1295–1400	1335	100%	24%	1305–1485	1295–1755	1425	100%	3%	72.3	72.2	0
exponential prior; modified Charcoal	1305–1400	1285–1540	1365	100%	9%	1320–1525	1300–1785	1445	100%	1%	74.4	74.4	0
Exponential prior; default Charcoal	1305–1405	1285–1595	1365	100%	9%	1315–1540	1305–1800	1450	100%	1%	74.4	74.4	0
Uniform prior; default Charcoal	1305–1405	1285–1585	1365	100%	8%	1325–1905	1320–1905	1520	100%	0%	74.3	74.3	0

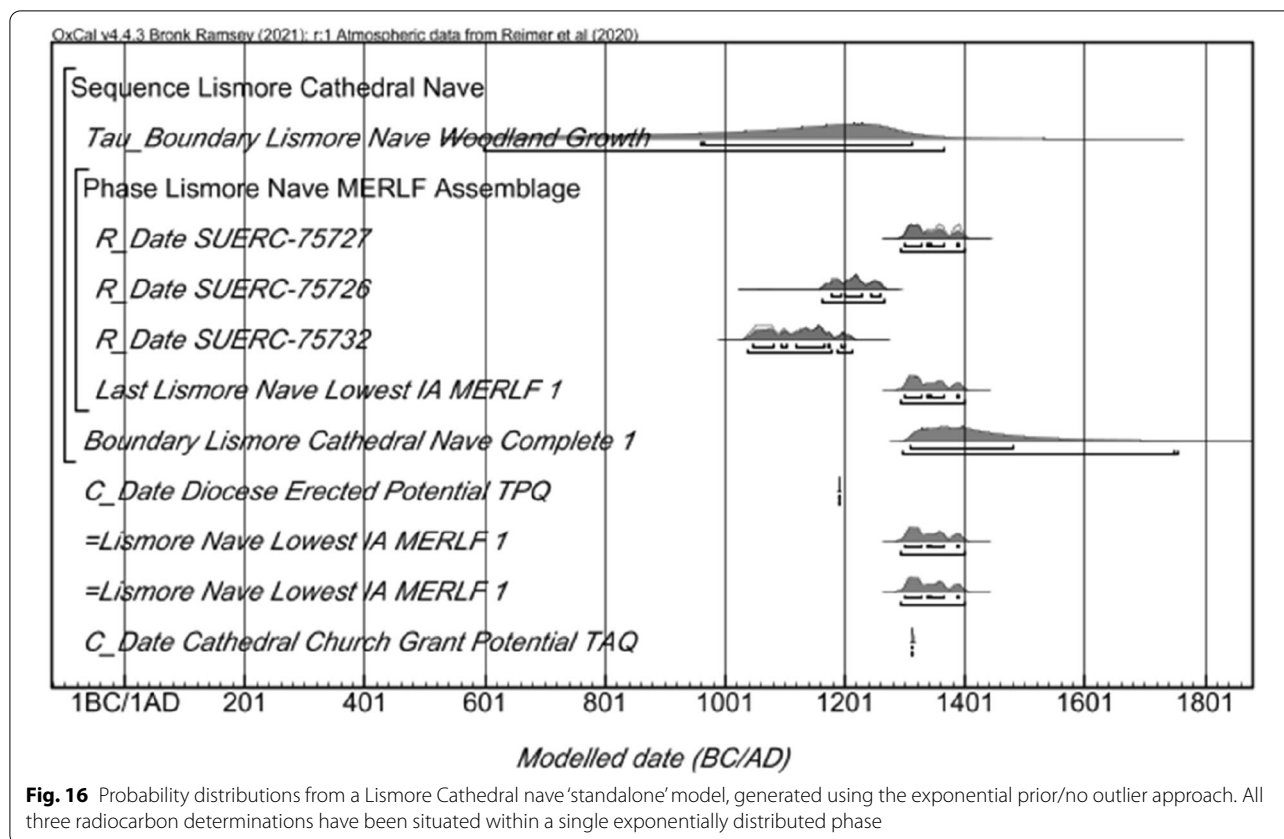


Table 28 Average percentages of accurate dates in TS1 and TS2 datasets (from Tables 2 and 11)

Dataset size	Specified dataset IA τ				
	10 years	50 years	100 years	200 years	500 years
20 date	95% (19/20)	65% (13/20)	58% 11.5/20	25% (5/20)	12.5% (2.5/20)
15 date	98% (14.7/15)	62% (9.3/15)	49% 7.3/15	33% (5/15)	8.7% (1.3/15)
10 date	97% (9.7/10)	77% (7.7/10)	40% (4/10)	33% (3/100)	13% (1.3/10)
5 date	94% (4.7/5)	66% (3.3/5)	66% (3.3/5)	20% (1/5)	6% (0.3/5)

Table 29 Average dataset age ranges in TS1 and TS2 (from Tables 2 and 11)

Dataset size	Specified dataset IA τ				
	10 years	50 years	100 years	200 years	500 years
20 date	5–235	105–325	330–550	465–680	2420–2705
15 date	10–240	75–285	195–390	560–815	2225–2490
10 date	– 10–225	65–270	185–435	315–565	1375–1670
5 date	– 5–225	45–250	110–350	375–615	1040–1350

were generated independently (Tables 33 and 34). Last distributions are generally more precise than End Boundary estimates at both 68% and 95% probability,

and thereby variations in dataset IA τ , dataset size, and model specification have a reduced impact. Conversely, given that reducing the Charcoal Outlier Model time-constant appears to have increased precision in broader 20 date TS1 End Boundary distributions subject to uniform priors and high dataset IA τ , it is reasonable to expect that time-constant variation would also have a greater effect where dataset size is very reduced and generated estimates broad (see below).

The older latest dates associated with smaller and higher IA τ datasets in TS1 and TS2 (Tables 2 and 11) generally result in End Boundaries with older lower limits, and the implications of this relationship for

Table 30 End Boundary and Last distribution accuracy in all TS1 and TS2 models. (from Tables 5 and 13)

Study code	Accurate end boundaries/ 68%	Accurate end boundaries/ 95%	Accurate last distributions/ 68%	Accurate last distributions/ 95%
TS1 (20 date datasets)	85%; 102/120	98%; 118/120		
TS2 (15–5 date datasets)	84%; 113/135	99%; 133/135	81%; 109/135	95%; 128/135
Total	84%; 215/255	98%; 251/255		

Table 31 End Boundary accuracy, model specification and dataset IAt in main models. (from Tables 5 and 13)

Specified dataset IAt	Study code	Exponential prior; no outlier	Exp. prior; modified Charcoal	Uniform prior; default Charcoal	All model and dataset specifications	
		68% (95%)	68% (95%)	68% (95%)	68%	95%
10 years	TS1	4/4 (4/4)	4/4 (4/4)	3/4 (4/4)	38/39	39/39
	TS2	9/9 (9/9)	9/9 (9/9)	9/9 (9/9)		
50 years	TS1	4/4 (4/4)	4/4 (4/4)	3/4 (4/4)	30/39	39/39
	TS2	7/9 (9/9)	7/9 (9/9)	5/9 (9/9)		
100 years	TS1	4/4 (4/4)	4/4 (4/4)	2/4 (4/4)	31/39	38/39
	TS2	8/9 (8/9)	7/9 (9/9)	6/9 (9/9)		
200 years	TS1	2/4 (4/4)	3/4 (4/4)	4/4 (4/4)	30/39	38/39
	TS2	6/9 (8/9)	7/9 (9/9)	8/9 (9/9)		
500 years	TS1	3/4 (4/4)	3/4 (4/4)	2/4 (3/4)	34/39	38/39
	TS2	8/9 (9/9)	9/9 (9/9)	9/9 (9/9)		
All datasets at 68%		85% 55/65	88% 57/65	78% 51/65	84% 163/195	
All datasets at 95%		97% (63/65)	100% (65/65)	98% (64/65)		98% 192/195
≤ 200-yr IAt datasets at 68%		85% 44/52	87% 45/52	77% 40/52	83% 129/156	
≤ 200-yr IAt datasets at 95%		96% (50/52)	100% (52/52)	100% (52/52)		99% 154/156

Table 32 Accuracy of different model specs and dataset sizes in TS1 and TS2 (from Tables 5 and 13)

Model specification	Last			End Boundary			
	15 date	10 date	5 date	20 date	15 date	10 date	5 date
exponential prior/no outlier	12/15 (12/15)	11/15 (13/15)	10/15 (12/15)	17/20 (20/20)	12/15 (14/15)	12/15 (14/15)	14/15 (15/15)
exponential prior/ Charcoal Outlier	12/15 (15/15)	12/15 (14/15)	13/15 (14/15)	18/20 (20/20)	13/15 (15/15)	13/15 (15/15)	13/15 (15/15)
uniform prior/ Charcoal Outlier	14/15 (15/15)	12/15 (15/15)	13/15 (15/15)	14/20 (19/20)	10/15 (15/15)	13/15 (15/15)	13/15 (15/15)
Totals 68%	38/45 84%	35/45 78%	36/45 80%	49/60 82%	35/45 78%	38/45 84%	40/45 89%
Totals 95%	42/45 93%	42/45 93%	41/45 91%	59/60 98%	44/45 98%	44/45 98%	45/45 100%

estimate accuracy are clearly illustrated where that latest dataset date does not contain the true event. In TS2 dataset MRRR1d run 3, for example, the latest date (MRRR5d) is too early at 68% confidence (1020–1160 cal AD) and 95% confidence (990–1160 cal AD),

and thereby the End Boundary and Last distributions generated by all models at 68% probability and the Last distributions generated by both exponential prior approaches at 95% probability are also too early (Table 12). No latest dataset dates are inaccurately late

Table 33 Average precision of End Boundary HPD intervals generated by the exponential prior/modified Charcoal Outlier Model approach in main TS1 and TS2 models, in years. (summarised from Tables 7 and 14)

Dataset IAT	Dataset size			
	20 date	15 date	10 date	5date
10 years	34 (53)	32 (53)	35 (57)	48 (118)
50 years	38 (63)	40 (72)	38 (75)	68 (170)
100 years	39 (71)	47 (90)	57 (120)	98 (230)
200 years	58 (120)	98 (152)	83 (172)	155 (398)
500 years	96 (216)	118 (263)	142 (328)	331 (882)

Table 34 Precision of Last distributions generated by the exponential prior/modified Charcoal Outlier Model approach in main TS1 and TS2 models, in years (summarised from Tables 8 and 14)

Dataset IAT	Dataset size			
	20 date	15 date	10 date	5 date
10 years	30 (50)	28 (52)	32 (53)	42 (73)
50 years	33 (58)	37 (67)	32 (63)	47 (92)
100 years	35 (68)	45 (80)	50 (102)	68 (137)
200 years	55 (110)	87 (133)	68 (147)	92 (217)
500 years	80 (210)	82 (203)	93 (243)	148 (332)

at 95% probability in these theoretical studies, but in TS1 dataset M1e run 3 the latest date (M5e) is too late at 68% confidence (1260–1300 cal AD), and the End Boundary distributions generated by all models from this dataset are also too late at 68% probability (Table 4). Indeed, the End Boundaries generated by both uniform prior/Charcoal Outlier Models from this dataset are also too late at 95% probability, and these are the only two inaccurate End Boundary HPD intervals at 95% probability in TS1.

The data associated with these examples also illustrate how model specification can mitigate against latest date variation, since the earlier distributions generated by models with exponential priors are generally more accurate where the latest dataset date is relatively late, whilst the older estimates generated by models incorporating the Charcoal Outlier Model are generally more accurate where the latest dataset date is relatively early. In TS2 dataset MRRR1c run 3, for example, the latest simulated date contains the true event at 95% confidence (1220–1380; MRRR1c) but is too late at 68% confidence (1260–1300 cal AD; MRRR1c; Additional file 2: Sect. 2.9.10); and in this instance both Charcoal Outlier modelling approaches

have generated inaccurately late End Boundaries at 68% probability, and only the exponential/no outlier approach has generated an accurate End Boundary at 68% probability. In contrast, the only two inaccurate End Boundaries at 95% probability in TS2 are too early (MR1c run 3 and MRR1d run 1) and, predictably therefore, these distributions are associated with comparatively early dataset latest dates and exponential prior/no outlier modelling approaches.

These processes also have implications for distribution selection; since the earlier Last distributions are often more accurate than End Boundaries where a comparatively late latest date pertains (e. g. TS2, MR1b run 2, exponential prior/no outlier) while End Boundaries are more accurate where an early latest date pertains. Indeed, given the preponderance of relatively early dates, this might explain the comparatively greater consistency of End Boundary distributions overall. The estimates generated from the TS2 dataset MRR1d run 1 illustrate how these processes affect both distribution and model selection, since the latest date (MRR3d) contains the true date at 95% confidence (1040–1270 cal AD) but is too early at 68% confidence (1050–1230 cal AD) (Table 11), and thereby: the End Boundary generated by the exponential prior/no outlier modelling approach is too early at 95% probability; the End Boundaries generated by both exponential prior models are too early at 68% probability; the Last distributions generated by both exponential prior models are also too early at 95% probability; and the Last distributions generated by all three modelling approaches are too early at 68% probability (Table 12). The uniform prior/Charcoal Outlier Model approach, however, has generated accurate End Boundary estimates at both 95% and 68% probability from this high IAT dataset, as well as an accurate Last distribution at 95% probability.

Ultimately, the Last and End Boundary distributions generated by different model specifications form a continuous chronological spectrum: from the very early and precise Last distributions generated from large low IAT datasets by the exponential prior/no outlier modelling approach; to the later and more imprecise End Boundary distributions generated from small high IAT datasets by the uniform prior/Charcoal Outlier Model approach. The evidence presented in TS2 also suggests this spectrum correlates with the accuracy of estimates generated from datasets subject to different IAT/size characteristics: wherein the exponential prior/no outlier approach has generated the most consistently accurate Last distributions from datasets with an IAT which is lower than 100 years (where latest dates are likely to be relatively late), and

the uniform prior/Charcoal Outlier approach has generated the most consistently accurate Last distributions from datasets of 100 years IA τ and above (where latest dates are likely to be relatively early) (Table 13). Unsurprisingly, given their precision, the proximity of the Last distribution median values to the true event date follows this same pattern (Table 15), while the accuracy threshold between these contrasting approaches is slightly broader in the End Boundary distribution evidence. Both exponential prior approaches present the most consistently accurate End Boundary distributions from datasets with an IA τ lower than 100 years in TS1 and TS2, and approaches which include a Charcoal Outlier Model are more consistently accurate from 200 years IA τ and above (although this breaks down at 500 years IA τ in TS1) (Table 31). That a considerable overlap between these theoretical Last and End Boundary spectra also pertains is clearly illustrated in the TS2 results, wherein the most consistently accurate End Boundaries have been generated by the exponential prior/Charcoal Outlier Model approach, whilst the most consistently accurate Last distributions have been generated by the uniform prior/Charcoal Outlier Model approach. Indeed, both approaches have generated accurate estimates from all datasets at 95% probability and 87% of all models at 68% probability, while closely comparable average precision and median values between these different distributions confirms they overlap considerably (Tables 13, 15 and 17).

These results are consistent with those presented by previous authors. If the 500yrs IA τ datasets are disregarded, then the uniform prior/Charcoal Outlier Model approach does indeed generate more consistently accurate End Boundary distributions than

the exponential prior/no outlier approach [17], with this latter approach once again returning some precise but inaccurate End estimates at 95% probability (Table 16). These inaccuracies are limited to datasets above 50 years IA τ , however, and the End Boundary estimates generated by the exponential prior/Charcoal Outlier Model approach are more consistently accurate overall. In the above studies this is even evident where dataset IA τ range is much reduced, and most particularly so with lower IA τ datasets where the less accurate and less precise uniform prior approach has been specified. These data, therefore, also support previous MERLF analysis protocols which had promoted a binary short-lived (exponential prior) and long-lived (Charcoal Outlier Model) approach [7]; but allows an increased role for exponential prior model specifications and further understanding of how these relate to Combine and Charcoal Outlier Model approaches. The accuracy of the Combine distributions generated from 10 years IA τ datasets is also resonant of Waterbolk's (1971) Group A samples which, he suggested, would extend up to 20 years [10]. Ultimately, these theoretical results provide a less binary Bayesian framework which can inform our interpretations of the datasets returned by MERLF materials from the six Scottish medieval case study buildings.

The case studies

The compositions presented by these case study MERLF assemblages confirm that a range of different locally available tree taxa were exploited for limekiln fuel in Scotland during this period, and the maximum age ranges presented by the resulting radiocarbon datasets are generally consistent with the taxa-specific and habitat-contingent IA τ of those woodland

Table 35 Case study MERLF assemblage and radiocarbon dataset character. (from Tables 16, 18, 20, 22, 24, 26, Appendix 1: Table 37).

Case study	Site and building name	Dataset size	MERLF taxa	5% statistical consistency	Combine agreement	Age range 95% (years)
CS1	Castle Fincharn main block	5	Corylus	Pass	Good	– 30 to 220
CS2	Aros Castle north-west block	5	Betula Corylus	Fail	Poor	35 to 190
CS3	Castle Roy enclosure and tower	5	Betula Pinus	Pass	Poor	– 75 to 210
CS4	Lochindorb Castle primary enclosure	5	Quercus	Fail	None	1555 to 1925
CS5	Achanduin Castle enclosure and hall	3	Betula Quercus	Pass	Good	0 to 155
CS6	Lismore Cathedral nave	3	Quercus/Corylus	Fail	Poor	125 to 345
CS4*	Lochindorb Castle reduced dataset	4	Quercus	Pass	Poor	10–220

MERLF taxa determining model time-constant are in bold

sources. This includes: the radiocarbon dataset associated with the *Corylus* sp. dominated assemblage from Castle Fincham, which generated an age range of – 30 to 220 years consistent with a 5 date mean lifespan of 10 years IA τ or less; the dataset associated with the *Betula* sp. dominated assemblage from Castle Aros which generated an age range of 35 to 190 years consistent with a 5 date mean lifespan of 50 years IA τ or less; and the smaller dataset associated with the *Quercus* sp. dominated assemblage from Lismore Cathedral nave, which nevertheless generated an age range of 125 to 345 years consistent with a 5 date mean lifespan of 200 years IA τ or less (Table 35).

The association of some taxa or environments with comparatively high mean lifespans does not of course preclude the exploitation of shorter-lived or immature wood, where growth habits and woodland population dynamics allow. Indeed, although the case study results presented here are biased by an analysis strategy which privileged the selection of shorter-lifespan taxa, it is evident from the statistical consistency and relatively narrow age ranges presented by the mixed assemblages from Castle Roy (CS3) and Achanduin Castle (CS5) that short-lived fragments of long life-span taxa were also included in limekiln charges (Table 35). The only case study dataset which generated an age range broader than expected is associated with the *Quercus* sp. dominated assemblage from Lochindorb Castle, which returned a dataset age range (1555 to 1925 years) consistent with a 5 date mean lifespan of over 500 years IA τ . This is improbable, and when the single very early radiocarbon determination (SUERC-75752) is manually excluded from the model, the age range of the remaining dataset (10–220 years; Additional file 3: Sect. 3.37) is consistent with a 5 date dataset of 50 years IA τ or less.

Pre-existing historical, architectural, and archaeological evidence has situated initial building construction at the six case study sites in the same long 13th-century period, and within chronological periods ranging between 18 and 122 years (Table 36). The relationships between this evidence and the masonry buildings under consideration are indirect and open to challenge, and these periods are much broader than the true event date from which the simulated datasets were generated in TS1 and TS2. The lack of terminal ring evidence in five of the case study assemblages, moreover, introduces a bridging period between these datasets and the constructional date which does not apply to those theoretical studies. However, all case study datasets contain at least one latest date which is consistent with the pre-existing evidence from other disciplines, five of the six present latest dataset dates

which extend past their potential historical TAQs, and none are inconsistently late (Table 36). This evidence suggests the volume of material missing material from these MERLF fragments (and so the extent of that bridging period) is quite limited and, although small dataset sizes limit the interpretive potential of their unmodelled distributions (Figs. 5, 7, 9, 11, 13, 15), these case study datasets generally contain high fractions of consistent dates.

As in both main theoretical studies, the Last and End Boundary distributions generated from these case study datasets present continuous chronological spectra: from the earliest and most precise Last distributions generated using the exponential prior/no Outlier approach; to the later and broader distributions generated using the uniform prior/Charcoal Outlier Model (Tables 14, 16, 18, 20, 22, 24). It is notable that modifying Charcoal Outlier Model time-constants to reflect the mean lifespans of the dominant taxa has increased Last and End Boundary precision in all six case studies and, in line with its increased effect on less precise distributions in TS1, this probably reflects the smaller size of these case study datasets. An overlap between the latest Last distributions and earliest End Boundary is again evident in these studies, and this is very clearly illustrated in overlapping estimate-TPQ/TAQ percentages.

The sum of these estimate-TPQ-TAQ percentages reflects contrasts in the precision of these different types of evidence, and these vary from Castle Fincham (whose high sum percentages reflect a low IA τ *Corylus* sp. dominated MERLF radiocarbon dataset and the moderate precision of the pre-existing documentary evidence relating to the wider site) and Lochindorb Castle and Lismore Cathedral nave (which are both associated with relatively high age range *Quercus* sp. dominated MERLF radiocarbon datasets). Except for the estimate generated by the uniform prior/Charcoal Outlier Model approach to the Lismore Cathedral nave dataset, all Last and End Boundary distributions generated by these different model specifications at 95% probability are consistent with the other evidence relating to these sites, and the proximity of some of these estimate-TPQ-TAQ probability sums to 200% indicates that these Bayesian estimates are closely consistent with that evidence. The consistency of this evidence usefully suggests that the masonry buildings from which these MERLF samples were removed can be reasonably associated with the wider evidence relating to these sites, and where late latest dates have defined comparatively late lower estimate limits (e. g. Aros Castle NW block and Lismore Cathedral nave) then considerable gains in

Table 36 Comparative summary of chronological evidence relating to case study buildings and sites. (from Tables 17, 19, 21, 22, 25, 27)

Case study site and building name	Potential TPQ-TAQ (AD)	TPQ-TAQ range (years)	Latest dataset date (cal AD)		Consistent dataset dates		Estimate/TPQ-TAQ probability sums		Most consistent Last estimates generated		Model
			68%	95%	68%	95%	End (%)	Last (%)	68%	95%	
Castle Fincharn main block	1240–1308	68	1230–1290	1220–1380	5/5	5/5	185–191	190–195	1250–1285	1230–1295	Exp. prior/ mod. Char
Aros Castle NW block	1270–1385	115	1300–1400	1290–1410	4/5	5/5	152–176	176–193	1295–1380	1290–1395	Exp. prior/ no outlier
Castle Roy enclosure/tower	1150–1226	76	1150–1220	1040–1260	4/5	5/5	142–162	164–173	1155–1220	1050–1225	Exp. prior/ no outlier
Lochindorb Castle enclosure	1258–1279	21	1170–1260	1160–1270	1/5	2/5	102–110	108–113	1185–1280	1160–1485	Exp. prior/ mod. Char
Achanduin enclosure/hall	1292–1310	18	1270–1380	1260–1390	2/3	2/3	114–129	133–141	1280–1320	1270–1405	Exp. prior/ mod. Char
Lismore Cathedral nave	1192–1314	122	1300–1400	1290–1400	2/3	3/3	100–103	108–124	1300–1395	1295–1400	Exp. prior/ no outlier

multidisciplinary interpretation precision have been made. It is salient that the datasets associated with both of these sites are high IA and statistically inconsistent at 5% probability, however, and therefore the End Boundary distributions generated from these data are relatively broad.

Recognising how we might retain accuracy while maximising precision through sample selection and model specification requires further comparison with the theoretical and ecological data. Variation in dataset age ranges and levels of statistical consistency across these studies suggests that the assemblages did include materials subject to some IA, and only two of these case study datasets have presented good Combine agreement indices (even including the reduced Lochindorb Castle CS4* dataset) (Table 35). That Combine distributions could be generated at all suggests the IA associated with five of these assemblages is reasonably limited, however, and comparison with the theoretical data from TS1 and TS2 suggests four of the six case studies (or five if the reduced Lochindorb Castle is included) present dataset age ranges consistent with mean lifespans associated with less than 50 years IA τ . Importantly, this situates these four-five studies below the considerable reduction in estimate precision associated with theoretical datasets subject to IA τ s of over 100 years in TS1 and TS2 (Tables 32 and 34), and all (100%) End Boundary and Last distributions generated from such narrowly distributed 5 date datasets were consistently accurate in TS2 at both 95% and 68% probability (Table 13). The estimate/TPQ-TAQ sum percentages also illustrate that interdisciplinary consistency generally increases with precision, and the most consistent estimates across all six case studies were Last distributions generated by exponential prior modelling specifications. Indeed, in most cases these Last distributions are very similar to each available latest dataset date, and constructional dates close to the lower limits of these distributions are often most convincing.

The association of higher IA τ and small datasets with earlier latest dates and decreased fractions of accurate dates in TS1 and TS2 (Table 28) suggests that it would be prudent to include a Charcoal Outlier Model within model specifications where radiocarbon datasets are less narrowly distributed, and yet the botany suggests different approaches to the case study evidence are probably required. Both *Quercus* sp. dominated case study assemblages (Lochindorb Castle enclosure and Lismore Cathedral nave) are

statistically inconsistent at 5% significance, but the Lochindorb dataset contains an extremely early determination, high age range, and low fraction of consistent dates. This assemblage is completely dominated by *Quercus* sp. samples, and although manual exclusion of the early determination has decreased dataset IA τ considerably, this still contains only two dates which are consistent with historical evidence at 95% probability and the latest date does not extend beyond the documentary TAQ at either 68% or 95% probability (Appendix 1: Table 37). Notably, this reduced dataset is also the only example to generate End Boundary estimates which are more consistent with the historical evidence than the earlier and more precise Last distributions, and the End Boundary generated by the exponential prior/modified Charcoal Outlier Model approach to the dataset is the most consistent overall (Appendix 1: Table 38). Archaeobotanical and statistical evidence suggests this approach is less relevant to the Lismore Cathedral nave study since, although the high age range associated with this small dataset is largely predicated on residuality in two early *Quercus* sp. fragments, the latest date is associated with a fragment of *Corylus*. Since the uniform prior/Charcoal Outlier Model approach to this dataset has generated the only inconsistent estimate in the data from all six studies (Table 27), it is entirely possible that the calibrated radiocarbon date associated with this latter fragment is relatively late. This latest determination allows the 200 years or less IA τ of the wider *Quercus*-dominated radiocarbon dataset and its relationship to the constructional event to be interpreted with greater confidence. Notably, this latest radiocarbon determination also calibrates to a date almost identical to the Last distribution generated from the wider dataset using the (most precise) exponential prior/no Outlier approach, and this currently represents the most convincing estimate for the construction of this fabric. The correlation between dataset IA τ and latest date does not hold for the radiocarbon evidence returned by this mixed-taxa assemblage, and the application of a Charcoal Outlier Model approach to this very small dataset is inappropriate.

Conclusion

This paper has presented further evidence that a range of different tree taxa were exploited for limekiln fuel in Scotland during the medieval period, and the range of MERLF taxa surviving from this process are generally consistent with regional phytogeographic

distributions. The samples selected from these assemblages for radiocarbon analysis have returned datasets characterised by an array of different age range distributions and most of these are associated with some level of IA. At this stage in the research cycle, however, the IA τ of these materials does appear to be constrained by the taxa-specific and habitat-contingent lifespans and post-mortem durabilities of the parent wood fuels. Given that shorter lifespan taxa were generally selected for radiocarbon analysis where possible, it seems probable that the carbon distributions in these assemblages are generally equivalent to the available woodland source. MERLF assemblages can therefore be considered an excellent source of palaeoenvironmental information, with a research potential again underscored by the stratigraphically secure mortar material within which these materials have been entrapped.

The MERLF assemblages considered in this paper are dominated by wood-charcoal fragments without surviving terminal ring evidence, and the range of radiocarbon determinations returned by selected samples suggests that calibrated dates from single determinations, unweighted mean averages of multiple determinations and/or bulk samples, cannot be accepted as direct evidence for the construction of masonry buildings without other forms of evidence. The TPQ role performed by such determinations can be of considerable value for multidisciplinary interpretation, particularly where the radiocarbon evidence is relatively late and documentary evidence is convincing and early. Increasing the potential for these buildings and materials to inform interdisciplinary (rather than multidisciplinary) discourse, however, requires accurate standalone constructional estimates of greater precision.

In the absence of non-residual intrusive materials, the generation of accurate Last and End Boundary distributions from MERLF radiocarbon datasets subject to significant IA relies more on the accuracy of the latest available determination, than on dataset IA τ , dataset size, or model specification. Last and End Boundary precision, however, is very closely related to all three of these parameters; decreasing with increasing dataset IA τ , decreasing dataset size, and model specifications which include uniform priors or Charcoal Outlier Models. These factors are interrelated and can be cumulative, and the Last and End Boundary distributions generated by different model specifications thereby present continuous and overlapping spectra. These range from the early and precise Last distributions generated from large low-IA τ datasets by models specified with an exponential prior/

no outlier approach; to the later and less precise End Boundary distributions generated from small high-IA τ datasets by models specified with uniform priors and the default Charcoal Outlier Model.

Different Bayesian model specifications can therefore be imposed on MERLF radiocarbon data to maximise precision whilst retaining accuracy. The data relating to the 13th-century events presented in this paper suggests that: (i) Where the IA τ of a dataset is limited in 10 years or less, then determinations are likely to be statistically consistent at 5% significance and a Combine average distribution is likely to represent an accurate and very precise constructional estimate; (ii) Where the IA τ of a dataset is limited to 50 years or less, then determinations are unlikely to be statistically consistent at 5% significance and Combine agreement indices will be poor, but the Last distribution generated by a model specified with exponential priors is likely to represent an accurate and reasonably precise constructional estimate; and (iii) Where the IA τ of a dataset is greater than 100 years, then a Last distribution generated by a model with a Charcoal Outlier Model is likely to generate an accurate but imprecise constructional estimate, while modification of the outlier time-constant is likely to increase precision where dataset size is limited.

The studies considered in this paper provide further evidence that Bayesian techniques can generate consistently accurate constructional estimates for medieval masonry buildings from MERLF radiocarbon data, whatever the ecological provenance of the limekiln fuel source. Estimate precision is contingent upon source ecology but can be increased by a more informed approach to materials analysis and interpretation. The radiocarbon evidence considered here and elsewhere [7, 76] is biased by the selection of single entity MERLF fragments from shorter lifespan tree taxa, where possible, and most of these have returned determinations consistent with (i) and (ii) above. It seems likely this has enabled the generation of more precise constructional estimates, although in many cases precision might be further increased by expanding these radiocarbon datasets to include higher precision (reduced error margin) analysis of short lifespan MERLF fragments.

Appendix 1

CS4*—Lochindorb Castle Phase 1 (*with reduced dataset manually excluding determination SUERC-75752)

See Tables 37 and 38; Figures 17 and 18.

Table 37 Radiocarbon results, dataset age ranges and Combine distributions associated with the reduced MERLF assemblage from Lochindorb Castle (CS4*), after manually excluding determination SUERC-75752

		Radiocarbon results		Modelled distributions	
		SUERC-75754	SUERC-75753	SUERC-75751	SUERC-75747
Laboratory code					
Sample taxon		<i>Quercus</i>	<i>Quercus</i>	<i>Quercus</i>	<i>Quercus</i>
$\delta^{13}\text{C}$ (‰)		- 26.1	- 24.7	- 25.3	- 26.5
^{14}C age (BP)		940 ± 31	932 ± 31	862 ± 31	835 ± 31
Calibrated date 68% probability (cal AD)		1040–1160	1040–1160	1160–1220	1170–1260
Calibrated date 95% probability (cal AD)		1020–1180	1030–1210	1050–1270	1160–1270
					60–175
					10–220
					1155–1210
					1050–1215

Table 38 Last and End Boundary distributions generated by different Bayesian models from the (reduced) 4 date Lochindorb Castle MERLF radiocarbon dataset, with TPQ and TAQ probabilities

Model specifications	Last HPD intervals/cal AD				End Boundary HPD intervals/cal AD				Agreement indices				
	68%	95%	median	after TPQ	before TAQ	68%	95%	median	after TPQ	before TAQ	Amodel	Aoverall	Ai
Exponential prior; no outlier	1175–1230	1165–1265	1210	3%	100%	1175–1270	1155–1420	1230	29%	81%	71.3	70.8	0
Exponential prior; modified Charcoal	1180–1260	1160–1355	1225	22%	88%	1185–1295	1160–1480	1250	44%	68%	74.4	74.2	0
Exponential prior; default Charcoal	1180–1260	1160–1370	1225	23%	87%	1185–1295	1160–1500	1250	45%	67%	74.4	74.2	0
Uniform prior; default Charcoal	1185–1265	1160–1390	1230	26%	85%	1180–1345	1160–1690	1280	61%	50%	74.9	74.5	0

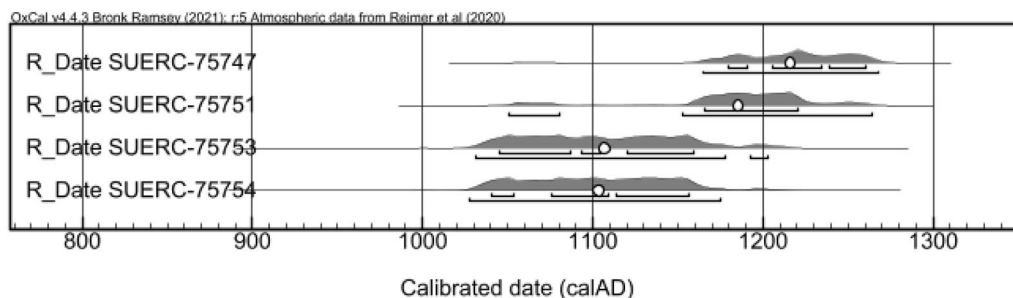


Fig. 17 Unmodelled calibrated probability distributions associated with four MERLF samples removed from the phase 1 enclosure of Lochindorb Castle. Small circles represent the mean average of each distribution

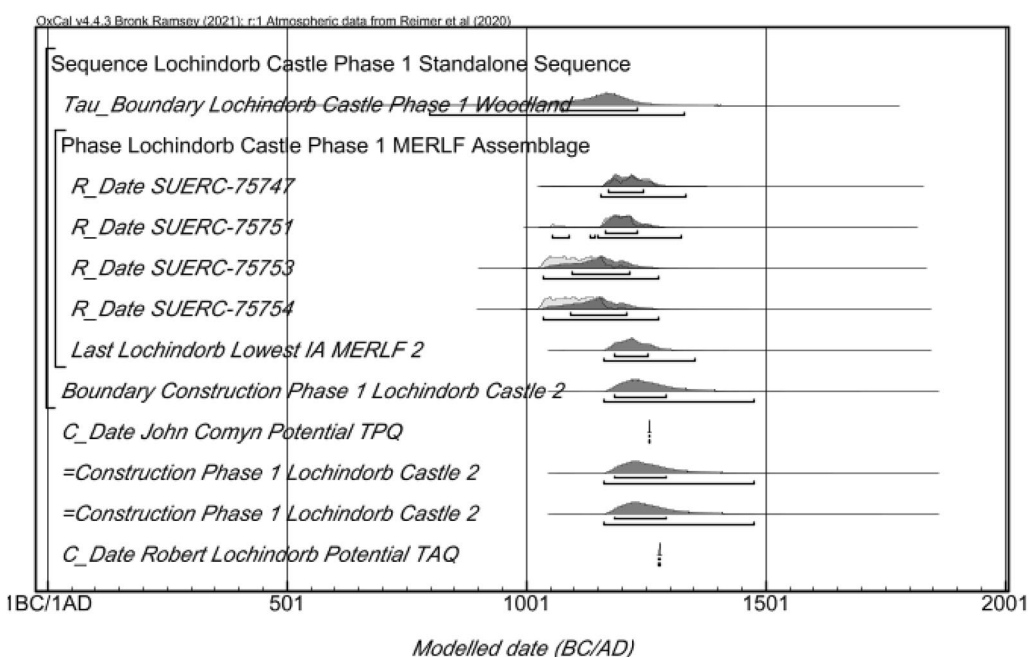


Fig. 18 Probability distributions generated from the reduced Lochindorb Castle dataset. All four radiocarbon determinations have been situated within a single phase with a Tau Start Boundary, and all four tagged with a 100% Outlier Probability within a Charcoal Outlier Model with a 300 year time-constant

Abbreviations

CS: Case Study; ESM: Electronic Supplementary Material; HPD: Highest Posterior Density; IA: Inbuilt Age; IA: Mean Dataset Inbuilt Age; MERLF: Mortar-Entrapped Relict Limekiln Fuel; TAQ: *terminus ante quem* (Limit before which); TPQ: *terminus post quem* (Limit after which); TS: Theoretical Study.

Supplementary Information

The online version contains supplementary material available at <https://doi.org/10.1186/s40494-021-00568-3>.

Additional file 1. Theoretical Study 1 (TS1).

Additional file 2. Theoretical Study 2 (TS2).

Additional file 3. Case Studies 1-6 (CS1-6 + CS4*).

Acknowledgements

The data reconsidered in this paper was generated during PhD research undertaken at the University of Edinburgh and post-doctoral research at the University of Stirling. Within these projects, charcoal identification was undertaken with Dr Mike Cressey (then at CFA Archaeology) and radiocarbon analysis was funded by Historic Environment Scotland. The author is grateful for the comments provided by two anonymous peers and the journal editor, which improved this paper significantly, and for their patience when the original manuscript was withdrawn in 2020 following the emergence of the new calibration curve.

Authors' contributions

This paper is the work of MT, who is sole author.

Funding

Not applicable.

Availability of data and materials

All the data relating to this paper are included in the main text and additional file.

Declarations

Competing interests

The authors declare that they have no competing interests.

Received: 17 May 2021 Accepted: 25 July 2021

Published online: 16 September 2021

References

- Gourdin W, Kingery W. The beginnings of pyrotechnology: Neolithic and Egyptian lime plaster. *J Field Archaeol*. 1975;2:133–50.
- Kingery W, Vandiver P, Prickett M. The beginnings of pyrotechnology, part II: production and use of lime and gypsum plaster in the pre-pottery Neolithic near-east. *J Field Archaeol*. 1988;15(2):219–34.
- Friesem D, Abadi I, Shaham D, Grosman L. Lime plaster cover of the dead 12000 years ago—new evidence for the origins of lime plaster technology. *Evol Hum Sci*. 2019;1:e9.
- Carò F, Riccardi M, Mazzilli SM. Characterization of plasters and mortars as a tool in archaeological studies: the case of Lardirago Castle in Pavia, northern Italy. *Archaeometry*. 2008;50:85–100.
- Elsen J, Mertens G, Van Balen K. Raw materials used in ancient mortars from the Cathedral of Notre-Dame in Tournai (Belgium). *Eur J Mineral*. 2011;23:871–82.
- Elsen J. Microscopy of historic mortars—a review. *Cem Concr Res*. 2006;36:1416–24.
- Thacker M. Dating medieval masonry buildings by radiocarbon analysis of mortar-entrapped relict limekiln fuels—a buildings archaeology. *J Archaeol Method Theory*. 2020. <https://doi.org/10.1007/s10816-020-09444-z>.
- Boaretto E. Dating materials in good archaeological contexts: the next challenge for radiocarbon analysis. *Radiocarbon*. 2009;51(1):275–81.
- Bayliss A, Bronk Ramsey C, van der Plicht J, Whittle A, Bradshaw and Bayes: towards a timetable for the Neolithic. *Camb Archaeol J*. 2007;17:1–28.
- Waterbolk H. Working with radiocarbon dates. *Proc Prehist Soc*. 1971;37:15–33.
- Warner R. A proposed adjustment for the "old-wood effect". In: Mook W, Waterbolk H (editors). In: Proceedings of the 2nd Symposium of 14C & Archaeology, Groningen 1987. 1990, p.159–72.
- Bowman S. Radiocarbon Dating. London: British Museum Publications; 1990. p. 50–1.
- Bronk RC. Dealing with outliers and offsets in radiocarbon dating. *Radiocarbon*. 2009;51(3):1023–45.
- Dean J. Independent dating in Archaeological Analysis. *Adv Archeol Method Theory*. 1978;1:223–55.
- McFadgen B. Dating New Zealand archaeology by radiocarbon. *NZ J Sci*. 1982;25:379–92.
- Dee M, Bronk Ramsey C, Shortland A, Higham T, Rowland J. Reanalysis of the chronological discrepancies obtained by the old and middle kingdom monuments project. *Radiocarbon*. 2009;51(3):1061–70.
- Dee M, Bronk RC. High-precision bayesian modeling of samples susceptible to inbuilt age. *Radiocarbon*. 2014;56(1):83–94.
- Ashmore P. Radiocarbon dating: avoiding errors by avoiding mixed samples. *Antiquity*. 1999;73:124–30.
- van Balen K. Understanding the lime cycle and its influence on historical construction practice. In: Huerta S, editor. In: Proceedings of the first international congress on construction history, Madrid, 20th–24th January 2003, Madrid.
- Enquist B, West G, Charnov E, Brown J. Allometric scaling of production and life-history variation in vascular plants. *Nature*. 1999;401:907–11.
- van Gelder H, Poorter L, Sterck F. Wood mechanics, allometry and life-history variation in a typical rain forest tree community. *New Phytol*. 2006;171(2):367–78.
- Marbà N, Duarte C, Agustí S. Allometric scaling of plant life history. *PNAS*. 2007;104(40):15777–80.
- Black B, Colbert J, Pederson N. Relationships between radial growth rates and lifespan within North American tree species. *Ecoscience*. 2008;15(3):348–57.
- Johnson S, Abrams M. Age class, longevity and growth rate relationships: protracted growth increases in old trees in the eastern United States. *Tree Physiol*. 2009;29:1317–28.
- Biondi F. From dendrochronology to allometry. *Forests*. 2020;11(2):146.
- Brown P. OLDLIST: a database of maximum tree ages. In: J Dean, D Meko, T Swetnam, editors. In: Tree rings, environment, and humanity: proceedings of the international conference, Tucson, Arizona, 17–21 May, 1994. *Radiocarbon* 1996, p. 727–31.
- Shorohova E, Kapitsa E. Influence of the substrate and ecosystem attributes on the decomposition rates of coarse woody debris in European boreal forests. *For Ecol Manage*. 2014;315:173–84.
- Gavin D. Estimation of Inbuilt Age in radiocarbon ages of soil charcoal for fire history studies. *Radiocarbon*. 2001;43(1):27–44.
- Di Filippo A, Pederson N, Baliva M, Brunetti M, Dinella A, Kitamura K, Knapp H, Schirone B, Piovesan G. The longevity of broadleaf deciduous trees in Northern Hemisphere temperate forests: insights from tree-ring series. *Front Ecol Evol* 2015; 3, article 46: 1–15.
- Rackham O. Ancient Woodland: its history, vegetation and uses in England. Kirkcudbrightshire: Castlepoint Press; 2003.
- Mitchell A. A field guide to the trees of Britain and Northern Europe. London: Collins; 1974.
- Cameron A. Managing birch woodlands for the production of quality timber. *Forestry*. 1996;69(4):357–71.
- Coppins A & Coppins B. *Atlantic Hazel*. Scottish Natural Heritage: Edinburgh; 2010.
- McVean D. Woodland and Scrub. In: J Burnett, editor. The Vegetation of Scotland. Oliver & Boyd: Edinburgh & London; 1964, pp 144–67.
- Jahn G. Temperate deciduous forests of Europe. In: Röhrig E, Ulrich B, editors. Ecosystems of the world 7: temperate deciduous forests; 1991, pp 377–502. Amsterdam: Elsevier. fig 13.12E.
- Stephenson N, et al. Rate of tree carbon accumulation increases continuously with tree size. *Nature*. 2014;507:90–3.
- Jenkins J, Chojnacky D, Heath L, Birdsey R. National-scale biomass estimators for United States tree species. *For Sci*. 2003;49(1):12–35.
- Harmon M, Franklin J, Swanson F, Sollins P, Gregory S, Lattin J, Anderson N, Cline S, Aumen N, Sedell J, Lienkaemper G, Cromack K, Cummins K. Ecology of coarse woody debris in temperate ecosystems. *Adv Ecol Res*. 1986;15:133–302.
- Manning S, Birch J, Conger M, Dee M, Griggs C, Hadden C, Hogg A, Bronk Ramsey C, Sanft S, Steier P, Wild E. Radiocarbon re-dating of contact-era Iroquoian history in north-eastern North America. *Sci Adv*. 2018. <https://doi.org/10.1126/sciadv.aav0280>.
- Ranius T, Niklasson M, Berg N. Development of tree hollows in pedunculate oak (*Quercus robur*). *For Ecol Manage*. 2009;257(1):303–10.
- White J. Forest and woodland trees in Britain. Oxford: Oxford University Press; 1995. p. 130.
- Nicholls G, Jones M. Radiocarbon dating with temporal order constraints. *J R Stat Soc Ser C Appl Stat*. 2001;50:503–21.
- Berger R. 14C Dating Mortar in Ireland. *Radiocarbon*. 1992;34(3):880–9.
- Berger R. Radiocarbon dating of early medieval Irish monuments. In: Proceedings of the royal Irish academy. Section C: Archaeology, Celtic Studies, History, Linguistics, Literature 95C 1995;(4): 159–74.
- Dee M, Wengrow D, Shortland A, Stevenson A, Brock F, Flink L, Bronk RC. An absolute Chronology for early Egypt using Radiocarbon dating and Bayesian Statistical Modelling. *Proc R Soc A*. 2013;469:20130395. <https://doi.org/10.1098/rspa.2013.0395>.
- van Strydonck M, van Der Borg K, de Jong A, Keppens E. Radiocarbon dating of lime fractions and organic material from buildings. *Radiocarbon*. 1992;34(3):873–9.
- Rutgers L, de Jong A, van der Borg K. Radiocarbon dates from the Jewish catacombs of Rome. *Radiocarbon*. 2002;44(2):541–7.
- Tubbs L, Kinder T. The use of AMS for the dating of lime mortars. *Nucl Instrum Methods Phys Res*. 1990;B52:438–41.
- Thacker M. The Castle of Achanduin, Lismore—a point of reference for the radiocarbon analysis of mortar-entrapped relict limekiln fuels. *Radiocarbon*. 2020;62(6):1563–75. <https://doi.org/10.1017/RDC.2020.57>.
- Ward G, Wilson S. Procedures for comparing and combining radiocarbon age determinations: a critique. *Archaeometry*. 1978;20:19–32.
- Bronk RC. Bayesian analysis of radiocarbon dates. *Radiocarbon*. 2009;51(1):337–60.

52. Thacker M. Castle Camus, Isle of Skye—buildings, materials & radiocarbon analysis in the borderlands of medieval Scotland. *Proc Soc Antiquaries Scotland*. 2020;149:277–301. <https://doi.org/10.9750/PSAS.149.1298>.
53. Reimer, et al. The IntCal20 Northern Hemisphere radiocarbon age calibration curve (0–55 cal kBP). *Radiocarbon*. 2020;62(4):725–57.
54. BSI. Durability of wood and wood-based products—Natural durability of solid wood—Part 2: guide to natural durability and treatability of selected wood species of importance in Europe. British Standards Institution: London; 2017.
55. Bronk RC. Radiocarbon calibration and analysis of stratigraphy: the OxCal program. *Radiocarbon*. 1995;37(2):425–30.
56. Bayliss A. Anglo-Saxon graves and grave goods of the 6th and 7th centuries AD: a chronological framework. 2017. Routledge: Oxford. p. 85–6.
57. Walters S, Betula L. in Britain. *Proc Bot Soc Br Isles*. 1968;7:179–80.
58. Gimingham C. Ecological aspects of Birch. *Proc R Soc Edinburgh Sect B Biol Sci*. 1984;85(1–2):65–72.
59. Pelham J, Gardiner A, Smith R, Last F. Variation in *Betula pubescens* Ehrh. (*Betulaceae*) in Scotland: its nature and association with environmental factors. *Bot J*. 1988;96(3):217–34.
60. Atkinson M. *Betula pendula* Roth (*B. verrucosa* Ehrh.) and *B. pubescens* Ehrh. *J Ecol*. 1992;80(4):837–70.
61. Edwards C, Mason W. Stand structure and dynamics of four native Scots pine (*Pinus sylvestris* L.) woodlands in northern Scotland. *Forestry*. 2006;79(3):261–77.
62. Mencuccini M, Oñate M, Peñuelas J, Rico L, Munne-Bosch S. No signs of meristem senescence in old Scots pine. *J Ecol*. 2014;102:555–65.
63. Stell G, Bailie M. The great hall and roof of Darnaway Castle, Moray. In: Sellar W, editor. *Moray: Province and People*. The Scottish Society for Northern Studies: Edinburgh; 1993. p. 163–86.
64. Crone A, Mills C. Timber in Scottish Buildings, 1450–1800—a dendrochronological perspective. *Proc Soc Antiqu Scotl*. 2012;142:329–69.
65. Wilson S. Native Woodlands of Scotland. Edinburgh: Edinburgh University Press; 2015. p. 133.
66. Thacker M. Constructing Lordship in North Atlantic Europe: the archaeology of masonry mortars in the medieval and later buildings of the Scottish North Atlantic. 3 Vols. Unpublished PhD. thesis. University of Edinburgh; 2016.
67. Thacker M. MacGillechrist's Castle: an environmental study in medieval buildings archaeology from Argyll. In: P Martin, editor. *Castles and Galleries. A re-assessment of the historic galley-castles of the Norse-Gaelic seaways*. IBT: Laxay; 2017. p. 157–71.
68. Thacker M. The medieval castle of Dun Aros: buildings archaeology and chronological consistency on the shores of the Sound of Mull. In: *Proceedings of the Society of Antiquaries of Scotland 2021*, Forthcoming.
69. Thacker M. Castle Roy: investigating medieval cultural landscapes, buildings and materials in Badenoch, Abernethy and Mar. *Int J Architect Herit*. 2020. <https://doi.org/10.1080/15583058.2020.1745321>.
70. Thacker M. An Ecology of Castle Construction: geoarchaeology, archaeobotany and radiocarbon analysis in the ecotone of Lochindorb Castle. In: *RILEM PRO 130; Proceedings of the 5th Historic Mortars Conference*, Pamplona. RILEM publications: Paris; 2019, p. 808–26.
71. Caldwell D, Stell G, Turner D. Excavations at Achanduin Castle, Lismore, Argyll, 1970–5: findings and commentary. *Proc Soc Antiqu Scotl*. 2015;145:349–69.
72. Thacker, M. Lismore Cathedral. *Discovery & Excavation in Scotland*; 2019.
73. Thacker in prep. *Materials Analysis at Lismore Cathedral* [working title].
74. Brown A, Duncan A. The cathedral church of Lismore. *Trans Scot Ecclesiol Soc*. 1957;15(1):41–55.
75. Fawcett R. *The Architecture of the Scottish Medieval Church*. New Haven & London: Yale University Press; 2011.
76. Thacker M. Medieval buildings & environmental change: chronology, ecology & political administration at Castle Sween, Knapdale. *Archaeol Anthropol Sci*. 2020;12:238. <https://doi.org/10.1007/s12520-020-01162-7>.

Publisher's Note

Springer Nature remains neutral with regard to jurisdictional claims in published maps and institutional affiliations.

Submit your manuscript to a SpringerOpen® journal and benefit from:

- Convenient online submission
- Rigorous peer review
- Open access: articles freely available online
- High visibility within the field
- Retaining the copyright to your article

Submit your next manuscript at ► [springeropen.com](https://www.springeropen.com)
